UNIVERSIDADE FEDERAL DE SÃO CARLOS
CENTRO DE CIÊNCIAS EXATAS E TECNOLOGIA
PROGRAMA DE PÓS-GRADUAÇÃO EM ENGENHARIA QUÍMICA

DEVELOPMENT OF STRATEGIES TO IMPROVE PHOSPHORUS AVAILABILITY IN SOILS THROUGH SOLID STATE FERMENTATION

DESENVOLVIMENTO DE ESTRATÉGIAS PARA MELHORAR A DISPONIBILIDADE DE FÓSFORO EM SOLOS ATRAVÉS DA FERMENTAÇÃO EM ESTADO SÓLIDO

Natalia Alvarez Rodrigues

SÃO CARLOS – SP

2025

UNIVERSIDADE FEDERAL DE SÃO CARLOS
CENTRO DE CIÊNCIAS EXATAS E TECNOLOGIA
PROGRAMA DE PÓS-GRADUAÇÃO EM ENGENHARIA QUÍMICA

DEVELOPMENT OF STRATEGIES TO IMPROVE PHOSPHORUS AVAILABILITY IN SOILS THROUGH SOLID STATE FERMENTATION

DESENVOLVIMENTO DE ESTRATÉGIAS PARA MELHORAR A DISPONIBILIDADE DE FÓSFORO EM SOLOS ATRAVÉS DA FERMENTAÇÃO EM ESTADO SÓLIDO

Natalia Alvarez Rodrigues

Tese de Doutorado apresentada ao Programa de Pós-Graduação em Engenharia Química da Universidade Federal de São Carlos como parte dos requisitos necessários para a obtenção do título de Doutora em Engenharia Química, área de concentração em Pesquisa e Desenvolvimento de Processos Químicos.

Orientadora: Profa. Dra. Cristiane Sanchez Farinas

SÃO CARLOS – SP

2025

UNIVERSIDADE FEDERAL DE SÃO CARLOS

Centro de Ciências Exatas e de Tecnologia
Programa de Pós-Graduação em Engenharia Química

Folha de Aprovação

Defesa de Tese de Doutorado da candidata Natalia Alvarez Rodrigues, realizada em 27/05/2025.

Comissão Julgadora:

Profa. Dra. Cristiane Sanchez Farinas (EMBRAPA)

Profa. Dra. Clarissa Hamaio Okino Delgado (Ikove Agro)

Prof. Dr. Rodrigo Klaic (BIOMA)

Profa. Dra. Mariane Molina Buffo (SENAI)

Prof. Dr. Alberto Colli Badino Junior (UFSCar)

O Relatório de Defesa assinado pelos membros da Comissão Julgadora encontra-se arquivado junto ao Programa de Pós-Graduação em Engenharia Química.

Dedico este trabalho aos meus pais, Cristina e João,
ao meu irmão, Guilherme, e ao meu noivo, Renato.

AGRADECIMENTOS

Agradeço, primeiramente, a Deus, por ter me concedido a força, a proteção e a sabedoria necessárias para a realização deste trabalho e por sua presença constante em minha vida.

À minha mãe, Cristina, ao meu pai, João, e ao meu irmão, Guilherme, que sempre rezaram por mim, torceram pelo meu sucesso e nunca mediram esforços para me ajudar de todas as maneiras.

Ao meu noivo, Renato, por todo apoio, companheirismo, amor e cuidado.

Às minhas orientadoras, Profª Drª Cristiane Sanchez Farinas e Profª Drª Fernanda Perpétua Casciatori, por todo o conhecimento compartilhado, apoio, incentivo, ensinamentos, conselhos, compreensão e fé na minha capacidade.

Aos membros da banca examinadora, pelas sugestões que contribuíram de forma significativa para o desfecho do presente trabalho.

Aos meus priminhos Laura, Luíza, Arthur e Henrique, que me motivam a ser uma pessoa melhor a cada dia.

Aos amigos e colegas de laboratório que sempre torceram por mim e tornaram esta jornada mais leve, Camila, Letícia, Felipe, Karine, Luana, Fabrício, Manu, Mariane, Mayara, Taise, Marina, Rauber e Ivan.

Aos amigos do grupo GICOM da Universidade Autônoma de Barcelona, que o doutorado sanduíche me trouxe, Anna, Jana, Nico, Esther, Goli, Arnau, Jose, Roberto, Mengqi, Nathaly, Marta, Davi, Michel, Elena e Carlos.

À minha supervisora do estágio no exterior, Profª Drª Adriana Artola, pela oportunidade, paciência e orientações.

Ao Programa de Pós-Graduação em Engenharia Química da Universidade Federal de São Carlos e aos órgãos de financiamento.

O presente trabalho foi realizado com apoio da Coordenação de Aperfeiçoamento de Pessoal de Nível Superior – Brasil (CAPES) – Código de Financiamento 001, da Fundação de Amparo à Pesquisa do Estado de São Paulo (FAPESP, processos nº 2019/25261-8 e nº 2024/09631-8), do Conselho Nacional de Desenvolvimento Científico e Tecnológico (CNPq, processos nº 441573/2023-1, nº 402713/2023-0, nº 303017/2022-8 e nº 401089/2022-3) e da Empresa Brasileira de Pesquisa Agropecuária (Embrapa).

"Por vezes sentimos que aquilo que fazemos não é senão uma gota de água do mar. Mas o mar seria menor se lhe faltasse uma gota."

(Madre Teresa de Calcutá)

ABSTRACT

The growing concern over the environmental impacts of intensive agriculture has intensified the search for sustainable alternatives, such as bioinoculants and biofertilizers. Among these strategies, the use of phosphate-solubilizing microorganisms (PSMs) is particularly promising, as they can reduce dependence on conventional phosphate fertilizers, whose production is associated with significant environmental damage. Solid-state fermentation (SSF) has emerged as a favorable cultivation method in this context, enabling the valorization of agro-industrial residues as fermentation substrates, thereby supporting circular economy principles. Given this scenario, this thesis aimed to investigate biotechnological strategies for producing phosphate biofertilizers via the cultivation of PSMs through SSF. Initially, the study focused on improving the solubilization process of phosphate rocks (PRs) through SSF by optimizing oxalic acid production by the fungus *Aspergillus niger*. Using sequential experimental designs, several variables were assessed, including substrate composition, sucrose supplementation, and methanol addition. A substrate mixture of sugarcane bagasse and soybean bran (1:1 w w^{-1}) was identified as the most effective for stimulating oxalic acid synthesis. Methanol addition proved to be a key factor in this process, increasing acid excretion threefold. Under optimized conditions - 7% methanol and 5 g of sucrose per kg of dry substrate (d.s.) -, substantial solubilization of Bayóvar, Itafós, and Registro PRs was achieved. Furthermore, the SSF process facilitated the release of organic P from the substrate itself, due to the production of enzymes such as phosphatases and cellulases. For Bayóvar PR, a maximum soluble P release of 12.1 g kg^{-1} d.s. was observed, corresponding to a solubilization efficiency of 63.8%. Based on these promising results, the process was evaluated in bench scale using a multilayer packed-bed bioreactor (PBB). Although the PBB system showed adequate operational behavior, methanol volatilization likely limited the solubilization efficiency to 24.6%. On the other hand, in situ drying of the fermented solids within the PBB successfully preserved both microbial viability and acid phosphatase activity over a 34-day storage period. Furthermore, greenhouse experiments revealed that substituting 50% of chemical fertilizer with the biofertilizers developed on a lab-scale did not compromise plant performance. Additionally, a different approach using the fungus *Trichoderma harzianum* was also explored, with a focus on optimize sporulation and enhancing the production of metabolites related to increased P acquisition by plants, such as indole derivatives and flavonoids. Cultivation was performed using beer draff and wheat straw as substrates. After optimization of aeration, proportion of substrates and inoculum size in 0.5 L PBBs, high values were achieved: 1.08×10^{10} spores g^{-1} dry matter (DM), 511.3 μg g^{-1} DM of indole derivatives, and 2.2 mg g^{-1} DM of total flavonoids. At bench scale (22 L PBB), the system still supported good sporulation (1×10^{9} spores g^{-1} DM) and indole derivative production (688 μg g^{-1} DM). However, overheating of up to 16.5°C above the optimal temperature (25°C) resulted in significant axial and radial thermal gradients, which notably impaired the production of acid phosphatase and flavonoids. Overall, this work provides significant contributions to the development of phosphate biofertilizers through SSF, identifying both promising strategies and key challenges for future advancement.

Keywords: Biofertilizers, Solid-state fermentation, Phosphate rock solubilization, Phosphate solubilizing microorganisms, Packed-bed bioreactor.

RESUMO

A crescente preocupação com os impactos ambientais da agricultura intensiva tem intensificado a busca por alternativas sustentáveis, como bioinoculantes e biofertilizantes. Dentre essas estratégias, o uso de microrganismos solubilizadores de fosfato (MSFs) se destaca por reduzir a dependência de fertilizantes fosfatados convencionais, cuja produção está associada a significativos danos ambientais. A fermentação em estado sólido (FES) tem se mostrado um método de cultivo promissor nesse contexto, ao viabilizar a valorização de resíduos agroindustriais como substratos fermentativos, promovendo os princípios da economia circular. Diante desse cenário, esta tese teve como objetivo investigar estratégias biotecnológicas para a produção de biofertilizantes fosfatados por meio do cultivo de MSFs através da FES. Inicialmente, o estudo concentrou-se na melhoria da solubilização de rochas fosfáticas (RFs) por meio da otimização da produção de ácido oxálico pelo fungo *Aspergillus niger*. Por meio de planejamentos experimentais sequenciais, foram avaliadas variáveis como composição de substratos, suplementação com sacarose e adição de metanol. Uma mistura de bagaço de cana-de-açúcar e farelo de soja (1:1 m m^{-1}) foi identificada como a mais eficaz para estimular a síntese de ácido oxálico. A adição de metanol mostrou-se um fator-chave, triplicando a excreção do ácido. Em condições otimizadas - 7% de metanol e 5 g de sacarose por kg de substrato seco (s.s.) - foi alcançada uma solubilização expressiva das RFs Bayóvar, Itafós e Registro. O processo de FES também favoreceu a liberação de fósforo (P) orgânico dos próprios substratos, devido à produção de enzimas como fosfatases e celulases. Para a RF Bayóvar, foi obtida uma liberação máxima de P solúvel de 12,1 g kg^{-1} s.s., correspondendo a uma eficiência de solubilização de 63,8%. Com base nesses resultados promissores, o processo foi avaliado em escala de bancada utilizando um biorreator de leito empacotado (BLE) multicamadas. Embora o sistema tenha apresentado bom desempenho operacional, a provável volatilização do metanol limitou a eficiência de solubilização a 24,6%. Por outro lado, a secagem in situ dos sólidos fermentados no próprio BLE preservou com sucesso a viabilidade microbiana e a atividade de fosfatase ácida ao longo de 34 dias de armazenamento. Além disso, ensaios em casa de vegetação demonstraram que a substituição de 50% do fertilizante químico pelos biofertilizantes desenvolvidos em escala laboratorial não comprometeu o desenvolvimento das plantas. Adicionalmente, o fungo *Trichoderma harzianum* também foi explorado, com foco na otimização da esporulação e no aumento da produção de metabólitos relacionados à maior aquisição de P pelas plantas, como derivados indólicos e flavonóides. Os cultivos foram realizados utilizando bagaço de malte de cerveja e palha de trigo como substratos. Após a otimização da aeração, proporção de substratos e tamanho de inóculo em BLEs de 0,5 L, foram alcançados valores de $1,08 \times 10^{10}$ esporos g^{-1} de matéria seca (MS), 511,3 μg g^{-1} MS de derivados indólicos e 2,2 mg g^{-1} MS de flavonóides totais. Em escala de bancada (BLE de 22 L), o sistema manteve boa esporulação (1×10^9 esporos g^{-1} MS) e produção de derivados indólicos (688 μg g^{-1} MS). No entanto, o superaquecimento - de até 16,5°C acima da temperatura ideal (25°C) - comprometeu a produção de fosfatase ácida e flavonoides. De modo geral, este trabalho oferece contribuições relevantes para o desenvolvimento de biofertilizantes fosfatados via FES, identificando estratégias promissoras e desafios a serem superados.

Palavras-chave: Biofertilizantes, Fermentação em estado sólido, Solubilização de rocha fosfática, Microrganismos solubilizadores de fosfato, Biorreator de leito empacotado.

LIST OF FIGURES

Fig. 2.1. World application and production of phosphate fertilizers in agriculture in 2022: a) use by world region, b) top 10 consuming countries and c) top 10 producing countries (FAO, 2025)…….24

Fig. 2.2. Simplified scheme of the phosphate fertilizer production process (Bertau et al., 2025)……25

Fig. 2.3. Main mechanisms involved in release of P by phosphate-solubilizing microorganisms (Kaur et al., 2024)…….33

Fig. 2.4. Annual Number of Scientific Publications Related to Phosphate-Solubilizing Microorganisms in Agriculture (2014 – 2024) (Web of Science, 2025)…….34

Fig. 2.5. Schematic representation of the main bioreactors for solid-state fermentation: a) rotating drum bioreactor; b) stirred drum bioreactor; c) tray bioreactor; and d) packed-bed bioreactor. Image extracted and adapted from Casciatori (2015)……41

Fig. 2.6. Trickle bed bioreactor proposed by Shahryari et al. (2020). Image extracted and adapted from Shahryari et al. (2020)……44

Fig. 2.7. Schematic representations of two air injection strategies in a packed-bed bioreactor: (a) 50% air injected at the bottom and 50% at the midsection (by walls); (b) injection via a longitudinally perforated tube (by the center). Image extracted and adapted from Perez et al. (2021)……..45

Fig. 2.8. Representation of multilayer packed-bed bioreactor operation modes: (a) cyclic and (b) continuous operations. Image extracted and adapted from Rodrigues et al. (2022).……46

Fig. 3.1. Schematic illustration of oxalic acid optimization steps by solid-state fermentation using the microorganism *Aspergillus niger*……...62

Fig. 3.2. Results from the mixture design experiments: a) contour plots showing the influence of the composition of wastes sugarcane bagasse (SCB), soybean bran (SB) and wheat bran (WB) on the pH variation (%) and b) production of oxalic and c) gluconic acids in g per kilogram of dry substrate (g kg^{-1} d.s.). Solid-state fermentations were carried out at 30°C for 4 days using *Aspegillus niger* C as microorganism……...69

Fig. 3.3. Results from the factorial design experiments: influence of the variables methanol, sucrose and pH of the saline solution. a) Pareto plot showing the effect of analyzed variables on the oxalic acid production. b) Contour plot showing the influence of the methanol and sucrose levels on oxalic acid production. c) Soluble proteins concentration in mg per kilogram of dry substrate (mg kg-1 d.s.) and final pH of liquid extract. d) Production of organic acids (g kg^{-1} d.s.). Electron microscopy of the final aspect of the fermented solids with e) 1% and f) 6% methanol addition. Solid-state fermentations were carried out at 30°C for 4 days using sugarcane bagasse and soybean bran (1:1 weight ratio) as solid substrates and *Aspegillus niger* C as microorganism…72

Fig. 3.4. Contour plots, resulting from the Box-Behnken design experiments, showing the influence of methanol, sucrose and rock phosphate concentrations on a) oxalic acid production in g per kg of dry substrate (g kg^{-1} d.s.), b) final pH of the liquid extract and c) solubilized P from the Bayóvar rock. Solid-state fermentations were carried out at

30°C for 4 days using sugarcane bagasse and soybean bran (1:1 weight ratio) as solid substrates and *Aspegillus niger* C as microorganism……..75

Fig. 3.5. a) Solubilization of Bayóvar phosphate rock in a medium under optimal conditions of fermentation determined by Box-Behnken design (sugarcane bagasse and wheat bran in a weight proportion 1:1, 5 g per kg of dry substrate (g kg^{-1} d.s.) of sucrose, 7% of methanol and 15 g kg^{-1} d.s. of rock) under different treatments: addition of 161 g kg^{-1} d.s. of abiotic oxalic acid (treatment 1) and solid-state fermentation by microorganism *Aspergillus niger* C (1×10^7 spores g^{-1} d.s.) (treatment 2). Electron microscopy of the solids at the end of incubation of treatments b) 1 c) and 2……79

Fig. 3.6. Time profiles for solubilized P, oxalic acid production in g per kg of dry substrate (g kg^{-1} d.s.) and final pH of the liquid extract during solid-state fermentation of *Aspergillus niger* C in the optimized condition: sugarcane bagasse and soybean bran in a weight proportion 1:1, 5 g kg^{-1} d.s. of sucrose, 7% methanol and 15 g kg^{-1} d.s. of Bayóvar rock……80

Fig. 3.7. Solubilization of different levels of Bayóvar, Itafós and Registro phosphate rocks by solid-state fermentation of *Aspergillus niger* C under the following conditions: sugarcane bagasse and soybean bran in a weight proportion 1:1, 5 g per kg of dry substrate (g kg^{-1} d.s.) of sucrose and 7% of methanol. Results for a) solubilized P (g kg^{-1} d.s.), b) P solubilization efficiency (%), c) Ratio between solubilized P and P added from rock and d) final pH of liquid extract and oxalic acid production (g kg^{-1} d.s.)…..82

Fig. 4.1. Schematic representation of the experimental apparatus at bench scale using a multilayer packed-bed bioreactor. Figure extracted and adapted from Rodrigues et al. (2022).……95

Fig. 4.2. a) Schematic representation and b) real image of the experimental setup used for drying fermented solids using the multilayer packed-bed bioreactor itself……...97

Fig. 4.3. a) Experimental pots prepared for lettuce cultivation; b) Overview of the greenhouse setup at the beginning of the trial……98

Fig. 4.4. Results of a) released P, P release efficiency, oxalic acid production, final pH, b) colony-forming units (CFU) and acid phosphatase (ACP) activity for the following treatments: (1) with sucrose and mineral salts, (2) without sucrose and with mineral salts, and (3) without sucrose and without mineral salts. All cultivations were carried out with the addition of 7% methanol (w w^{-1}) and 120 g kg-1 d.s. of Registro rock. Different letters indicate statistically significant differences between treatments ($\alpha \leq 0.05$), while the same letters indicate no significant difference……101

Fig. 4.5. Effect of adding 6, 9 and 12% of ethanol to the cultivation medium on the following responses: a) released P, P release efficiency, oxalic acid production, final pH, b) colony-forming units (CFU) and acid phosphatase (ACP) activity. All cultivations were carried out with the addition of 120 g kg^{-1} d.s. of Registro rock. Different letters indicate statistically significant differences between treatments ($\alpha \leq 0.05$), while the same letters indicate no significant difference……102

Fig. 4.6. Thermal behavior and CO_2 production in solid-state fermentation using a multilayer packed-bed bioreactor: temperature profiles of each layer for the batches a) 1, b) 2 e c) 3; maximum and average temperatures of each layer for the batches d) 1, e) 2 e f) 3; and CO_2 profiles and accumulated CO_2 for the batches g) 1, h) 2 e i) 3. FL1,

FL2 and FLA3 mean fermentative layer 1, 2 and 3, respectively. FL1 - FL3 denote fermented layers 1 - 3 (FL1: closest to air inlet; FL3: furthest)……106

Fig. 4.7. Results of the solid-state fermentation using a multilayer packed-bed bioreactor for each layer and batch: a) released P; b) P release efficiency; c) Final pH; d) oxalic acid production; e) acid phosphatase (ACP); and f) colony-forming units (CFU). FL1, FL2 and FLA3 mean fermented layer 1, 2 and 3, respectively. FL1 - FL3 denote fermentative layers 1 - 3 (FL1: closest to air inlet; FL3: furthest)……107

Fig. 4.8. Study of the drying of fermented solids after the solid-state fermentation process using the multilayer packed-bed bioreactor itself: a) relative humidity of the air leaving the drying system over time; b) CFU values and ACP activity of the dry fermented solids stored under refrigeration over 34 days……109

Fig. 5.1. Schematic representation of the experimental apparatus at lab and bench scales: (a) 0.5 L Erlenmeyer flask, (b) 0.5 L PBB and (c) 22 L PBB……...120

Fig. 5.2. Effect of different methanol and ethanol concentrations on *Trichoderma. harzianum* SSF using beer draff:wheat straw 7:3 as substrates and 3.5% of struvite as inorganic P source. The evaluated responses include: a) spore production and final pH; b) phenotypic aspect of the fermented solids; c) Acid phosphatase (ACP) activity, released P, and P solubilization efficiency and d) time-course analysis (without struvite) comparing 8% ethanol addition versus no ethanol. SSF was conducted at 25°C for 4 days in Erlenmeyer flasks……..128

Fig. 5.3. Surface plots, resulting from the Box-Behnken design experiments, showing the influence of airflow, proportion of beer draff (BD) and wheat straw (WS) and inoculum size on sporulation. a) Inoculum size fixed in 5.05×10^6 spores g^{-1} DM. b) Air flow fixed in 55 mL min^{-1}. c) Proportion of substrates fixed in 5:5 BD:WS. SSF were carried out at 25ºC for 4 days in 0.5 L packed-bed bioreactors……132

Fig. 5.4. Time course analysis under optimized conditions in 0.5 L PBBs. Profiles of a) Specific oxygen uptake rate (sOUR) and Cumulative Oxygen Consumption (COC), b) spores, c) Acid phosphatase (ACP) activity and released P, and d) indole derivatives and total flavonoids. SSF was conducted at 25°C in 0.5 L packed-bed bioreactors……136

Fig. 5.5. Thermal behavior during SSF in the 22 L packed-bed bioreactor: a) position of temperature sensors inside the bioreactor; b) temperature profiles over time for the two batches; c) maximum and d) average temperatures recorded at each sensor position……..142

Fig. 5.6. Results from SSF process in the 22 L packed-bed bioreactor (PBB), compared to the 0.5 L PBB. Profiles of a) Specific oxygen uptake rate (sOUR) and Cumulative oxygen consumption (COC), b) spore production, c) ACP activity, and d) production of indole derivatives and total flavonoids……..144

LIST OF TABLES

Table 2.1. Diversity of organic acid produced by phosphate-solubilizing microorganisms (PSMs)……..29

Table 2.2. Examples of commercial biofertilizer products based on phosphate-solubilizing microorganisms. ……..35

Table 3.2. Matrix and results of the mixture design carried to evaluate the influence of the composition of agro-industrial by-products sugarcane bagasse (SCB), soybean bran (SB) and wheat bran (WB) on the pH variation (%) and production of organic acids by *Aspergillus niger* C in solid-state fermentation at 30°C for 4 days…….63

Table 3.3. Matrix and results of the factorial design 23 carried out to evaluate the influence of methanol (Met), sucrose (Suc) and initial pH of the saline solution (pH of SS) on the final pH of the liquid extract (Final pH), oxalic acid production (OA) and soluble proteins (SP)……64

Table 3.4. Matrix and results of the Box-Behnken design carried out to evaluate the influence of methanol (Met), sucrose (Suc) and Bayóvar rock (BR) on the final pH of the liquid extract, oxalic acid production (OA) and solubilized P (P exp and P pred)…65

Table 4.1. Physicochemical analysis of the Registro phosphate rock (Favaro et al., 2022)……91

Table 4.2. Process conditions and average responses for the three batches conducted in the multilayer packed-bed bioreactor……104

Table 4.3. Effect of 50% replacement of chemical fertilizer with biofertilizers on lettuce growth parameters. The quantity of total P per plant pot was standardized to 60 mg..110

Table 5.1. Characterization of materials employed in the SSF processes…….119

Table 5.2. Matrix and results of the Box-Behnken design carried out to evaluate the influence of air flow, proportion of beer draff (BD):wheat straw (WS) and inoculum size on the sporulation by *Trichoderma harzianum* in 0.5 L packed-bed bioreactors……133

Table 5.3. Operating conditions and main results for the two batches conducted in the 22 L packed-bed bioreactor……...140

SUMÁRIO

Chapter 1 ..... **17**
1.1. Introduction **17**
1.2. General objective **18**
1.2.1. Specific objectives 18
References **20**
Chapter 2 ..... **21**
2. Theoretical basis and state of the art **21**
2.1. Phosphorus in agriculture **21**
2.1.1. Role of phosphorus in plant development 21
2.1.3. Phosphate fertilization 25
2.2. Phosphate-solubilizing microorganisms **28**
2.2.1. Action mechanism 28
2.2.2. Current scenario 34
2.2.3. Production methods 38
2.3. Solid-state fermentation **39**
2.3.1. General concepts 39
2.3.2. Bioreactors for solid-state fermentation 41
2.3.2.1. Recent advances in packed-bed bioreactors 44
2.3.3. SSF-based strategies for the development of phosphate bioinputs 47
2.4. Conclusions **49**
References **50**
Chapter 3 ..... **58**
3. New approaches for solubilization of phosphate rocks through solid-state fermentation by optimization of oxalic acid production **58**
ABSTRACT **58**
3.1. Introduction **58**
3.2. Materials and methods **60**
3.2.1. Characterization of mineral rocks 60
3.2.2. Microorganism and substrates 61
3.2.3. Solid-state fermentation 62
3.2.3.1. Oxalic acid optimization 63
3.2.3.1.1. Mixture design 63

3.2.3.1.2. Factor design 2^3 64
3.2.3.1.3. Box-Behnken design 65
3.2.3.1.4. P solubilization of different types and contents of phosphate rocks 66
3.2.4. Comparative study on the action of the microorganism in phosphorus release 67
3.2.5. Analytic determinations 67
3.2.5.1. Soluble proteins 67
3.2.5.2. Organic acids 67
3.2.5.3. Soluble phosphorus 67
3.2.5.4. Total phosphorus 68
3.2.5.5. Phosphorus solubilization efficiency 68
3.2.5.6. Enzymatic assays 68
3.2.6. Statistical analyzes 68
3.3. Results and discussion 69
3.3.1 Effect of the combination of agro-industrial by-products on the production of oxalic acid by *Aspergillus niger* 69
3.3.2 Factor screening in oxalic acid production 72
3.3.3 Optimization of oxalic acid production and Bayóvar rock solubilization 75
3.3.3.1 Time profiles of the P solubilization process in the optimized conditions 81
3.3.4. Evaluation of phosphorus solubilization in different types and contents of phosphate rocks 82
3.4. Conclusions 86
References 86
Chapter 4 90
4. Bioconversion of phosphate rock by *Aspergillus niger* in packed bed bioreactors: toward scalable biofertilizer production for agricultural use 90
ABSTRACT 90
4.1. Introduction 90
4.2. Material and methods 92
4.2.1. Characterization of mineral rocks 92
4.2.2. Microorganism and substrates 93
4.2.3. Solid-state fermentation 93
4.2.3.1. Lab-scale experiments 94
4.2.3.1.1. Effect of sucrose and mineral salt addition to the cultivation medium 94
4.2.3.1.2. Effect of ethanol in the solubilization process of phosphate rock 95
4.2.3.2. Experiments at bench scale 95
4.2.3.2.1 Drying process of the fermented solids 97

4.2.4. Application of biofertilizers in soil-plant system 98
4.2.5. Analytical procedures 100
4.2.5.1. Colony-forming unit counting 100
4.2.5.2. Oxalic acid determination 100
4.2.5.3. Soluble and total P determination 101
4.2.5.4. Phosphatase activity assays 101
4.2.6. Statistical analyzes 102
4.3. Results and discussion 102
4.3.1. Effect of sucrose and mineral salt addition to the cultivation medium 102
4.3.2. Effect of ethanol in the solubilization process of phosphate rock 103
4.3.3. Evaluation of the solubilization process of phosphate rock in the multilayer packed-bed bioreactor 105
4.3.3.1. Bed drying using the multilayer packed-bed bioreactor itself 110
4.3.4. Application of biofertilizers in lettuce 111
4.4. Conclusions 112
References 113
Chapter 5 116
5. *Trichoderma harzianum* as a multifunctional microbial agent: optimizing solid-state fermentation in packed-bed bioreactors to produce essential metabolites for phosphorus availability 116
ABSTRACT 116
5.1. Introduction 116
5.2. Material and methods 119
5.2.1 Microorganisms and solid substrates 119
5.2.2 Solid-state fermentation 120
5.2.2.1 Evaluation of P release in flasks 121
5.2.2.2 Optimization of spore production in 0.5 L PBB 122
5.2.2.3 Time course analysis under optimized conditions in 0.5 L PBB 123
5.2.2.4 Process scale-up to a 22 L PBB 124
5.2.2.5 Assessment of Oxygen Consumption 125
5.2.3 Analytical procedures 125
5.2.3.1 Spore counting 126
5.2.3.2 Soluble and total P determination 126
5.2.3.3 Phosphatase activity assays 127
5.2.3.4 Quantification of indole derivatives 127
5.2.3.5 Quantification of total flavonoids 127

5.2.4 Statistical analysis 128
5.3. Results and discussion 128
5.3.1 Effect of the addition of alcohols on P release 128
5.3.2 Optimization of spore production in 0.5 L PBB 132
5.3.3 Time-course analysis of sporulation and associated metabolic responses in 0.5 L PBBs 136
5.3.4 Scale-up: 22 L packed-bed bioreactor 140
5.4. Conclusions 147
References 147
Chapter 6 152
6. Conclusions 152
Chapter 7 154
7. Suggestions for future work 154

Chapter 1

1.1. Introduction

In recent years, global consumption of water, food, and energy has intensified due to population growth, increased longevity, rapid urbanization, and changes in consumer behavior. The global population is expected to increase by approximately 30% until 2100, requiring a substantial intensification of agricultural production to ensure food security (United Nations, 2022). However, achieving this intensification in a sustainable manner poses major challenges. Most of the anticipated increase in food production is expected to rely on intensified use of existing agricultural lands. This strategy, although essential, can have unintended consequences, including negative impacts on soil carbon stocks, biodiversity, and long-term ecosystem stability (Chan et al., 2021).

Among the essential nutrients for plant growth, phosphorus (P) plays a key role in several metabolic processes. It comprises about 0.2 to 0.8% of plant dry weight (Sharma et al., 2013) and is absorbed by plants in the form of orthophosphates ($H_2PO_4^-$ or HPO_4^{2-}) (Ibrahim et al., 2022). To address phosphate deficiency in soils, synthetic phosphate fertilizers have been widely applied. However, these fertilizers have low use efficiency - only about 5 to 25% of the applied P is absorbed by plants - since phosphate ions rapidly form insoluble complexes with calcium, iron, and aluminum in the soil (Schnug et al., 2016). This not only reduces crop productivity but also leads to environmental issues such as soil acidification, water pollution, and eutrophication (Chaney et al., 2012).

In response to these challenges, the use of phosphate-solubilizing microorganisms (PSMs) in agriculture has expanded significantly (Timofeeva et al., 2022). This growth is driven by a greater awareness of the environmental and health risks posed by chemical inputs and by advances in the understanding of the ecological functions of soil microbiota. Their use can reduce the dependency on synthetic fertilizers, representing a sustainable strategy for enhancing P availability in agroecosystems (Bagga et al., 2024).

Despite their potential, the widespread adoption of PSM-based products faces technical and economic challenges, particularly regarding the development of stable, effective formulations and scalable production processes (Kumawat et al., 2021). A

successful microbial product must ensure efficacy, persistence, and commercial viability - attributes typically achieved through robust fermentation and formulation strategies. In this context, solid-state fermentation (SSF), which involves the cultivation of microorganisms on moist, solid substrates with minimal or no free water, has emerged as a promising alternative. One of its main advantages is the possibility to use agro-industrial residues as substrates, thereby contributing to circular economy principles while reducing environmental problems associated with improper waste disposal (Mattedi et al., 2023).

Given the importance of efficient and scalable microbial production systems, the development of SSF-based strategies for producing PSMs represents an important step toward more sustainable agricultural practices. Therefore, this thesis explores the potential of SSF to obtain biofertilizers through different strategies, including the biological solubilization of phosphate rocks using *Aspergillus niger* and the production of metabolites associated with enhanced P acquisition by plants using *Trichoderma harzianum*.

1.2. General objective

This thesis aimed to evaluate strategies for producing phosphate biofertilizers through the cultivation of phosphate-solubilizing microorganisms using solid-state fermentation.

1.2.1. Specific objectives

- To optimize the production of oxalic acid by *Aspergillus niger* through solid-state fermentation and evaluate the solubilization of different types of phosphate rocks during cultivation;
- To evaluate the solid-state fermentation process by *Aspergillus niger* under optimized conditions for oxalic acid production in a multilayer packed-bed bioreactor with a working volume of 4.5 L, as well as the drying of fermented solids in the bioreactor itself;
- To apply the biofertilizers obtained from *Aspergillus niger* cultivation in a soil - plant system;

- To optimize the growth and evaluate the production of metabolites related to phosphorus acquisition by plants by a strain of *Trichoderma harzianum* through solid-state fermentation;
- To evaluate the solid-state fermentation process under optimized conditions for the growth of *Trichoderma harzianum* in a 22 L packed-bed bioreactor.

To present the steps taken to achieve the objectives of this thesis, the work was structured into some chapters. Chapter 2 is currently being prepared for publication in an international journal as a review article; Chapter 3 was published in 2024 in the journal "Bioresource Technology"; Chapter 4 is also currently being prepared for publication in an international journal; and Chapter 5 is in the submission phase for publication in an international journal. A brief description of each chapter is provided below:

- **Chapter 2 – Theoretical basis and state of the art:** This chapter outlines the key theoretical concepts that support the relevance and development of the research. It also provides an overview of existing studies on the production of phosphate biofertilizers using phosphate-solubilizing microorganisms.
- **Chapter 3 – New approaches for solubilization of phosphate rocks through solid-state fermentation by optimization of oxalic acid production:** This chapter describes a sequence of experimental designs carried out to optimize oxalic acid production by *Aspergillus niger* through solid-state fermentation. Under optimized conditions, the solubilization of different phosphate rocks during cultivation was also evaluated.
- **Chapter 4 – Bioconversion of phosphate rock by *Aspergillus niger* in packed-bed bioreactors: toward scalable biofertilizer production for agricultural use:** This chapter presents the development of strategies to perform the optimized fermentation process from the previous chapter in a multilayer packed-bed bioreactor. It also includes an evaluation of the feasibility of drying the fermented solids in the bioreactor itself. In addition, this chapter presents the application of different forms of the biofertilizer - produced under optimized conditions at lab scale - in lettuce cultivation.
- **Chapter 5 – *Trichoderma harzianum* as a multifunctional microbial agent: optimizing solid-state fermentation in packed-bed bioreactors to produce**

essential metabolites for phosphorus availability: This chapter focuses on optimizing the growth of a *Trichoderma harzianum* strain and evaluating its production of key metabolites - such as phosphatases, indole-3-acetic acid, and flavonoids - that enhance plant phosphorus acquisition. The development of the process in a 22 L packed-bed bioreactor is also presented.

- **Chapter 6 – Conclusions:** This chapter summarizes the main findings of the thesis, highlighting the scientific and technological contributions of the work.
- **Chapter 7 – Suggestions for future work:** This final chapter presents recommendations for future research, considering the limitations encountered and the potential applications.

References

Bagga, D., Chauhan, S., Bhavanam, A., GN, N., Meena, S.S., Mohanty, A., 2024. Recent advancements in fermentation strategies for mass production and formulation of biofertilizers: Towards waste valorization. J. Soil Sci. Plant Nutr. 24, 5868–5897.

Chan, J., Havlik, P., Leclère, D., de Vries, W., Valin, H., Deppermann, A., Hasegawa, T., Obersteiner, M., 2021. Reconciling regional nitrogen boundaries with global food security. Nat. Food 2, 700–711.

Chaney, R.L., 2012. Food safety issues for mineral and organic fertilizers. Adv. Agron. 117, 51–116.

Ibrahim, M., Iqbal, M., Tang, Y.T., Khan, S., Guan, D.X., Li, G., 2022. Phosphorus mobilization in plant–soil environments and inspired strategies for managing phosphorus: A review. Agronomy 12, 2539.

Kumawat, K.C., Keshani, Nagpal, S., Sharma, P., 2021. Present scenario of bio-fertilizer production and marketing around the globe. In: Biofertilizers. Elsevier, Amsterdam, The Netherlands, pp. 389–413.

Mattedi, A., Sabbi, E., Farda, B., Djebaili, R., Mitra, D., Ercole, C., Pellegrini, M., 2023. Solid-state fermentation: Applications and future perspectives for biostimulant and biopesticides production. Microorganisms 11, 1408.

Schnug, E., Haneklaus, S.H., 2016. The enigma of fertilizer phosphorus utilization. In: Schnug, E. (Ed.), Phosphorus in Agriculture: 100% Zero. Springer, Dordrecht, The Netherlands, pp. 7–26.

Sharma, S.B., Sayyed, R.Z., Trivedi, M.H., Gobi, T.A., 2013. Phosphate solubilizing microbes: Sustainable approach for managing phosphorus deficiency in agricultural soils. Springerplus 2, 587.

Timofeeva, A., Galyamova, M., Sedykh, S., 2022. Prospects for using phosphate-solubilizing microorganisms as natural fertilizers in agriculture. Plants 11, 2119.

United Nations, Department of Economic and Social Affairs, Population Division, 2022. World Population Prospects 2022: Summary of Results. https://population.un.org/wpp/ (accessed 2 May 2025).

Chapter 2

2. Theoretical basis and state of the art

2.1. Phosphorus in agriculture

2.1.1. Role of phosphorus in plant development

Phosphorus (P) is a primary macronutrient essential for plant development, alongside nitrogen (N) and potassium (K), acting as a structural and functional component of several vital biomolecules (Silva et al., 2023). One of its most critical roles is in energy transfer and storage, through the formation of molecules such as adenosine triphosphate (ATP), adenosine diphosphate (ADP), and NADPH. These molecules are key to essential physiological processes, including photosynthesis, cellular respiration, the biosynthesis of organic compounds, and active nutrient transport across cell membranes (Bisson et al., 2017). Cell membranes themselves are composed of phospholipids, which contain P in their structure and are crucial for maintaining membrane integrity and fluidity. Additionally, P plays a direct role in nucleic acid synthesis, forming the phosphodiester backbone of DNA and RNA. Thus, P is fundamental to plant metabolism, contributing to carbohydrate synthesis, enzyme regulation (activation and inactivation), and physiological processes such as germination, root development, flowering, and seed formation (Malhotra et al., 2018).

Several studies also highlight P's role in regulating physiological responses and promoting plant tolerance to various abiotic stresses, including drought, heat, salinity, and the presence of heavy metals in soil (Bechtaoui et al., 2021; Khan et al., 2023). Plants can detect and respond to variations in P availability through specific signaling pathways, leading to changes in root architecture and stomatal morphology. By modulating phosphate metabolism, plants develop adaptive mechanisms that enhance tolerance to environmental stressors (Shen et al., 2011).

Under low moisture conditions, for instance, P contributes to root proliferation and improved root architecture, increasing root volume and hydraulic conductance. This enhanced root development enables more efficient water and nutrient uptake, strengthens resource sensing and signaling, and improves absorption in the rhizosphere under abiotic stress (Khan et al., 2023). In a field study, Hansel et al. (2017) evaluated the effects of triple superphosphate and soil preparation on soybean root systems under drought conditions. Their results showed that P application promoted deeper root

growth and increased drought resistance. Similarly, Tariq et al. (2017) investigated the combined effects of phosphate fertilization and two irrigation regimes (well-watered and water-stressed) on *Phoebe zhennan* seedlings. They observed that P application positively influenced root biomass, enhancing the plant's ability to extract water from the soil.

Adequate P supply also contributes to tolerance against heat stress by modulating root system architecture. Fahad et al. (2017) demonstrated that high temperatures impair plants' ability to absorb and utilize water and nutrients effectively. In their study on rice, the combined application of biochar and P under heat stress improved growth, productivity, and grain quality. The benefits were attributed to enhanced stomatal conductance, increased photosynthetic rate, better water-use efficiency, and larger grain size.

Regarding tolerance to saline stress, the mechanisms by which plants respond under adequate or deficient P conditions remain somewhat controversial. One well-established plant strategy under saline conditions is the excretion of salts through salt glands, a mechanism common in halophytes. This process is energy-intensive, relying on ATPases and therefore dependent on sufficient P availability (Assaha et al., 2017). However, excessive P supplementation under salinity may have adverse effects; for instance, Tang et al. (2019) reported that high P doses increased Na^+ concentrations in the aerial parts of plants, potentially due to alterations in root physiology. Conversely, moderate or low levels of phosphate fertilization have shown positive outcomes under saline conditions. Loudari et al. (2022) observed that limited phosphate input mitigated the detrimental effects of salt stress, enhancing photosynthetic efficiency, nutrient uptake, and overall plant growth.

Adequate P availability also plays a significant role in alleviating heavy metal stress. P can immobilize toxic metals in the soil by forming stable complexes, thereby reducing their bioavailability and limiting their uptake by plant roots (Zeng et al., 2017). Heavy metal contamination can severely inhibit plant growth and development, particularly in roots and shoots, by disrupting nutrient balance through ionic competition (Zhao et al., 2018). Although P supplementation does not entirely prevent metal absorption, it helps decrease their accumulation in plant tissues - especially in leaves - thus reducing their toxicity.

Li et al. (2012) studied the effects of P application on lead (Pb) availability and the growth of perennial ryegrass (*Lolium perenne*). At a P/Pb ratio of 2, Pb concentration in roots was reduced by 25.6%, and plant productivity increased by 804%. Similarly, Bechtaoui et al. (2021) evaluated the accumulation of cadmium (Cd), lead (Pb), and zinc (Zn) in the aerial parts of wheat, sedum, rice, corn, and canola under both high and low P conditions. Adequate P supply led to significant reductions in metal accumulation, with the highest decreases observed being 55.4% for Cd in wheat, 37.5% for Zn in corn, and 50.6% for Pb in wheat.

P deficiency induces cellular and physiological changes in plants. Meng et al. (2021), for example, demonstrated that low P availability restricted the accumulation of dry matter in leaves and branches of grapefruit (*Citrus grandis*). Moreover, P deficiency impairs the absorption of other nutrients, primarily due to reduced energy availability for active transport mechanisms, ultimately hindering plant development.

2.1.2. Soil phosphorus dynamics

P in soil exists predominantly in two forms: inorganic and organic. The relative proportions of these forms vary depending on soil formation and development processes, which are influenced by factors such as mineralogy, climate, and biological activity. It is estimated that organic P accounts for approximately 30–50% of the total soil P, while inorganic P represents 35–70% (Nesme et al., 2018; Wilson et al., 2019). The inorganic fraction includes soluble and weakly adsorbed P, as well as P bound to aluminum (Al-P), iron (Fe-P), calcium (Ca-P), reduced P forms, and occluded P. The organic fraction, in turn, consists mainly of phytates, nucleic acids, and phospholipids - compounds that are integral to soil organic matter. These different P forms behave distinctly in the soil due to their interactions with specific physicochemical and biological processes (Brady; Weil, 2008). Regardless of its origin, P must be in the form of orthophosphate ions ($H_2PO_4^-$ and HPO_4^{2-}) to be absorbed by plants. These ions are present in very low concentrations in the soil solution due to P's low mobility, slow diffusion, and strong fixation onto soil colloids (Ibrahim et al., 2022).

Primary inorganic P minerals, such as apatites ($Ca_5(PO_4)_3(F, Cl, OH)$), originate primarily from magmatic crystallization and slowly release P through chemical weathering processes, including acid-mediated dissolution. However, the rate of P release from these sources is too slow to meet the nutritional demands of agricultural

crops (Cardoso Filho et al., 2021). Secondary phosphates, such as variscite ($AlPO_4 \cdot 2H_2O$) and strengite ($FePO_4 \cdot 2H_2O$), form from the reaction of soluble P (originating from fertilizers or organic matter decomposition) with cations like Fe^{3+}, Al^{3+}, and Ca^{2+}. Their solubility depends largely on soil pH and particle size (Pierzynski et al., 2005).

Thus, soil P exists in a dynamic and complex equilibrium, ranging from highly stable, unavailable forms to more labile fractions that are readily taken up by plants (Shen et al., 2011). Under conditions of P deficiency, other P reserves may be mobilized; however, this process is typically slow and inadequate to meet crop demands. As P is rapidly absorbed by roots, a sharp concentration gradient develops near the root-soil interface, reducing the availability of P in this critical zone. Because P diffusion in soil is generally very limited, this gradient is seldom naturally replenished, leading to frequent P deficiency (Kruse et al., 2015).

Studies have shown that limited P uptake is one of the key constraints to plant growth worldwide. Therefore, the root system architecture plays a crucial role in P acquisition efficiency (Luo et al., 2020). In response to low P availability, many plants exhibit morphological adaptations such as increased root branching, enhanced root hair development, and the formation of longer, thinner roots that explore deeper or more nutrient-rich soil sublayers (Lyu et al., 2016). Indeed, Chen et al. (2024) investigated the effects of phosphate fertilizer placement at different soil depths (5–20 cm) on maize cultivation. They found that deeper fertilizer application stimulated deeper root growth, improving the coordination between shoot and root development. In treatments where fertilizer was applied at a depth of 15 cm, mature biomass and grain yield were 12.5% and 22.0% higher, respectively, compared to fertilizer applied at a depth of 5 cm.

Despite these adaptive strategies, the naturally low availability and limited mobility of P in soils continue to impose significant constraints on agricultural productivity. This limitation is particularly pronounced in tropical regions, such as in Brazilian soils, where P availability is inherently low due to specific chemical and mineralogical characteristics. These soils are typically highly weathered and rich in Fe and Al oxides and hydroxides, which have a strong affinity for P, leading to its fixation as poorly soluble compounds. The acidic nature of these soils further intensifies this effect by enhancing the precipitation of P with these metals (Campos et al., 2016). As a result, the large-scale application of phosphate fertilizers becomes essential to ensure

adequate nutrient supply and to sustain high agricultural productivity (Jahan et al., 2025). However, it is estimated that only 10–20% of the total P applied to soil is taken up by plants (Helfenstein et al., 2018).

Although P is generally considered immobile in soils due to its strong adsorption to minerals, under certain conditions - such as in sandy soils, soils with low organic matter, or with excessive phosphate application - P can become prone to leaching. This phenomenon, although less frequent than N leaching, raises environmental concerns, particularly due to its contribution to the eutrophication of water bodies (Withers et al., 2014a). Leached P, predominantly in dissolved reactive or particulate-bound forms, may be carried through surface runoff or percolation, ultimately reaching aquatic systems and contributing to eutrophication and declining water quality. This underscores the importance of balanced fertilization practices and improved P use efficiency in agriculture to minimize environmental risks (Sharpley et al., 2013; Sattari et al., 2012).

2.1.3. Phosphate fertilization

Globally, the demand for phosphate fertilizers has steadily increased, driven by the need to sustain agricultural productivity and feed a growing population (Bertau et al., 2025). In 2022, approximately 41.9 million tons of phosphate fertilizers were used worldwide, with Asia accounting for more than half of this total - around 23 million tons (Fig. 2.1a).

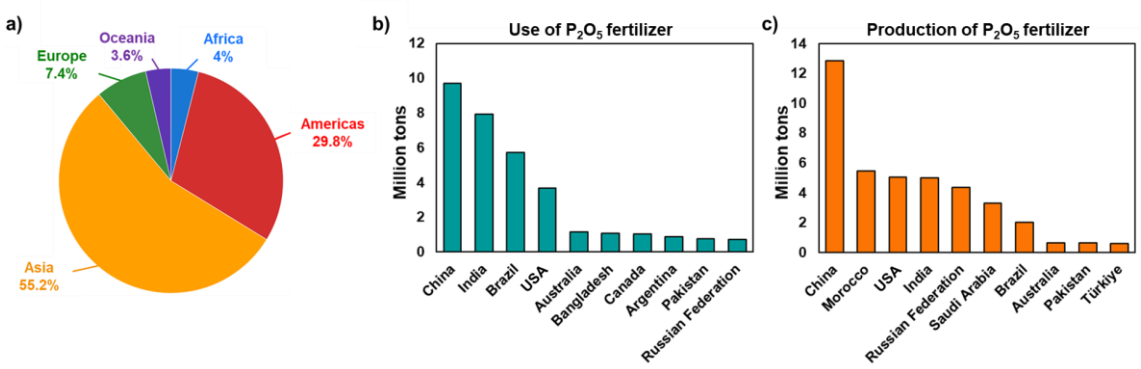

Fig. 2.1. World application and production of phosphate fertilizers in agriculture in 2022: a) use by world region, b) top 10 consuming countries and c) top 10 producing countries (FAO, 2025).

Brazil ranked as the third-largest consumer, following China and India (Fig. 2.1b), with an estimated usage of 5.7 million tons in 2022, representing 13.7% of global consumption. Notably, 68% of the phosphate fertilizers used in Brazil were imported, highlighting the country's significant dependence on external sources for this essential agricultural input (FAO, 2025).

In terms of fertilizer production, Brazil occupies the seventh position, as shown in Fig. 2.1c. Countries such as China, Morocco, and the United States - the three largest producers in 2022 - benefit from abundant reserves of phosphate rock, the primary raw material for phosphate fertilizer production. This process typically involves the mining of phosphate rock, followed by chemical treatment to produce concentrated products such as single superphosphate (SSP), triple superphosphate (TSP), and monoammonium phosphate (MAP) or diammonium phosphate (DAP), which contain approximately 18, 44, 52 and 46% of P_2O_5, respectively (Leikam; Achorn, 2005). The main steps involved in this process are illustrated in Fig. 2.2.

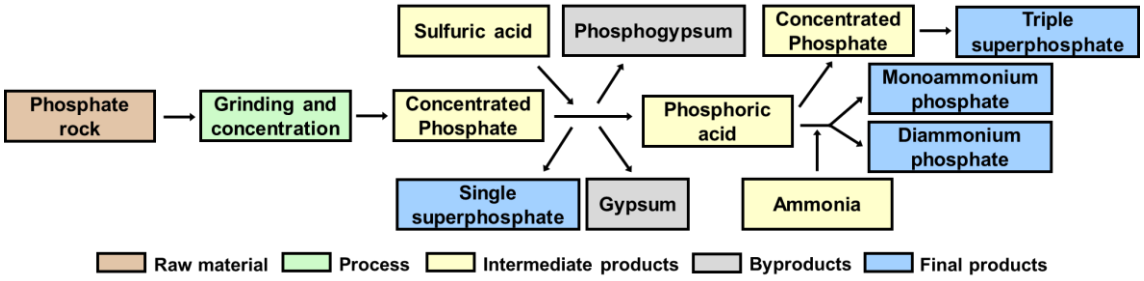

Fig. 2.2. Simplified scheme of the phosphate fertilizer production process (Bertau et al., 2025).

As shown in Fig. 2.2, the addition of sulfuric acid (H_2SO_4) to beneficiated phosphate rock initiates a reaction that produces SSP and phosphoric acid (H_3PO_4) - a key intermediate for manufacturing TSP, MAP and DAP. The process also generates two by-products: gypsum and phosphogypsum. Although both have potential applications, particularly in the construction industry, phosphogypsum is produced in such large volumes that its reuse rate remains very low - less than 15% globally (Chernysh et al., 2021). For every mole of fluorapatite processed, 5 moles of phosphogypsum are generated, as represented in Eq. (2.1) (Sherkuziev, 2021).

$$Ca_5(PO_4)3F + 5H_2SO_4 + 10H_2O \rightarrow 3H_3PO_4 + 5CaSO_4.2H_2O + HF \quad (2.1)$$

Worldwide, over 200 million tons of phosphogypsum are produced annually (Chernysh et al., 2021). Due to concerns over radionuclides, heavy metals, and fluoride, its use is strictly regulated in many countries. Consequently, most phosphogypsum is stored in large stacks or ponds near production facilities, posing long-term environmental risks such as leachate generation, acidic drainage, and potential structural failure (Tayibi et al., 2009).

In addition to the high generation of phosphogypsum, this process consumes large quantities of water and concentrated sulfuric acid, a compound that, in itself, requires a significant energy input for its production, further aggravating the environmental impact of the production of phosphate fertilizers (Withers et al., 2014b). Another growing concern is the potential depletion of phosphate rock, a finite resource. Recent estimates suggest that current reserves could be exhausted within 200 to 400 years (IFA, 2023).

In response to these challenges, a range of strategies has been investigated to improve the efficiency of phosphate fertilizer use in agriculture. These strategies aim to reduce P losses in the soil and to limit its conversion into forms unavailable to plants. Four main categories of technologies have been explored: phosphate fertilizers with fixation inhibitors; synergistic phosphate fertilizers; chemically modified phosphate fertilizers; and controlled-release phosphate fertilizers (Guelfi et al., 2022).

Phosphate fertilizers with fixation inhibitors are formulations that incorporate additives designed to limit P precipitation and adsorption in the soil. Common additives include oxysulfates and carbonates, which help neutralize acidity, as well as competing anions like molybdates and organic acids that function as cation chelators or adsorption blockers (Koilraj et al., 2013).

Synergistic phosphate fertilizers are conventional fertilizers enhanced with additional components such as nutrients, beneficial microorganisms, nanoparticles, or biostimulants that enhance P uptake by plants. For instance, magnesium plays a key role in facilitating P transport across root cell membranes, while certain microbial strains aid in the solubilization and mineralization of soil-bound P (Guelfi et al., 2022).

Chemically modified phosphate fertilizers undergo physical, chemical, or combined treatments to alter the solubility or chemical form of P. These modifications

may involve incorporating nanomaterials or substances like graphene oxide, which influence the behavior and availability of P in the soil (Andelkovic et al., 2018).

Controlled-release phosphate fertilizers consist of conventional phosphate sources coated with materials that regulate the release rate of P into the soil. Coating materials act as diffusion barriers and may include plastic resins, thermoplastics, polyurethane, polyethylene, and similar compounds (Wu et al. 2019).

Among these technologies for increasing the efficiency of phosphate fertilizer use, biological approaches have gained attention as complementary or alternative strategies for improving P availability in agricultural systems, such as one of the approaches of the synergistic phosphate fertilizers. One promising approach involves the inoculation of soils or crops with phosphate-solubilizing microorganisms (PSMs), which can enhance P availability and uptake by plants (Timofeeva et al., 2022). The next section will explore in more detail the mechanisms of action of these microorganisms as well as the current state of research and application in this field.

2.2. Phosphate-solubilizing microorganisms

2.2.1. Action mechanism

PSMs can convert insoluble forms of P into plant-available forms ($H_2PO_4^-$ and HPO_4^{2-}). Through this transformation, PSMs contribute to enhancing P availability in soils and can reduce the need for chemical phosphate fertilizer inputs in agricultural systems. Hussain et al. (2019) reported that the combined application of PSMs and phosphate fertilizer in wheat cultivation increased grain yield by 22% and P uptake by 26%, while enabling a 30% reduction in fertilizer input. Besides solubilizing P, some PSMs also demonstrate potential as biocontrol agents against some plant pathogens. They manage these pathogens by producing antifungal compounds (such as phenolics and flavonoids), siderophores, antibiotics, hydrogen cyanide and lytic enzymes all of which enhance inhibition of the growth of plant pathogens (Alori et al., 2017).

This diverse group includes bacteria, fungi, actinomycetes, and algae. They are commonly found in the rhizosphere, agricultural soils, forest soils, organic matter, and sediments. The rhizosphere is considered the primary reservoir of PSMs, as it hosts metabolically active microbial populations closely associated with plant roots. It is estimated that bacteria constitute 1–50% of the total PSM population, while fungi account for approximately 0.1–0.5% (Kalayu et al., 2019). Some potential genera of P

solubilizing fungi include *Aspergillus, Penicillium*, *Trichoderma*, *Glomus*, *Acremonium* and *Mortierella*. While some potential genera of P solubilizing bacteria include *Pseudomonas*, *Enterobacter*, *Bacillus*, *Serratia*, *Pantoea*, *Rhizobium*, *Arthrobacter* and *Burkholderia*, (Alori et al., 2017).

The mechanisms by which PSMs enhance P availability in soils can be categorized into two primary processes: the solubilization of insoluble inorganic phosphates (such as tricalcium phosphate, apatite, and iron and aluminum phosphates) and the mineralization of organic P compounds (e.g., phytate, phosphomonoesters, and phosphodiesters) (Richardson; Simpson, 2011; Kalayu et al., 2019).

Inorganic phosphate solubilization primarily occurs through the secretion of organic acids such as citric, oxalic, malic, gluconic, and lactic acids, among others. These acids lower the pH of the surrounding environment, promoting the dissociation of phosphate complexes. Two main processes are involved: acidification of the microenvironment, which enhances phosphate mineral dissolution, and chelation of metal cations (e.g., Ca^{2+}, Fe^{3+}, and Al^{3+}), which releases phosphate ions previously bound in insoluble forms (Kalayu et al., 2019; Rawat et al., 2021). Eqs. (2.2) and (2.3) exemplify the processes responsible for P release: acidification of fluorapatite and Fe chelation with oxalic acid, respectively.

$$Ca_3(PO_4)_2 + 6H^+ \rightarrow 3Ca^{2+} + 2H_3PO_4 \quad (2.2)$$

$$Fe(PO_4)_2 + 3H_2C_2O_4 \rightarrow Fe(C_2O_4)_3^{3-} + H_3PO_4 \quad (2.3)$$

Bononi et al. (2020) inoculated soybean plants with selected *Trichoderma* strains isolated from the Amazon and cultivated them in soil amended with a gradient of rock phosphate and triple superphosphate. The study revealed that 19.5% of the isolates were capable of solubilizing phosphate, primarily through the production of various organic acids. These strains showed positive effects on soybean growth - ranging from 2.1% to 41.1% - and significantly enhanced P uptake efficiency, with increases of up to 141%. Table 2.1 presents examples of organic acids produced by different PSMs.

Table 2.1. Diversity of organic acid produced by phosphate-solubilizing microorganisms (PSMs).

	PSM	Organic acids	Reference
Bacteria	*Achromobacter*	Gluconic, oxalic, lactic, acetic, malic, tartaric	Nacoon et al. (2020)
	Acinetobacter rhizosphaerae	Gluconic, formic, oxalic	Gulati et al. (2010)
	Bacillus cereus	Oxalic, malic, formic, acetic, tartaric, gluconic	Chawngthu et al. (2020)
	Bacillus licheniformis	Citric, acetic, propionic	Carmo et al. (2019)
	Bacillus megaterium	Citric, acetic, propionic	Carmo et al. (2019)
	Bacillus subtilis	Oxalic, malic, formic, acetic, tartaric, gluconic	Chawngthu et al. (2020)
	Burkholderia	Gluconic, oxalic, lactic, acetic, malic, tartaric	Nacoon et al. (2020)
	Enterobacter ludwigii	Citric, fumaric, acetic, succinic, gluconic, oxalic	Rfaki et al. (2020)
	Klebsiella	Gluconic, oxalic, lactic, acetic, malic, tartaric	Nacoon et al. (2020)
	Paenibacillus sp.	Oxalic, malic, formic, acetic, tartaric, gluconic	Chawngthu et al. (2020)
	Pantoea agglomerans	Citric, fumaric, acetic, succinic, gluconic, oxalic	Rfaki et al. (2020)
	Pantoea vagans	Citric, fumaric, acetic, succinic, gluconic, oxalic	Rfaki et al. (2020)
	Pseudomonas azotoformans	Citric, fumaric, acetic, succinic, gluconic, oxalic	Rfaki et al. (2020)

Table 2.1. Continuation.

	PSM	Organic acids	Reference
	Pseudomonas poae	Citric, gluconic, oxalic	Vyas and Gulati (2009)
	Pseudomonas trivialis	Gluconic, succinic, lactic, fumaric, malic	Vyas and Gulati (2009)
	Serratia marcescens	Citric, lactic, propionic, gluconic	Chen et al. (2006)
	Serratia quinivorans	Citric, fumaric, acetic, succinic, gluconic, oxalic	Rfaki et al. (2020)
Fungi	*Aspergillus foetidus*	Oxalic, citric, gluconic, succinic, tartaric	Singal et al. (1994)
	Aspergillus japonicus	Oxalic, citric, gluconic, succinic, tartaric	Singal et al. (1994)
	Aspergillus niger	Citric, glycolic, succinic, gluconic, oxalic, lactic, acetic, formic, tartaric, malic	Li et al. (2016); Mendes et al. (2013); Rodrigues et al. (2024)
	Penicillium canescens	Gluconic, oxalic, citric, acetic	Mendes et al. (2013)
	Penicillium islandicum	Gluconic, oxalic, citric, acetic	Mendes et al. (2013)
	Penicillium janthinellum	Gluconic, succinic, acetic, butyric, valeric, citric, fumaric, propionic	Scrervino et al. (2010)
	Penicillium oxalicum	Oxalic, formic, tartaric, malic, citric, succinic, acetic	Li et al. (2016)
	Penicillium purpurogenum	Gluconic, succinic, acetic, butyric, valeric, citric, fumaric, propionic	Scrervino et al. (2010)

Table 2.1. Continuation.

	PSM	Organic acids	Reference
Fungi	*Trichoderma sp.*	Lactic, fumaric, ascorbic, isocitric, malic, citric, phytic	Bononi et al. (2020)

The mineralization of organic P in soils is predominantly mediated by extracellular enzymes that hydrolyze organic P-containing compounds, converting them into forms readily assimilable by plants ($H_2PO_4^-$ and HPO_4^{2-}). Among these enzymes, acid and alkaline phosphatases are the most extensively studied and are classified based on the optimal pH at which they function (Liang et al., 2020). These enzymes are nonspecific and catalyze the dephosphorylation of phosphoanhydride or phosphoester linkages in organic phosphate compounds. For example, the hydrolysis of phosphomonoester bonds ($R–O–PO_3^{2-}$) produces alcohols (R–OH) and orthophosphate Examples of phosphomonoesters commonly found in soil include nucleotides, phosphorylated sugars, and glycerophosphate, among others (Sharma et al., 2013).

Additionally, there is an important class of phosphatases with high substrate specificity, the phytases. Phytases are essential for the stepwise hydrolysis of phytic acid (myo-inositol hexakisphosphate), a prevalent form of organic P in soils, releasing up to six molecules of inorganic P per molecule of substrate (Sharma et al., 2013). Furthermore, cellulolytic and other hydrolytic enzymes indirectly enhance P mineralization by decomposing soil organic matter and exposing otherwise inaccessible P substrates to phosphatases. This synergistic action highlights the complex enzymatic network involved in organic P cycling in soils (Richardson; Simpson, 2011).

Several fungal species are well known for their high phytase production capacity. Notable examples include *Aspergillus candidus*, *Aspergillus Aspergillus fumigatus*, *Aspergillus niger*, *Aspergillus parasiticus*, *Aspergillus rugulosus*, *Aspergillus terreus*, *Penicillium rubrum*, *Penicillium simplicissimum*, *Pseudeurotium zonatum*, *Trichoderma harzianum*, and *Trichoderma viride* (Tarafdar et al., 2003). While fewer bacterial genera are efficient phytase producers, strains belonging to *Bacillus*, *Streptomyces*, and *Pseudomonas* have demonstrated this enzymatic capability (Kalayu et al., 2019).

Experimental evidence supports the effectiveness of microbial phosphatases in improving P availability. For example, Singh and Banik (2019) reported that the

application of purified alkaline phosphatases from *Bacillus licheniformis* MTCC 2312 led to a 2.35-fold and 1.76-fold increase in P content in roots and stems of *Zea mays* L., respectively. Furthermore, Della Monica et al. (2020) observed that co-inoculation with the phosphate-solubilizing fungus *Talaromyces helices* L7B and the arbuscular mycorrhizal fungus *Rhizophagus irregularis* significantly boosted soil alkaline phosphatase activity, accompanied by a 50% rise in soluble P levels.

In addition to these direct mechanisms, some PSMs employ indirect strategies to enhance plant P uptake, such as siderophore production, exopolysaccharides production and root growth stimulation. Siderophores are low molecular weight, high-affinity Fe-chelating compounds secreted by microorganisms and plants under Fe-deficient conditions (Rawat et al., 2020). Under alkaline environments, several phosphate-solubilizing bacteria - including *Bacillus megaterium*, *Bacillus subtilis*, *Rhizobium radiobacter*, and *Pantoea allii* - have been shown to produce siderophores at concentrations ranging from 80 to 140 μmol L^{-1}. This not only supports microbial survival under stress conditions but also improves P solubilization by sequestering metal cations that would otherwise immobilize phosphate (Ferreira et al., 2019).

Exopolysaccharides are carbohydrate polymers secreted by microorganisms in response to stress or biofilm formation. These compounds can bind metal ions in soil, which may help in P solubilization. Research by Yi et al. (2008) demonstrated that the ability of 4 phosphate-solubilizing bacterial strains to dissolve tricalcium phosphate was influenced by the concentration of exopolysaccharides and the microbial strain, highlighting their role in P mobilization.

Root growth promotion growth may occur via both mycorrhizal associations and the biosynthesis of plant hormones (Richardson; Simpson, 2011). Mycorrhizal fungi establish symbiotic relationships with plant roots, effectively expanding the root system and increasing the soil volume explored for phosphate acquisition (Browne et al., 2009). Additionally, some PSMs produce phytohormones like indole-3-acetic acid (IAA), a key regulator of plant growth. IAA stimulates the formation of lateral roots and root hairs, improving P uptake capacity (Richardson and Simpson, 2011). Fig. 2.3 illustrates the primary mechanisms by which PSMs enhance P acquisition in plants.

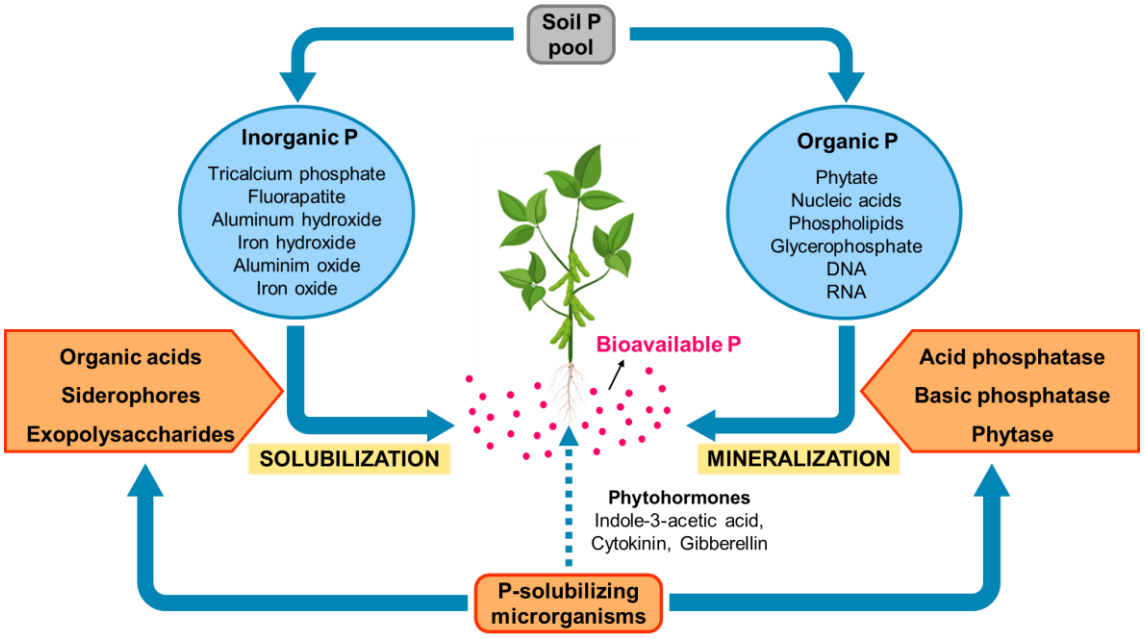

Fig. 2.3. Main mechanisms involved in release of P by phosphate-solubilizing microorganisms (Kaur et al., 2024).

2.2.2. Current scenario

Several studies have demonstrated the beneficial effects of inoculating agricultural crops with PSMs, particularly in enhancing plant biomass, P accumulation in plant tissues, and crop productivity (Sharma et al., 2013; Timofeeva et al., 2022; Kaur et al., 2024). Among microbial inoculants, PSMs represent approximately 15% of global bioinoculant use, while nitrogen-fixing bacteria dominate the market with about 80% and other growth-promoting inoculants at approximately 5% (Soumare et al., 2020).

PSMs are increasingly valued not only for their capacity to enhance P availability in soils - thereby reducing dependence on mineral phosphate fertilizers - but also for their potential multifunctionality. Many microbial formulations now combine biofertilization properties with biocontrol activity, targeting phytopathogens or weeds. Between 2020 and 2024, 114 patents were filed related to microbial biofertilizers; of these, 53 were associated with PSMs, and 54 included dual functionality as both biofertilizers and biopesticides, particularly for the control of bacterial and fungal pathogens (Reis et al., 2024).

From a market perspective, the biofertilizer sector has been expanding at a significantly faster pace than its synthetic counterpart. While the global synthetic fertilizer market reached an estimated value of USD 202 billion in 2022, its projected compound annual growth rate (CAGR) for the coming decade remains modest, ranging from 2.7% to 3.3%. In contrast, the biofertilizer market - valued between USD 1.5 and 2.8 billion in 2022 - is expected to grow rapidly, with a projected CAGR of 10.9% to 12.8% between 2023 and 2032 (Aloo et al., 2022). This trend reflects not only the increasing demand for sustainable agricultural solutions but also a growing trust in biological technologies.

According to data from the Web of Science, the number of publications - including journal articles and book chapters - that include the terms “phosphate-solubilizing microorganisms” or “phosphorus-solubilizing microorganisms” and “agriculture” in any field has steadily increased between 2014 and 2024, as shown in Fig. 2.4. This upward trend highlights the rising scientific interest and relevance of this research area. Notably, journal articles constitute 87% of the total publications.

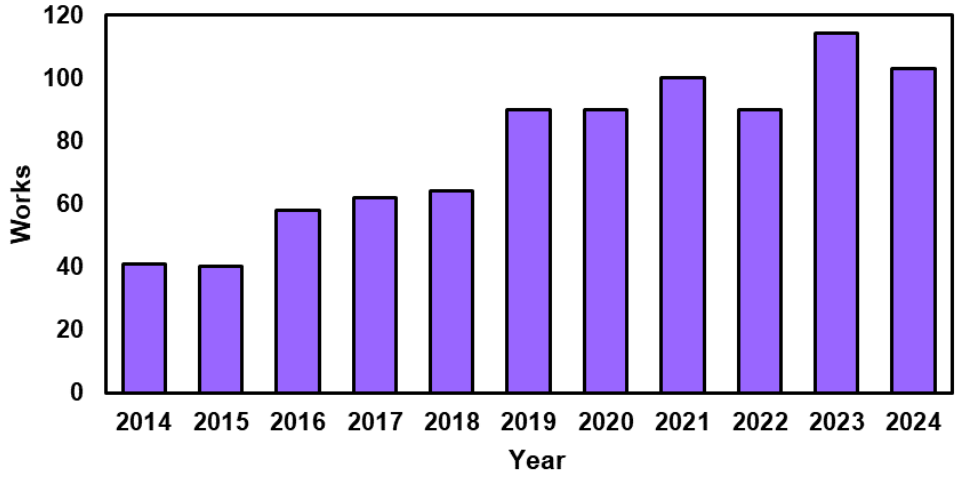

Fig. 2.4. Annual Number of Scientific Publications Related to Phosphate-Solubilizing Microorganisms in Agriculture (2014 – 2024) (Web of Science, 2025).

Most commercially available phosphate biofertilizers are formulated with bacterial strains, with *Bacillus megaterium* being the most commonly used species, as summarized in Table 2.2 Among fungal-based products, species from the *Penicillium* genus are the most prevalent.

Table 2.2. Examples of commercial biofertilizer products based on phosphate-solubilizing microorganisms.

Product name	PSM	Manufacturing company/Country	Reference
BiomaPhos	*Bacillus megaterium* (CNPMS B119), *Bacillus subtilis* (CNPMS B2084)	Bioma/ Brazil	Bioma (2025)
BioPhos+	*Bacillus megaterium, Bacillus polymyxa, Pseudomonas putida, Penicillium bilaii*	CoastBio/ USA	Coast Bio (2025)
Fosfotal	*Rhizobium pusense* (strain B02)	AGROSAVIA/ Colombia	AGROSAVIA (2025)
Bi Fosfor	*Bacillus megaterium*	Agrarius/ Poland	Agrarius (2025)
P-Sol B®-BM	*Bacillus megaterium* (MCC 0053)	Agri Life/ India	Agri Life (2025)
JumpStart®	*Penicillium bilaiae*	Novobac/ China	Novobac (2025)

The increasing scientific and commercial momentum behind PSMs highlights their potential as key components in sustainable nutrient management strategies. However, despite promising advances, their practical deployment faces both regulatory and agronomic challenges (Aloo et al., 2022).

One of the primary barriers to widespread adoption of PSMs lies in outdated regulatory and legal frameworks that were originally designed for synthetic agrochemicals. These frameworks often impose stringent requirements that are not tailored to the unique nature of biological products, thereby delaying registration and market entry. Fortunately, this scenario is gradually changing. Regulatory authorities, particularly in regions such as Europe, are recognizing the importance of alternative fertilization technologies and are working to amend current regulations to accommodate microbial inputs (Aloo et al., 2022; European Parliament and Council of the European

Union, 2019). Such efforts are expected to support the development and dissemination of sustainable agricultural inputs.

Brazil, one of the world's leading agricultural producers, has emerged as a prominent example of regulatory modernization in support of biological inputs. The country has revised its legal framework to accelerate the registration and commercialization of microbial inoculants and biofertilizers (Soares et al. 2023). According Brazilian legislation, inoculants are products containing microorganisms that have a favorable impact on plant growth (MAPA, 2020A), while biofertilizers are products containing organic substances, microorganisms or both, with the main function of providing nutrients to plants or improving the physical, chemical or biological characteristics of the soil (MAPA, 2020b). In the current moment, only for pest control, there are 629 biological products registered in Brazil (FAPESP, 2024). In 2011, this number was 26 (AgroPages, 2023).

This progress is the result of coordinated efforts among public institutions, private enterprises, and research bodies, which have collectively established standardized procedures to ensure product quality and efficacy throughout the production and commercialization pipeline. Given the rapid pace of innovation in microbial technologies, regulatory systems are expected to remain dynamic and adaptive (Soares et al. 2023).

Beyond the regulatory landscape, technical challenges in field application continue to constrain the performance of PSMs. The efficacy of these inoculants is strongly influenced by environmental variables such as soil pH, texture, organic matter content, native microbiota, climatic conditions, and the plant species involved (Lopes et al., 2021). While many formulations demonstrate strong potential under laboratory or greenhouse conditions, their performance in the field is often less consistent. One major obstacle is the ability of inoculated strains to establish and compete in complex soil microbial communities (Aloo et al., 2022). Furthermore, the economic competitiveness of PSM-based products depends not only on their biological performance but also on the overall upstream and downstream operational costs, encompassing production, formulation, distribution, application, and field effectiveness.

To overcome these limitations, various strategies have been explored. These include the use of protective carriers, encapsulation techniques, co-formulation with supportive additives, and the selection of strains with demonstrated adaptability to

specific environmental conditions (Brondi et al., 2022; Velloso et al., 2024; Lopes et al., 2024). Continued research into these approaches is essential to improve the reliability and resilience of PSM-based products under real-world agricultural conditions.

Despite advances in strategies to protect microorganisms and enhance their efficiency in soil environments, the successful application of PSMs in agriculture also relies on the development of efficient, scalable, and economical cultivation methods.

2.2.3. Production methods

The cultivation of PSMs can be achieved basically through two fermentation process: solid-state fermentation (SSF) and submerged fermentation (SmF). Each method presents distinct advantages and limitations, and the choice between them typically depends on the characteristics of the target microorganism, the desired bioproduct, and the overall production process. Factors such as the cultivation mode, downstream processing, and scalability must be carefully evaluated (Vassileva et al., 2021).

In SSF, microorganisms grow on a solid support without the availability of free-flowing water. This approach offers several benefits, including the use of low-cost and environmentally friendly materials as substrates, such as agro-industrial residues, as well as reduced consumption of water and energy (Pandey, 2003). Moreover, SSF can provide a growth environment that more closely mimics natural microbial habitats, which can enhance biomass quality and the production of specific metabolites (Farinas, 2015). However, challenges related to downstream processing, large-scale operation, and process control remain significant barriers to industrial implementation (Bagga et al., 2024).

In contrast, SmF involves microbial cultivation in liquid media and is the dominant method used in industrial bioprocesses. Its widespread adoption is attributed to advantages related to instrumentation and control (monitoring of pH, dissolved oxygen, temperature, concentration of water-soluble molecules), separation of biomass after fermentation, mixing, aeration and scale-up. SmF allows the use of different types of bioreactors and cultivation modes (batch, fed-batch, or continuous), enabling the creation of tailored environments for microbial growth (Farinas, 2015).

Typically, SmF is preferred for the cultivation of bacterial strains, while SSF is generally more suitable for fungal cultivation. Interestingly, fungal species may hold

particular importance in phosphate solubilization in soil ecosystems, as they often demonstrate greater mobility through soil matrices and higher production of organic acids compared to bacteria (Sharma et al., 2013).

Considering the sustainability advantages of SSF and the growing need for environmentally conscious production methods, the following section (2.3) explores in greater detail the fundamentals, bioreactor designs, and specific applications of solid-state fermentation for the cultivation of PSMs.

2.3. Solid-state fermentation

2.3.1. General concepts

According to Mitchell et al. (2006), SSF is the cultivation of microorganisms on moist solid particles, where the amount of water is sufficient to support microbial growth and metabolism, but does not exceed the water retention capacity of the porous solid matrix. The space between the particles contains a continuous gaseous phase, usually saturated with water to maintain adequate moisture content.

The solid matrix can be either inert or biodegradable: in the first case, it serves solely as a physical support impregnated with nutrients; in the second, it acts both as support and as the main carbon and energy source for microbial growth (Pandey, 2003). Agro-industrial residues are frequently used as substrates in SSF, contributing not only to sustainability but also to a significant reduction of bioprocess costs - up to 25 - 50% according to Sathya et al. (2009). Considering that approximately 998 million tons of agricultural residues are produced annually worldwide, including rice and wheat straw, corn stover and a number of other economic crop leftovers (Yu et al., 2021), SSF represents a promising strategy for valorizing these materials (Mattedi et al., 2023).

To optimize microbial development, it is common to humidify the solid substrates with pH-adjusted nutrient solutions that correct nutrient deficiencies and adjust the initial moisture content (Rodrigues et al., 2022; Casciatori et al., 2024). Sequestering agents can also be added to remove metal ions that may negatively affect bioprocess yields (Pandey, 2003).

The properties of solid substrates - such as surface area, particle size, crystallinity, and porosity - are crucial in SSF, in addition to chemical composition (Soccol et al., 2017). Among these, porosity is particularly critical. An optimal porous matrix ensures effective transmission of respiratory gases and efficient removal of

metabolic heat. Casciatori et al. (2024) performed SSF in a packed-bed bioreactor with different filamentous fungi, investigating how particle shape, size, bed porosity, and packing density affected enzyme yields and thermal conditions. They reported that lower packing densities, with higher proportions of sugarcane bagasse fibers, led to temperature increases of less than 1°C. In contrast, higher packing densities using sugarcane bagasse powder or wheat bran resulted in temperature rises of 7 - 16°C, leading to lower enzymatic activities. These findings highlight the importance of strategically designing the porous media composition and packing technique for successful scale-up.

Moisture content is another critical factor in SSF. The ideal moisture level depends on the specific combination of substrate and microorganism and must be individually optimized. For example, the optimal moisture content for maximum P solubilization from an orange peel–rock phosphate system by *Aspergillus awamori* was found to be 75% (Gaind, 2017). For *Metarhizium anisopliae* spore production, ideal moisture contents varied between 22% and 75%, depending on the cereal substrate used (Sala et al., 2019; Šelo et al., 2021). Excessively high moisture can fill the matrix's pore spaces, promoting bed compaction, restricting gas diffusion, and impairing heat transfer. Porosity decreases with increasing humidity, a factor that must be considered due to its impact on heat and mass transfer (Casciatori et al., 2014). On the other hand, low moisture availability can hinder nutrient transport and absorption and compromise the stability of biological structures such as proteins and carbohydrates (Farinas, 2015).

While humidity and temperature control at laboratory scale is relatively simple, SSF presents significant challenges at pilot and industrial scales (Perez et al., 2019). Unlike SmF, where the culture medium is considered homogeneous and microbial growth is primarily limited by oxygen transfer at the gas-liquid interface, SSF is highly heterogeneous. Growth may be limited by the transfer of heat, oxygen, nutrients, metabolites, and water, in addition to fermentation stage and bioreactor design and operation (Casciatori et al., 2016).

Despite these challenges, SSF remains the predominant method for fungal spore production, as it enables high yields due to cultivation conditions that closely resemble the natural habitat of these microorganisms. It also is less susceptible to bacterial contamination and substrate inhibition, promotes higher final product concentrations, and allows the direct use of agro-industrial wastes in their natural form. SSF generates

minimal wastewater and supports sustainable solid waste management, aligning with circular economy principles (Singhania et al., 2009). A notable advantage of current SSF systems is the possibility of using the culture substrates themselves in the formulation of inoculants, serving as physical supports or carriers and thereby facilitating the formulation process (Vassileva et al., 2021). In addition to filamentous fungi, SSF can also support the growth of certain bacteria - including *Bacillus* spp. and *Streptomyces* spp. (Sukumaran et al., 2009; Olanrewaju et al., 2019) - and has demonstrated superior enzymatic productivity due to the enhanced transcription of biosynthetic genes. The enzymes produced tend to be more stable across pH and temperature variations and are less susceptible to substrate inhibition (Farinas, 2015).

Despite these challenges, SSF remains the predominant method for fungal spore production, as it enables high yields due to cultivation conditions that closely resemble the natural habitat of these microorganisms. Additionally, SSF requires less energy for sterilization, is less susceptible to bacterial contamination and substrate inhibition, promotes higher final product concentrations, and facilitates the direct use of agro-industrial wastes in their natural form. It also generates less wastewater and contributes to more sustainable solid waste management, aligning with the principles of the circular economy (Singhania et al., 2009).

Currently, due to the challenges associated with metabolic heat removal and the formation of gradients in temperature, moisture, and metabolite concentrations, industrial SSF is typically conducted by growing fungi on moistened cereal grains kept in plastic bags or trays under controlled environmental conditions. However, there is a linear increase in the number of publications over time, which is still growing, both for scientific research papers and deposed patent documents, reflecting the growing interest in this technology. The following section will explore the main bioreactor configurations developed to advance SSF processes (Vandenberghe et al., 2021).

2.3.2. Bioreactors for solid-state fermentation

At the lab scale, SSF processes are usually conducted using a few grams of solid matrix in Erlenmeyer flasks, plastic bags, or Raimbault columns. At this stage, optimal conditions - such as pH, temperature, inoculum size, substrates, cultivation time, and necessary additives - are typically determined, and gradients of temperature, moisture, and metabolites are generally not observed. However, at bench, pilot and industrial

scales, appropriate bioreactors are necessary to ensure the best possible yields (Mattedi et al., 2023).

Various SSF bioreactor models have been developed and are classified based on the type of mixing system employed: stirred bioreactors or static bioreactors (Arora et al., 2018). Fig. 2.5 illustrates the main types. The rotating drum bioreactor is an example of a moving bed system, where movement can be achieved either by rotating the wall (Fig. 2.5a) or by rotating an internal shaft equipped with blades (Fig. 2.5b**).** These bioreactors may also include an inlet for water spraying (Grajales et al., 2025).

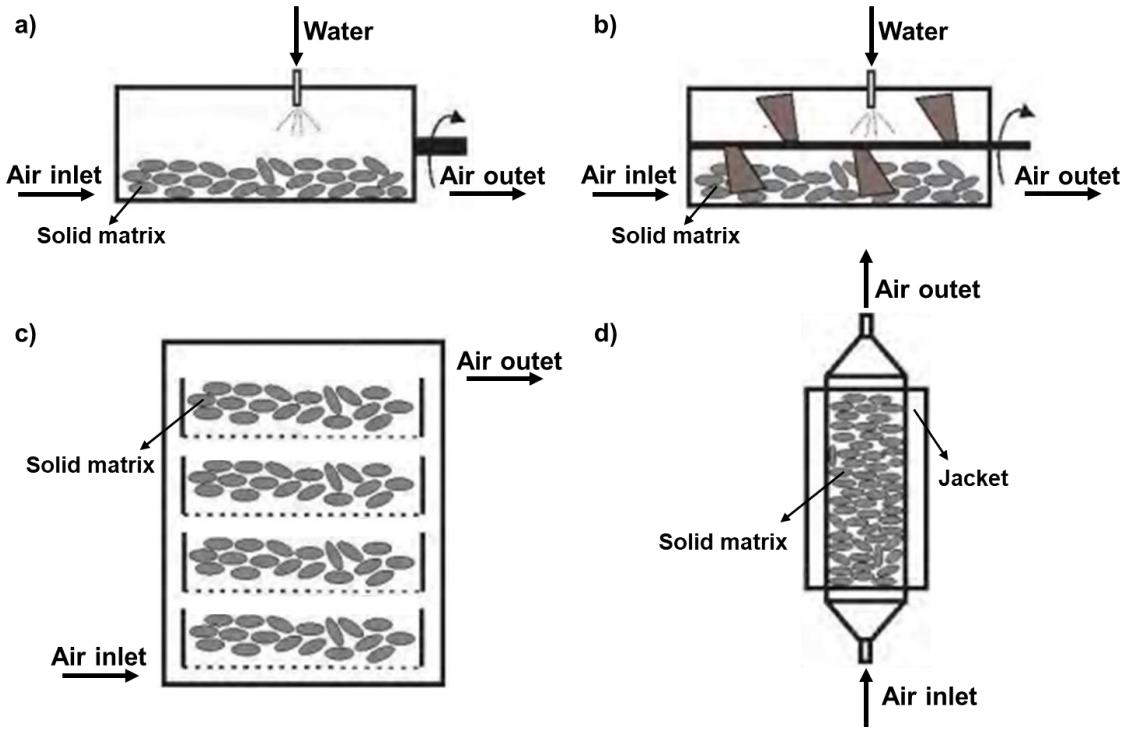

Fig. 2.5. Schematic representation of the main bioreactors for solid-state fermentation: a) rotating drum bioreactor; b) stirred drum bioreactor; c) tray bioreactor; and d) packed-bed bioreactor. Image extracted and adapted from Casciatori (2015).

Saithi and Tongta (2016) investigated the growth of *Aspergillus niger* and its phytase production in a 600 L rotating drum bioreactor. They reported a production of 580 U per gram of dry mass, approximately half the value obtained in Erlenmeyer flasks. The reduction in production was mainly attributed to difficulties in controlling temperature rise, which increased by 12°C above the optimum. In contrast, Grajales et al. (2025) evaluated cellulase production by *Myceliophthora thermophila* in a 42 L

rotating drum bioreactor and were able to successfully control the temperature, mainly by employing water spraying during cultivation. As a result, the enzymatic activity obtained was comparable to that achieved under static conditions using plastic bags containing 5 g of substrate. However, agitation can also have detrimental effects depending on the combination of substrates and microorganisms. Cassaro et al. (2015) reported losses in the production of endoglucanase, glucosidase, and xylanase during the fermentation of wheat bran by *A. niger* due to agitation.

Fixed bed bioreactors are another option, particularly suitable for microorganisms sensitive to agitation. Examples include tray bioreactors (Fig. 2.5**c**), which may or may not have a perforated bottom, and packed-bed bioreactors (Fig. 2.5d**),** which may or may not feature a jacketed wall. Tray bioreactors have a relatively simple design, but at industrial scales, they require large physical areas and intensive labor, as the trays must be placed in air-conditioned chambers for temperature and humidity control. Moreover, since they are not closed systems, they are more susceptible to contamination (Arora et al., 2018).

Packed-bed bioreactors (PBBs), in contrast, have a closed structure, occupy less space, and are less prone to contamination. Sala et al. (2022) conducted a comparative study between a 22 L packed-bed bioreactor and a 43.5 L tray bioreactor for the production of *Beauveria bassiana* and *Trichoderma harzianum* conidia using rice husk or beer draff supplemented with wood chips. They reported that volumetric production (total conidia produced per liter) was 2 - 10 times higher in all cultivations conducted in the PBB, highlighting the more efficient use of space of this type of equipment.

However, the thicker bed layers of PBBs can lead to significant axial temperature gradients and, consequently, humidity gradients. Even when the percolating air is saturated upon entering the bioreactor bed, the increase in temperature during fermentation may cause it to fall below saturation, enabling the air to remove water from the solid matrix. Agro-industrial residues typically have low thermal conductivity, and the low airflow rates needed to avoid bed drying further reduce both static and dynamic effective thermal conductivities, complicating heat removal (Casciatori et al., 2018). As a result, even radial temperature gradients can occur, particularly in large-diameter bioreactors where the jacket effectively controls temperature only near the walls (Casciatori et al., 2016).

Nevertheless, given the advantages of PBBs - including their closed structure, smaller footprint, and the ability to accommodate microorganisms sensitive to agitation - several improvements have been proposed over time to address these challenges and facilitate their industrial application. The most recent strategies developed for this purpose are discussed in the Section 2.3.2.1**.**

2.3.2.1. Recent advances in packed-bed bioreactors

To overcome the limitations associated with PBBs and enhance their scalability, several innovative strategies have been developed in recent years. Shahryari et al. (2020) designed a bioreactor named the *trickle bed bioreactor* (Fig. 2.6) and tested it for phytase production by *Aspergillus ficuum* using wheat straw as substrate. In this system, a perforated helical bed acts as a support for the substrate. The rotation of the bed inside a baffled column promotes gentle mixing and helps to separate agglomerated substrate particles. During fermentation, water is dripped over the bed to partially remove heat and soluble metabolites. After three days of incubation, water was recycled at a flow rate of 195 mL min^{-1} for one minute per day. The helical bed was occasionally rotated to further prevent substrate compaction and improve the distribution of both liquid and air. Compared to a conventional PBB operated in parallel, the trickle bed bioreactor achieved 54.95% higher phytase production and significantly lower temperature increases. However, the system tested had a relatively small scale (10 cm diameter × 30 cm height), and its scalability to larger dimensions remains to be evaluated.

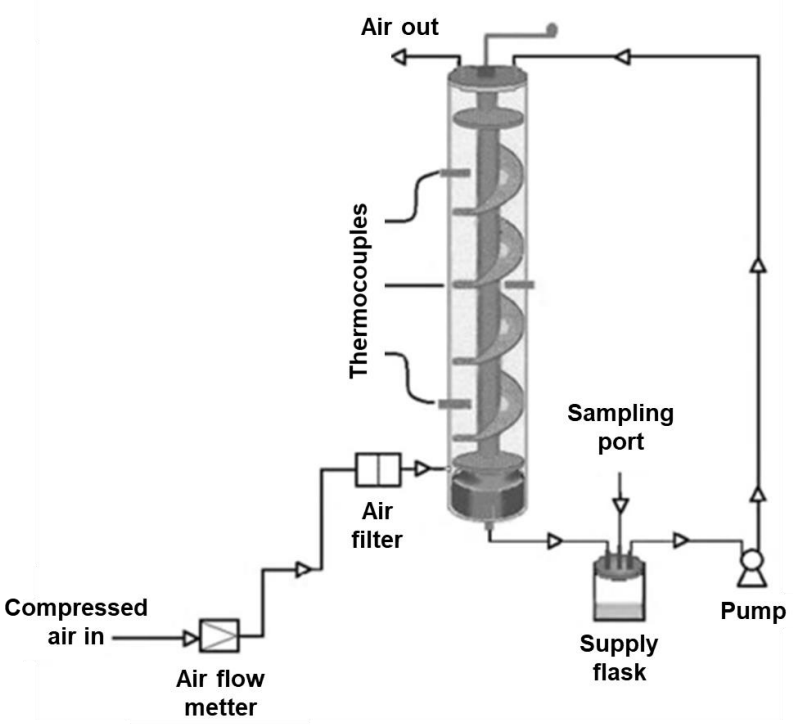

Fig. 2.6. Trickle bed bioreactor proposed by Shahryari et al. (2020). Image extracted and adapted from Shahryari et al. (2020).

Perez et al. (2021) investigated different air injection strategies in a multilayer PBB - an approach initially proposed by Lu et al. (1998) to mitigate compaction problems. Two configurations were tested: splitting the air flow into two equal parts, injected separately at the bottom and at the midsection of the column (Fig. 2.7a), and injecting air through a perforated tube positioned longitudinally at the center of the column (Fig. 2.7b). Their results showed that neither strategy significantly affected overheating, as the thermal profiles were similar to those observed with conventional bottom-only aeration. However, the radial air injection strategy promoted a slight improvement in enzyme production, likely due to more uniform air distribution and better O_2 availability across the bed.

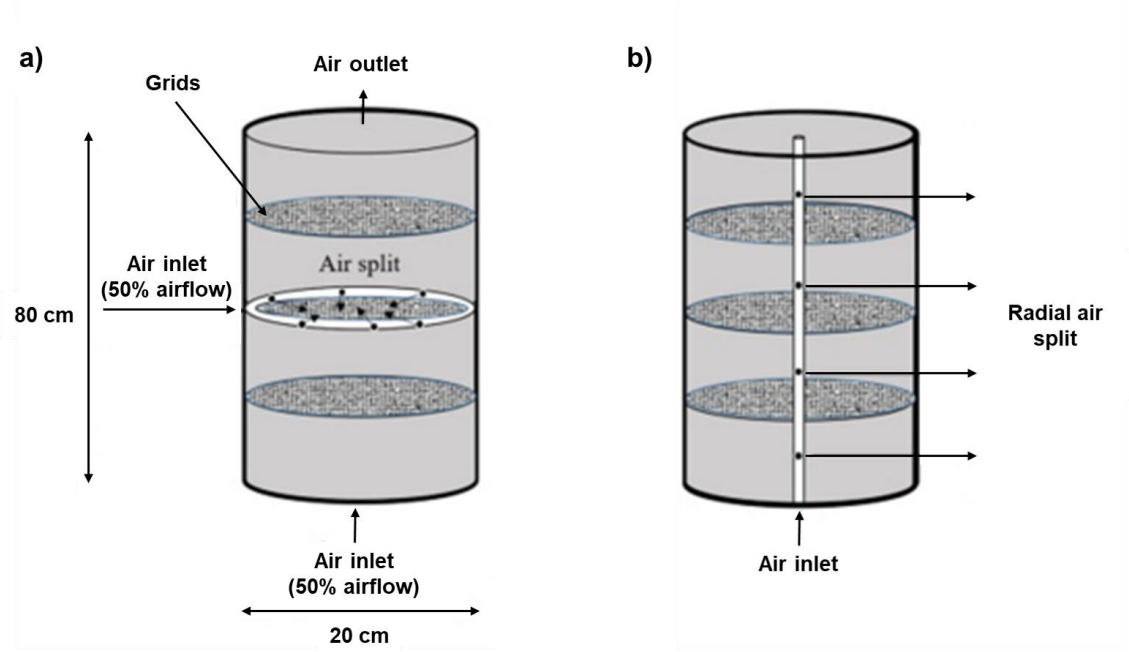

Fig. 2.7. Schematic representations of two air injection strategies in a packed-bed bioreactor: (a) 50% air injected at the bottom and 50% at the midsection (by walls); (b) injection via a longitudinally perforated tube (by the center). Image extracted and adapted from Perez et al. (2021).

Beyond structural innovations, different operating modes for multilayer PBBs have also been explored. Inspired by the modeling and simulation work of Mitchell et al. (2010), Rodrigues et al. (2022) evaluated cyclic and continuous operations in addition to the traditional batch mode. In the cyclic batch mode, the bed layers were repositioned once per day (Fig. 2.8a), whereas in the continuous mode, fresh inoculated layers were added daily at the bottom of the bioreactor and fully fermented layers were simultaneously removed from the top, maintaining a constant bed height once steady state was achieved (Fig. 2.8b). The authors reported that under continuous operation, maximum CO_2 concentrations were 60% lower than under batch mode, suggesting better gas exchange and lower heat accumulation. This strategy offers promising potential to support continuous SSF processes, minimizing heat buildup, improving O_2 availability, and reducing heterogeneity.

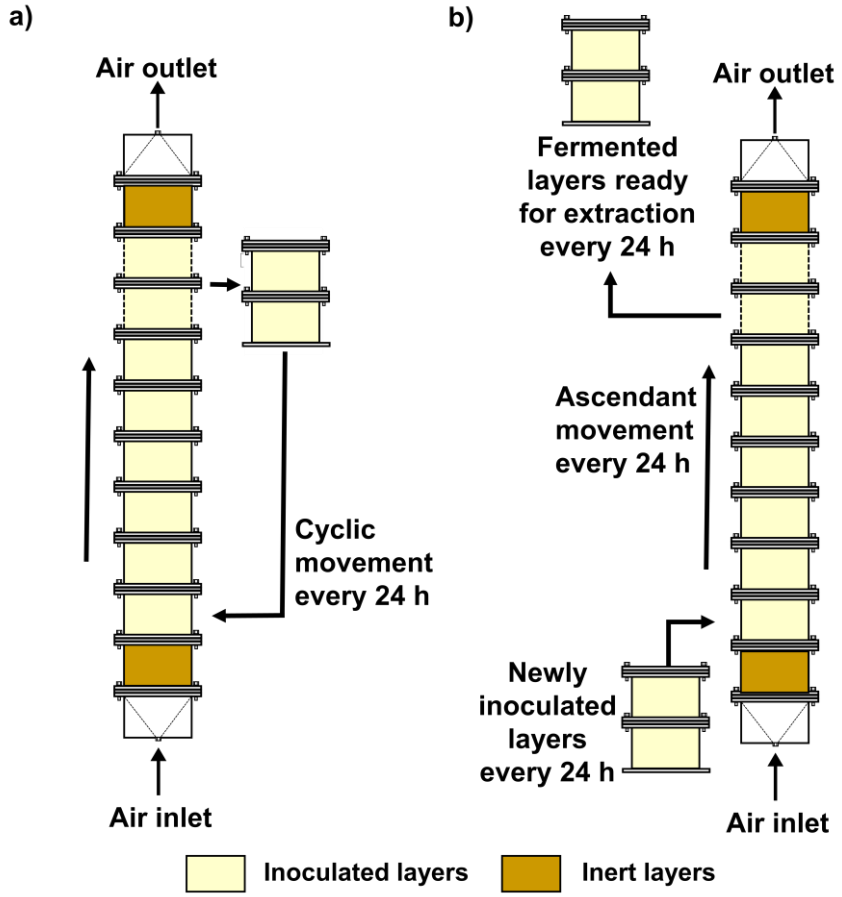

Fig. 2.8. Representation of multilayer packed-bed bioreactor operation modes: (a) cyclic and (b) continuous operations. Image extracted and adapted from Rodrigues et al. (2022).

In addition to changes in bioreactor design and operation, increasing bed porosity has also been proven effective in improving SSF performance in PBBs. Sala et al. (2022) used 60% wood chips as a bulking agent in a 22 L PBB and reported no overheating issues. Similarly, Rodrigues et al. (2022) observed a maximum temperature increase of only 3°C across all operation modes evaluated, using a substrate bed composed of 70% sugarcane bagasse, which ensured high porosity and enhanced airflow.

2.3.3. SSF-based strategies for the development of phosphate bioinputs

SSF process can contribute to improving P availability in soils through the production of PSMs and their associated metabolites. Depending on the desired

application, the process can be optimized to favor the production of microbial biomass, specific metabolites - such as phosphatases, cellulases, IAA, siderophores, organic acids - or both (Mattedi et al., 2023; Rocha et al., 2024).

The most established application of SSF in the bioinput industry is the large-scale production of spores from biocontrol agents, particularly fungi from the genus *Trichoderma*, commonly cultivated on rice-based substrates (Mascarin et al., 2019). However, in research contexts, several studies have demonstrated that not only various *Trichoderma* species but also other fungi and even bacteria - such as *Bacillus thuringiensis*, *Bacillus subtilis*, and *Bacillus amyloliquefaciens* - can grow and sporulate under SSF using alternative substrates like rice husk, wheat straw, soybean meal, wheat bran, and beer draff (Mattedi et al., 2023).

Although these genera are widely recognized for their entomopathogenic and phytopathogenic effects, certain strains also possess the potential to act as phosphate biofertilizers, reinforcing the idea that agricultural bioinputs can exhibit multiple beneficial modes of action. For instance, Sauka et al. (2021) showed that a *Bacillus thuringiensis* strain isolated from soil in Corrientes, Argentina, exhibited insecticidal activity against *Lepidoptera* and *Diptera* larvae, as well as the ability to solubilize hydroxyapatite, Patagonian phosphate rock, and, to a lesser extent, aluminum phosphate. Likewise, Ghoreishi et al. (2023) cultivated *Trichoderma harzianum* on grass clippings and pruning residues by SSF and demonstrated that optimizing parameters such as moisture content, temperature, and tryptophan supplementation significantly enhanced the recovery of IAA and spores.

Substrate composition in SSF strongly influences the type and yield of microbial products. Prado et al. (2019) evaluated several strains of *Aspergillus*, *Trichoderma*, and *Bacillus* for their ability to produce IAA and its derivatives, as well as phytases, via SSF, and attempted to correlate product yields with substrate characteristics. According to the authors, all genera produced the evaluated compounds when 1% tryptophan was added. However, for *Bacillus* and *Trichoderma*, a negative correlation was observed between IAA production and the lignin content of the substrates. The highest levels of indole derivatives and phytase activity were observed in combinations such as wheat bran with *B. subtilis*, and maize distillers' dried grains with solubles (DDGS) with *T. atroviride*, respectively.

Beyond spore and metabolite production, SSF has also been used to evaluate the solubilization of insoluble P sources in vitro systems. Mendes et al. (2015) investigated the solubilization of phosphate rock from Araxá, Brazil, by SSF using sugarcane bagasse and sucrose as substrates, *Aspergillus niger* as the inoculum, and biochar to mitigate the rock's potentially harmful effects. Following process optimization, the authors achieved 9.43 mg of soluble P per gram of bagasse. Application of the incinerated fermented material to common bean cultivation significantly enhanced both plant growth and P uptake.

In addition to natural phosphate rocks, other renewable P sources can also be used in SSF, aligning with circular economy principles and the goals of sustainable agriculture. Raymond et al. (2018) explored the potential of various phosphorus-rich sewage sludge biochars and ashes to serve as substrates and P sources for the phosphate-solubilizing fungus *Penicillium bilaiae*. The amount of soluble P increased significantly under high-glucose conditions, with the greatest relative increase observed for incineration ash (>100-fold after 10 days). These findings underscore the potential of using PSMs to recover P from thermally treated sewage sludge; however, further studies are needed to evaluate the process at larger scales and to assess its performance in soil–plant systems.

2.4. Conclusions

PSMs are promising tools for sustainable agriculture, promoting biological P cycling, reducing reliance on synthetic fertilizers, and minimizing environmental impacts such as eutrophication and resource depletion. Their integration into regenerative farming systems could play a key role in addressing global food security challenges. In this context, SSF presents a valuable strategy for developing phosphate bioinputs, allowing the production of PSM biomass, beneficial metabolites (e.g., IAA, phytases, organic acids), and soluble P. However, large-scale application faces significant challenges, mainly due to the difficulty of obtaining appropriate equipment for scale-up.

Limitations also include the reduced persistence of PSMs in soil due to microbial competition and abiotic stressors, along with the need for technical support for field application. Moreover, many farmers remain unaware of PSM benefits, and current distribution networks are often insufficient to ensure timely access, especially in

remote areas. Overcoming these barriers requires coordinated efforts in research, policy support, education, and infrastructure development. Expanding farmer awareness, improving availability, and reducing production costs will be essential to increase adoption and fully realize the potential of PSMs as biofertilizers in sustainable agriculture.

References

Agrarius, 2025. Bi-Fosfor 2 – Fertilizer microbial product. https://agrarius.eu/en/our-solutions/fertilizer-microbial-products/bi-fosfor-2/ (accessed 21 April 2025).

AgroPages, 2023. Brazil registers 616 new biological products in 2023, totaling 567 active ingredients. https://news.agropages.com/News/NewsDetail---49574.htm (accessed 29 April 2025).

AGROSAVIA, 2025. Fosfotal - Biofertilizante solubilizador de fosfato. https://www.agrosavia.co/productos-y-servicios/oferta-tecnol%C3%B3gica/l%C3%ADnea-agr%C3%ADcola/cultivos-transitorios-y-agroindustriales/bioproductos/768-fosfotal-biofertilizante-solubilizador-de-fosfato (accessed 21 April 2025).

Aloo, B.N., Tripathi, V., Makumba, B.A., Mbega, E.R., 2022. Plant growth-promoting rhizobacterial biofertilizers for crop production: The past, present, and future. Front. Plant Sci. 13, 1002448.

Alori, E.T., Glick, B.R., Babalola, O.O., 2017. Microbial phosphorus solubilization and its potential for use in sustainable agriculture. Front. Microbiol. 8, 971.

Andelkovic, I.B., Kabiri, S., Tavakkoli, E., Kirby, J.K., McLaughlin, M.J., Losic, D., 2018. Graphene oxide-Fe(III) composite containing phosphate—A novel slow release fertilizer for improved agriculture management. J. Clean. Prod. 185, 97–104.

Arora, S., Rani, R., Ghosh, S., 2018. Bioreactors in solid state fermentation technology: Design, applications and engineering aspects. J. Biotechnol. 269, 16–34.

Assaha, D.V.M., Ueda, A., Saneoka, H., Al-Yahyai, R., Yaish, M.W., 2017. The role of Na+ and K+ transporters in salt stress adaptation in glycophytes. Front. Physiol. 8, 509.

Bagga, D., Chauhan, S., Bhavanam, A., GN, N., Meena, S.S., Mohanty, A., 2024. Recent advancements in fermentation strategies for mass production and formulation of biofertilizers: Towards waste valorization. J. Soil Sci. Plant Nutr. 24(3), 5868–5897.

Bechtaoui, N., Rabiu, M.K., Raklami, A., Oufdou, K., Hafidi, M., Jemo, M., 2021. Phosphate-dependent regulation of growth and stresses management in plants. Front. Plant Sci. 12, 679916.

Bertau, M., Wellmer, F.W., Scholz, R.W., Mew, M., Zenk, L., Aubel, I., Steiner, G., 2025. The future of phosphoric acid production – Why we have to leave trodden paths. ChemSusChem 18(3), e202401155.

Bioma, 2025. Produtos Bioma. https://bioma.ind.br/ (accessed 21 April 2025).

Bisson, C., Adams, N.B., Stevenson, B., Brindley, A.A., Polyviou, D., Bibby, T.S., Hitchcock, A., 2017. The molecular basis of phosphite and hypophosphite recognition by ABC-transporters. Nat. Commun. 8, 1746.

Bononi, L., Chiaramonte, J.B., Pansa, C.C., Moitinho, M.A., Melo, I.S., 2020. Phosphorus-solubilizing *Trichoderma* spp. from Amazon soils improve soybean plant growth. Sci. Rep. 10, 1–13.

Brady, N.C., Weil, R.R., 2008. The soils around us. The nature and properties of soils, 14th ed. Pearson Prentice Hall, Upper Saddle River, NJ, USA, 1–31.

Brondi, M., Florencio, C., Mattoso, L., Ribeiro, C., Farinas, C., 2022. Encapsulation of *Trichoderma harzianum* with nanocellulose/carboxymethyl cellulose nanocomposite. Carbohydr. Polym. 295, 119876.

Browne, P., Rice, O., Miller, S.H., Burke, J., Dowling, D.N., Morrissey, J.P., O'Gara, F., 2009. Superior inorganic phosphate solubilization is linked to phylogeny in the *Pseudomonas fluorescens* complex. Appl. Soil Ecol. 43, 131–138.

Campos, M., Antonangelo, J.A., Alleoni, L.R.F., 2016. Phosphorus sorption index in humid tropical soils. Soil Tillage Res. 156, 110–118.

Cardoso Filho, J.A., 2021. Microbial solubilizers of rock-forming minerals: Opportunities and challenges. Agri-Based Bioeconomy, 179–218.

Carmo, T.S., Moreira, F.S., Cabral, B.V., Dantas, R.C., de Resende, M.M., Cardoso, V.L., Ribeiro, E.J., 2019. Phosphorus recovery from phosphate rocks using phosphate-solubilizing bacteria. Geomicrobiol. J. 36, 195–203.

Casciatori, F.P., 2015. Produção de celulases fúngicas por fermentação em estado sólido: ampliação de escala de biorreatores de leito fixo. PhD thesis, Universidade Estadual Paulista (UNESP), Brazil.

Casciatori, F.P., Bück, A., Thoméo, J.C., Tsotsas, E., 2016. Two-phase and two-dimensional model describing heat and water transfer during solid-state fermentation within a packed-bed bioreactor. Chem. Eng. J. 287, 103–116.

Casciatori, F.P., Laurentino, C.L., Taboga, S.R., Casciatori, P.A., Thoméo, J.C., 2014. Structural properties of beds packed with agro-industrial solid by-products applicable for solid-state fermentation: Experimental data and effects on process performance. Chem. Eng. J. 255, 214–224.

Casciatori, F.P., Mafra, N.S.C., Rodrigues, N.A., Sales, E.H., Maia, M.M.S., Dias, A.C.P., Grajales, L.M., 2024. Flow configuration and packing density of sugarcane bagasse and wheat bran affecting enzymes production by solid-state fermentation. Bioenergy Res. 17(1), 187–197.

Casciatori, F.P., Thoméo, J.C., 2018. Heat transfer in packed-beds of agricultural waste with low rates of air flow applicable to solid-state fermentation. Chem. Eng. Sci. 188, 97–111.

Cassaro, E.G., Fonseca, R.F., Farinas, C.S., 2015. Assessment of the effects of intermittent mixing on solid-state fermentation for biomass-degrading enzymes production by different fungal strains.

Chawngthu, L., Hnamte, R., Lalfakzuala, R., 2020. Isolation and characterization of rhizospheric phosphate solubilizing bacteria from wetland paddy field of Mizoram, India. Geomicrobiol. J. 37, 366–375.

Chen, X., Ren, H., Zhang, J., Zhao, B., Ren, B., Wan, Y., Liu, P., 2024. Deep phosphorus fertilizer placement increases maize productivity by improving root-shoot coordination and photosynthetic performance. Soil Tillage Res. 235, 105915.

Chen, Y.P., Rekha, P.D., Arun, A.B., Shen, F.T., Lai, W.A., Young, C.C., 2006. Phosphate solubilizing bacteria from subtropical soil and their tricalcium phosphate solubilizing abilities. Appl. Soil Ecol. 34, 33–41.

Chernysh, Y., Yakhnenko, O., Chubur, V., Roubík, H., 2021. Phosphogypsum recycling: A review of environmental issues, current trends, and prospects. Appl. Sci. 11(4), 1575.

Coast Bio, 2025. Phosphorus Solubilizing Bacteria Blend – BioPhos. https://coastbio.com/products/phosphorus-solubilizing-bacteria-blend-biophos/ (accessed 21 April 2025).

Reis, G.A., Martínez-Burgos, W.J., Pozzan, R., Pastrana Puche, Y., Ocán-Torres, D., de Queiroz Fonseca Mota, P., Soccol, C.R., 2024. Comprehensive review of microbial inoculants: Agricultural applications, technology trends in patents, and regulatory frameworks. Sustainability 16(19), 8720.

European Parliament and Council of the European Union, 2019. Regulation (EU) 2019/1009 of the European Parliament and of the Council of 5 June 2019 laying down rules on the making available on the market of EU fertilising products and amending Regulations (EC) No 1069/2009 and (EC) No 1107/2009 and repealing Regulation (EC) No 2003/2003. Off. J. Eur. Union L170, 1–114. https://eur-lex.europa.eu/eli/reg/2019/1009/oj

Fahad, S., Bajwa, A.A., Nazir, U., Anjum, S.A., Farooq, A., Zohaib, A., et al., 2017. Crop production under drought and heat stress: Plant responses and management options. Front. Plant Sci. 8, 1147.

FAO. Food and Agriculture Organization of the United Nations, 2025. FAOSTAT. Database. Available from: https://www.fao.org/faostat/en/#data/RFN (accessed 25 April 2025).

FAPESP, 2024. Registration of biological pest control products exceeds that of agrochemicals in Brazil. ODS FAPESP. https://ods.fapesp.br/registration-of-biological-pest-control-products-exceeds-that-of-agrochemicals-in-brazil/10600 (accessed 25 April 2025).

Farinas, C.S., 2015. Developments in solid-state fermentation for the production of biomass-degrading enzymes for the bioenergy sector. Renew. Sustain. Energy Rev. 52, 179–188.

Ferreira, C.M., Vilas-Boas, A., Sousa, C.A., Soares, H.M., Soares, E.V., 2019. Comparison of five bacterial strains producing siderophores with ability to chelate iron under alkaline conditions. AMB Express 9, 1–12.

Gaind, S., 2017. Exploitation of orange peel for fungal solubilization of rock phosphate by solid-state fermentation. Waste Biomass Valor. 8, 1351–1360.

Grajales, L.M., Wang, H., Casciatori, F.P., Thoméo, J.C., 2025. Intensified rotary drum bioreactor for cellulase production from agro-industrial residues by solid-state cultivation. Chem. Eng. Process. Process Intensif. 110223.

Guelfi, D., Nunes, A.P.P., Sarkis, L.F., Oliveira, D.P., 2022. Innovative phosphate fertilizer technologies to improve phosphorus use efficiency in agriculture. Sustainability 14(21), 14266.

Gulati, A., Sharma, N., Vyas, P., Sood, S., Rahi, P., Pathania, V., Prasad, R., 2010. Organic acid production and plant growth promotion as a function of phosphate solubilization by *Acinetobacter rhizosphaerae* strain BIHB 723 isolated from the cold deserts of the trans-Himalayas. Arch. Microbiol. 192, 975–983.

Hansel, F.D., Amado, T.J.C., Ruiz Diaz, D.A., Rosso, L.H.M., Nicoloso, F.T., Schorr, M., 2017. Phosphorus fertilizer placement and tillage affect soybean root growth and drought tolerance. Agron. J. 109, 2936–2944.

Helfenstein, J., Tamburini, F., von Sperber, C., Massey, M.S., Pistocchi, C., Chadwick, O.A., Frossard, E., 2018. Combining spectroscopic and isotopic techniques gives a dynamic view of phosphorus cycling in soil. Nat. Commun. 9, 312–320.

Hussain, A., Adnan, M., Iqbal, S., Fahad, S., Saeed, M., Mian, I.A., Muhammad, M.W., Romman, M., Perveez, R., Wahid, F., Subhan, F., 2019. Combining phosphorus (P) with phosphate solubilizing bacteria (PSB) improved wheat yield and P uptake in alkaline soil. Pure Appl. Biol. 8, 1809–1817.

Ibrahim, M., Iqbal, M., Tang, Y.T., Khan, S., Guan, D.X., Li, G., 2022. Phosphorus mobilization in plant–soil environments and inspired strategies for managing phosphorus: A review. Agronomy 12, 2539.

IFA. International Fertilizer Association, 2023. Phosphate rock resources and reserves. https://www.fertilizer.org/wp-content/uploads/2023/04/2023_Argus_IFA_Phosphate_Rock_Resources_and_Reserves_Final.pdf

Jahan, N., Mahmud, U., Khan, M.Z., 2025. Sustainable plant-soil phosphorus management in agricultural systems: Challenges, environmental impacts and innovative solutions. Discov. Soil 2, 1–8.

Kalayu, G., 2019. Phosphate solubilizing microorganisms: Promising approach as biofertilizers. Int. J. Agron. 2019, 4917256.

Kaur, H., Mir, R.A., Hussain, S.J., Prasad, B., Kumar, P., Aloo, B.N., Dubey, R.C., 2024. Prospects of phosphate solubilizing microorganisms in sustainable agriculture. World J. Microbiol. Biotechnol. 40, 291.

Khan, F., Siddique, A.B., Shabala, S., Zhou, M., Zhao, C., 2023. Phosphorus plays key roles in regulating plants' physiological responses to abiotic stresses. Plants 12, 2861.

Koilraj, P., Antonyraj, C.A., Gupta, V., Reddy, C.R.K., Kannan, S., 2013. Novel approach for selective phosphate removal using colloidal layered double hydroxide nanosheets and use of residue as fertilizer. Appl. Clay Sci. 86, 111–118.

Kruse, J., Abraham, M., Amelung, W., Baum, C., Bol, R., Kühn, O., Leinweber, P., 2015. Innovative methods in soil phosphorus research: A review. J. Plant Nutr. Soil Sci. 178, 43–88.

Leikam, D.F., Achorn, F.P., 2005. Phosphate fertilizers: Production, characteristics, and technologies. In: Sims, J.T., Sharpley, A.N. (Eds.), Phosphorus: Agriculture and the Environment, vol. 46, pp. 23–50.

Li, L., Xing, W., Ma, C., Zhang, Y., Wang, G., Yang, L., 2012. Phosphorus amendment of a lead-spiked soil with low phosphorus availability: Roles of phosphorus on soil and plant lead. Commun. Soil Sci. Plant Anal. 43, 1053–1064.

Li, Z., Bai, T., Dai, L., Wang, F., Tao, J., Meng, S., Hu, Y., Wang, S., Hu, S., 2016. A study of organic acid production in contrasts between two phosphate solubilizing fungi: Penicillium oxalicum and Aspergillus niger. Sci. Rep. 6, 25313.

Liang, Y., Li, M., Pan, F., Ma, J., Yang, Z., Ling, T., 2020. Alkaline phosphomonoesterase-harboring microorganisms mediate soil phosphorus transformation with stand age in Chinese Pinus massoniana plantations. Front. Microbiol. 11, 571209.

Lopes, M.J.S., Dias-Filho, M.B., Gurgel, E.S.C., 2021. Successful plant growth-promoting microbes: Inoculation methods and abiotic factors. Front. Sustain. Food Syst. 5, 606454.

Lopes, M.M., Lodi, L.A., Oliveira-Paiva, C.A., Farinas, C.S., 2024. Emulsion/cross-linking encapsulation of Bacillus in starch/PVA-based microparticles for agricultural applications. ACS Agric. Sci. Technol. 4, 490–499.

Loudari, A., Mayane, A., Zeroual, Y., Colinet, G., Oukarroum, A., 2022. Photosynthetic performance and nutrient uptake under salt stress: differential responses of wheat plants to contrasting phosphorus forms and rates. Front. Plant Sci. 13, 1038672.

Lu, M.Y., Maddox, I.S., Brooks, J.D., 1998. Application of a multi-layer packed-bed reactor to citric acid production in solid-state fermentation using Aspergillus niger. Process Biochem. 33, 117-123.

Luo, X., Mahdi, A.-K., Han, X.-Z., Chen, X., Yan, J., Biswas, A., Zou, W.-X., 2020. Long-term application of fertilizer and manures affect P fractions in Mollisol. Sci. Rep. 10, 14793.

Lyu, Y., Tang, H., Li, H., Zhang, F., Rengel, Z., Whalley, W.R., Shen, J., 2016. Major crop species show differential balance between root morphological and physiological responses to variable Phosphorus supply. Front. Plant Sci. 7, 1939.

Malhotra, H., Vandana, Sharma, S., Pandey, R., 2018. Phosphorus nutrition: plant growth in response to deficiency and excess. Plant Nutr. Abiotic Stress Toler. 171-190.

MAPA (Ministério da Agricultura, Pecuária e Abastecimento), 2020a. Instrução Normativa nº 13, de 24 de março de 2020. Dispõe sobre os critérios para registro de inoculantes. Diário Oficial União, Brasília, DF.

MAPA (Ministério da Agricultura, Pecuária e Abastecimento), 2020b. Instrução Normativa nº 61, de 8 de julho de 2020. Estabelece os critérios para registro de biofertilizantes. Diário Oficial União, Brasília, DF.

Mascarin, G.M., Matsumura, A.T.S., Weiler, C.A., Kobori, N.N., Silva, M.E.da, Berlitz, D.L., Matsumura, A.S., 2019. Produção industrial de Trichoderma. Embrapa.

Mattedi, A., Sabbi, E., Farda, B., Djebaili, R., Mitra, D., Ercole, C., Pellegrini, M., 2023. Solid-state fermentation: Applications and future perspectives for biostimulant and biopesticides production. Microorganisms 11, 1408.

Mendes, G.O., Dias, C.S., Silva, I.R., Junior, J.I.R., Pereira, O.L., Costa, M.D., 2013. Fungal rock phosphate solubilization using sugarcane bagasse. World J. Microbiol. Biotechnol. 29, 43-50.

Mendes, G. O., Silva, N. M. R. M., Anastácio, T. C., Vassilev, N. B., Ribeiro Jr, J. I., da Silva, I. R., Costa, M. D., 2015. Optimization of *Aspergillus niger* rock phosphate solubilization in solid-state fermentation and use of the resulting product as a P fertilizer. Microb. Biotechnol. 8, 930-939.

Meng, X., Chen, W.W., Wang, Y.Y., Huang, Z.R., Ye, X., Chen, L.S., Yang, L.T., 2021. Effects of phosphorus deficiency on the absorption of mineral nutrients, photosynthetic system performance and antioxidant metabolism in Citrus grandis. PLoS One 16, e0246944.

Mitchell, D.A., Cunha, L.E.N., Machado, A.V.L., Luz Junior, L.F.L., Krieger, N., 2010. A model-based investigation of potential advantages of multi-layer packed-beds in solid-state fermentation. Biochem. Eng. J. 48, 195-203.

Mitchell, D.A., Krieger, N., Beroviˇc, M., 2006. Solid-state fermentation bioreactors. Springer, 19.

Nacoon, S., Jogloy, S., Riddech, N., Mongkolthanaruk, W., Kuyper, T.W., Boonlue, S., 2020. Interaction between phosphate solubilizing bacteria and arbuscular mycorrhizal fungi on growth promotion and tuber inulin content of Helianthus tuberosus L. Sci. Rep. 10, 1-10.

Nesme, T., Metson, G.S., Bennett, E.M., 2018. Global phosphorus flows through agricultural trade. Glob. Environ. Chang. 50, 133-141.

Novobac, 2025. Penicillium bilaiae. https://www.novobac.com/product/penicillium-bilaiae/ (accessed 21 April 2025).

Olanrewaju, O.S., Babalola, O.O., 2019. Streptomyces: implications and interactions in plant growth promotion. Appl. Microbiol. Biotechnol. 103, 1179-1188.

Pandey, A., 2003. Solid-state fermentation. Biochem. Eng. J. 13, 81-84.

Perez, C.L., Casciatori, F.P., Thoméo, J.C., 2021. Improving enzyme production by solid-state cultivation in packed-bed bioreactors by changing bed porosity and airflow distribution. Bioprocess Biosyst. Eng. 44, 537-548.

Perez, C.L., Casciatori, F.P., Thoméo, J.C., 2019. Strategies for scaling-up packed-bed bioreactors for solid-state fermentation: The case of cellulolytic enzymes production by a thermophilic fungus. Chem. Eng. J. 361, 1142-1151.

Pierzynski, G.M., McDowell, R.W., Thomas Sims, J., 2005. Chemistry, cycling, and potential movement of inorganic phosphorus in soils. Phosphorus Agric. Environ. 46, 51-86.

Rawat, P., Das, S., Shankhdhar, D., Shankhdhar, S.C., 2021. Phosphate-solubilizing microorganisms: mechanism and their role in phosphate solubilization and uptake. J. Soil Sci. Plant Nutr. 21, 49-68.

Rfaki, A., Zennouhi, O., Aliyat, F.Z., Nassiri, L., Ibijbijen, J., 2020. Isolation, selection and characterization of root-associated rock phosphate solubilizing bacteria in moroccan wheat (Triticum aestivum L.). Geomicrobiol. J. 37, 230-241.

Richardson, A.E., Simpson, R.J., 2011. Soil microorganisms mediating phosphorus availability update on microbial phosphorus. Plant Physiol. 156, 989-996.

Rocha, T.M., Marcelino, P.R.F., Da Costa, R.A.M., Rubio-Ribeaux, D., Barbosa, F.G., da Silva, S.S., 2024. Agricultural bioinputs obtained by solid-state fermentation: From production in biorefineries to sustainable agriculture. Sustainability 16, 1076.

Rodrigues, N.A., Katayama, E.T., Casciatori, F.P., 2022. Alternative strategies to perform solid-state cultivation in a multilayer packed-bed bioreactor: Continuous and cyclic operations. Chem. Eng. J. 448, 137726.

Saithi, S., Tongta, A., 2016. Phytase production of Aspergillus niger on soybean meal by solid-state fermentation using a rotating drum bioreactor. Agric. Agric. Sci. Procedia 11, 25-30.

Sala, A., Barrena, R., Artola, A., Sánchez, A., 2019. Current developments in the production of fungal biological control agents by solid-state fermentation using organic solid waste. Crit. Rev. Environ. Sci. Technol. 49, 655-694.

Sala, A., Echegaray, T., Palomas, G., Boggione, M.J., Tubio, G., Barrena, R., Artola, A., 2022. Insights on fungal solid-state fermentation for waste valorization: Conidia and chitinase production in different reactor configurations. Sustain. Chem. Pharm. 26, 100624.

Sattari, S.Z., Bouwman, A.F., Giller, K.E., van Ittersum, M.K., 2012. Residual soil phosphorus as the missing piece in the global phosphorus crisis puzzle. Proc. Natl. Acad. Sci. U.S.A. 109, 6348-6353.

Sauka, D.H., Piccinetti, C.F., Vallejo, D.A., Onco, M.I., Pérez, M.P., Benintende, G.B., 2021. New entomopathogenic strain of Bacillus thuringiensis is able to solubilize different sources of inorganic phosphates. Appl. Soil Ecol. 160, 103839.

Šelo, G., Planinić, M., Tišma, M., Tomas, S., Koceva Komlenić, D., BucićKojić, A., 2021. A comprehensive review on valorization of agro-food industrial residues by solid-state fermentation. Foods 10, 927.

Shahryari, Z., Fazaelipoor, M.H., Shaabani, M.S., Ghasemi, Y., 2020. Production of fungal phytase in an innovative trickle bed bioreactor. Waste Biomass Valorization 11, 3273-3280.

Sharma, S.B., Sayyed, R.Z., Trivedi, M.H., Gobi, T.A., 2013. Phosphate solubilizing microbes: sustainable approach for managing phosphorus deficiency in agricultural soils. Springerplus 2, 587.

Sharpley, A., Jarvie, H.P., Buda, A., May, L., Spears, B., Kleinman, P., 2013. Phosphorus legacy: overcoming the effects of past management practices to mitigate future water quality impairment. J. Environ. Qual. 42, 1308-1326.

Shen, J., Yuan, L., Zhang, J., Li, H., Bai, Z., Chen, X., Zhang, W., Zhang, F., 2011. Phosphorus dynamics: from soil to plant. Plant Physiol. 156, 997-1005.

Sherkuziev, D., 2021. Simple superphosphate by two-stage acid treatment of phosphate raw materials. IOP Conf. Ser. Earth Environ. Sci. 939, 012057.

Silva, L.I.D., Pereira, M.C., Carvalho, A.M.X.D., Buttrós, V.H., Pasqual, M., Dória, J., 2023. Phosphorus-solubilizing microorganisms: a key to sustainable agriculture. Agriculture 13, 462.

Singal, R., Gupta, R., Saxena, R.K., 1994. Rock phosphate solubilization under alkaline conditions by Aspergillus japonicus and A. foetidus. Folia Microbiol. 39, 33-36.

Singhania, R., Kumar, A., Soccol, C.R., Pandey, A., 2009. Recent advances in solid-state fermentation. Biochem. Eng. J. 44, 13-18.

Soares, C.R.F.S., Hernández, A.G., Da Silva, E.P., De Souza, J.E.A., Bonfim, D.F., Zabot, G.L., Brunetto, G., 2023. Applications and Market of Micro-Organism-Based and Plant-Based Inputs in Brazilian Agriculture. Plants 12, 3844.

Soumare, A., Diedhiou, A.G., Thuita, M., Hafidi, M., Ouhdouch, Y., Gopalakrishnan, S., Kouisni, L., 2020. Exploiting Biological Nitrogen Fixation: A Route Towards a Sustainable Agriculture. Plants 9, 1011.

Sukumaran, R.K., Singhania, R.R., Mathew, G.M., Pandey, A., 2009. Cellulase production using biomass feed stock and its application in lignocellulose saccharification for bio-ethanol production. Renew. Energy 34, 421-424.

Tang, H., Niu, L., Wei, J., Chen, X., Chen, Y., 2019. Phosphorus limitation improved salt tolerance in maize through tissue mass density increase, osmolytes accumulation, and Na+ uptake inhibition. Front. Plant Sci. 10, 856.

Tarafdar, J., Bareja, M., Panwar, J., 2003. Efficiency of some phosphatase-producing soil fungi. Indian J. Microbiol. 43, 27-32.

Tariq, A., Pan, K., Olatunji, O.A., Graciano, C., Li, Z., Sun, F., et al., 2017. Phosphorus application improves drought tolerance of Phoebe zhennan. Front. Plant Sci. 8, 1561.

Tayibi, H., Choura, M., López, F.A., Alguacil, F.J., López-Delgado, A., 2009. Environmental impact and management of phosphogypsum. J. Environ. Manage. 90, 2377-2386.

Timofeeva, A., Galyamova, M., Sedykh, S., 2022. Prospects for using phosphate-solubilizing microorganisms as natural fertilizers in agriculture. Plants 11, 2119.

Vandenberghe, L.P., Pandey, A., Carvalho, J.C., Letti, L.A., Woiciechowski, A.L., Karp, S.G., Soccol, C.R., 2021. Solid-state fermentation technology and innovation for the production of agricultural and animal feed bioproducts. Syst. Microbiol. Biomanuf. 1, 142-165.

Vassileva, M., Malusà, E., Sas-Paszt, L., Trzcinski, P., Galvez, A., Flor-Peregrin, E., Vassilev, N., 2021. Fermentation strategies to improve soil bio-inoculant production and quality. Microorganisms 9, 1254.

Velloso, C.C., Borges, R., Badino, A.C., Oliveira-Paiva, C.A., Ribeiro, C., Farinas, C.S., 2024. Modulation of starch-based film properties for encapsulation of microbial inoculant. Int. J. Biol. Macromol. 283, 137605.

Vyas, P., Gulati, A., 2009. Organic acid production in vitro and plant growth promotion in maize under controlled environment by phosphate-solubilizing fluorescent Pseudomonas. BMC Microbiol. 9, 1-15.

Wilson, H., Elliott, J., Macrae, M., Glenn, A., 2019. Near surface soils as a source of Phosphorus in snow melt runoff from crop land. J. Environ. Qual. 23, 445-455.

Withers, P.J., Neal, C., Jarvie, H.P., Doody, D.G., 2014a. Agriculture and eutrophication: where do we go from here? Sustainability 6, 5853-5875.

Withers, P.J., Sylvester-Bradley, R., Jones, D.L., Healey, J.R., Talboys, P.J., 2014b. Feed the crop not the soil: rethinking phosphorus management in the food chain. Environ. Sci. Technol. 48, 6523-6530.

Wu, K., Du, C., Ma, F., Shen, Y., Liang, D., Zhou, J., 2019. Degradation of Metal-Organic Framework Materials as Controlled-Release Fertilizers in crop fields. Polymers 11, 947.

Yi, Y., Huang, W., Ge, Y., 2008. Exopolysaccharide: a novel important factor in the microbial dissolution of tricalcium phosphate. World J. Microbiol. Biotechnol. 24, 1059-1065.

Yu, S., Sun, J., Shi, Y., Wang, Q., Wu, J., Liu, J., 2021. Nanocellulose from Various Biomass Wastes: Its Preparation and Potential Usages towards the High Value-Added Products. Environ. Sci. Ecotechnol. 5, 100077.

Zeng, G., Wan, J., Huang, D., Hu, L., Huang, C., Cheng, M., et al., 2017. Precipitation, adsorption and rhizosphere effect: The mechanisms for Phosphate-induced Pb immobilization in soils-A review. J. Hazard. Mater. 339, 354-367.

Zhao, S., Qiu, S., He, P., 2018. Changes of heavy metals in soil and wheat grain under long-term environmental impact and fertilization practices in North China. J. Plant Nutr. 41, 1970-1979.

Chapter 3

3. New approaches for solubilization of phosphate rocks through solid-state fermentation by optimization of oxalic acid production

ABSTRACT

This study explores the enhancement of phosphate rock (PR) solubilization through solid-state fermentation (SSF) by optimizing oxalic acid production using *Aspergillus niger*. Key process parameters, including the use of agro-industrial by-products (sugarcane bagasse (SCB), wheat bran (WB), soybean bran (SB)), pH levels, sucrose supplementation, and methanol addition, were systematically evaluated through sequential experimental designs. The results identified SCB and SB in a 1:1 ratio as the most effective substrate. Remarkably, the inclusion of methanol (7%) and sucrose (0.5%) resulted in a 3-fold increase in oxalic acid production. Under these optimized conditions, significant phosphorus (P) solubilization of Bayóvar, Itafós, and Registro PRs was achieved. Additionally, the SSF process effectively released organic P from the substrates. In the process using Bayóvar rock, up to 12.1 g of soluble P per kg of dry substrate was released (63.8% efficiency). These findings hold promise for advancing the bio-based economy and developing future industrial biofertilizers.

Keywords: Phosphorus, Biofertilizer, Biological solubilization, *Aspergillus niger*, Organic acids.

3.1. Introduction

Phosphorus is a crucial macronutrient for plant development and is one of the most limiting elements in crop production. This limitation arises because most of the P in the soil is not readily available to plants. This is primarily due to leaching and the formation of low-solubility phosphates with iron (Fe), aluminum (Al), or calcium (Ca) when phosphate anions interact with these elements in the soil (Penn and Camberato, 2019). As a result, frequent applications of soluble P fertilizers are necessary to ensure satisfactory plant growth. In 2021, global agricultural use of processed phosphate fertilizers was 46.3 Mt P_2O_5 (FAO, 2024). These fertilizers are mainly produced by

chemically processing phosphate rocks (PRs) through an energy-intensive treatment with strong acids, generating undesirable contaminants and causing significant environmental issues (Vassilev et al., 2006). Therefore, it is critical to reduce the use of agrochemicals and develop green alternatives to enhance agricultural productivity.

An alternative approach showing promise for P management in agriculture is the use of phosphorus-solubilizing microorganisms (PSMs) in biotechnological processes (Mendes et al., 2015; Klaic et al., 2018; Klaic et al., 2021). Biological P-solubilization primarily occurs through the production of organic acids, which chelate cations bound to phosphate and convert it into soluble forms that plants can assimilate (Mendes et al., 2014). Several studies have explored this process and reported promising results (Klaic et al., 2017; Klaic et al., 2018; Lodi et al., 2021). However, previous work has demonstrated that the biological solubilization process is strongly limited by the PR content in the culture system. This limitation is mainly due to the release of trace elements such as iron, aluminum, and fluorine from PR, which can have toxic effects on microbial growth. Consequently, as the rock content in the culture system increases, the P-solubilization yield tends to decrease (Xiao et al., 2008; Klaic et al., 2018). Therefore, these biological P-solubilization processes still need to be improved to make them viable and competitive.

There are two main options for using PSMs to release P from PRs: applying them directly to the soil along with PRs (Jain et al., 2010) or using in vitro systems to produce soluble P fertilizers from PR (Vassilev et al., 2014; Klaic et al., 2018; Klaic et al., 2021). The second option allows for controlled optimization of organic acid production, which is difficult to achieve in the soil. SSF is a promising strategy for PR solubilization, as it enables the use of agro-industrial by-products as substrates, reducing costs and providing versatility since the product can be used in liquid or solid form (Farinas, 2015). Additionally, SSF is particularly advantageous for cultivating filamentous fungi, as it simulates their natural habitat.

Typically, studies on the biological solubilization of PRs via SSF exhibit lower yields compared to those achieved through submerged fermentation (SF) (Mendes et al., 2015; Klaic et al., 2017; Klaic et al., 2018; Favaro et al., 2022). However, few SSF studies have focused on maximizing organic acid production to enhance PR solubilization (Klaic et al., 2021). In this process, the type and concentration of organic acids produced are crucial for PR solubilization. Mendes et al. (2020) demonstrated that

oxalic acid was the most effective for PR solubilization, even outperforming sulfuric acid by releasing more P per mmol of applied acid. Thus, exploring microorganisms that can effectively produce oxalic acid under SSF present a promising alternative for solubilizing PRs. Among them, the filamentous fungus *Aspergillus niger* is renowned for producing various enzymes and organic acids, including oxalic acid (Klaic et al., 2018; Wang et al., 2022). However, the type of acid produced during *A. niger* metabolism is influenced by process conditions, such as the pH of the culture medium and the type and initial concentration of the carbon source (Yang, Lubeck and Lubeck, 2017). Additionally, the excretion of produced acids can be enhanced by the addition of low molecular weight alcohols (Anwar et al., 2009).

Despite the potential of *Aspergillus niger* for phosphate solubilization, the challenge remains to maximize the efficiency of oxalic acid production in SSF systems. This study addresses this challenge by systematically optimizing the process conditions, including the selection of agro-industrial by-products (SCB, WB, and SB), pH, sucrose, and methanol addition. Following optimization with Bayóvar rock, other low-reactive PRs and higher rock:dry substrate ratios were explored to increase process yield. By refining these variables, the aim to enhance the solubilization of PRs, making biological systems a viable and competitive alternative to conventional chemical processes. This approach contributes to the development of sustainable and cost-effective biofertilizers, thus addressing critical environmental and agricultural needs.

3.2. Materials and methods

3.2.1. Characterization of mineral rocks

In the solubilization experiments, the PRs Bayóvar, from Sechura (Peru), Itafós, which was kindly donated by the Itafós Company (Arraias, TO, Brazil), and Registro, which was kindly donated by Nutrisafra Fertilizantes Ltda. (Cosmopolis, SP, Brazil) were used. The rocks were dried in a stove (Model 035, Marconi, Brazil) at 110ºC for 48 hours to reduce humidity content and stored in dry boxes at room temperature for further use in the experiments. After that, all the rocks were submitted to mechanical treatment for 20 min aiming to improve the solubilization process, as reported by Klaic et al. (2017), in an orbital mill (Model CT-251, Servitec) consisting of a porcelain jar and alumina balls.

The characterizations of the Bayóvar, Itafós and Registro rocks were carried out by Klaic et al. (2017), Klaic et al. (2018) and Favaro et al. (2022), respectively. The results are presented in Table 3.1. Analyzes consisted of X-ray diffraction (XRD) and X-ray fluorescence (XRF) to determine the 10 most common oxides found in the ores and specific ion analysis to determine fluorine (F).

Table 3.1. Physicochemical analysis of the Bayóvar, Itafós and Registro phosphate rocks.

Oxide species	Bayóvar rock (mass %)[a]	Itafós rock (mass %)[b]	Registro rock (mass %)[c]
SiO_2	4.42	36.40	2.21
Al_2O_3	0.96	4.60	3.91
Fe_2O_3	0.87	2.03	14.1
CaO	46.6	30.40	34.9
MgO	0.53	0.52	0.36
TiO_2	0.07	0.22	0.63
P_2O_5	30.73	20.29	28.08
Na_2O	1.98	0.30	0.51
K_2O	0.3	0.88	0.08
MnO	0.01	0.1	1.69
Loss on ignition	10.57	4.33	6.54
Total	97.04	100	93.01
F	2.24	1.87	1.18

[a] Klaic et al. (2017).
[b] Klaic et al. (2018).
[c] Favaro et al. (2022).

3.2.2. Microorganism and substrates

The filamentous fungus *Aspergillus niger* C (BRMCTAA 82) was obtained from the Embrapa Food Agroindustry collection (Rio de Janeiro, Brazil). This strain of *A. niger* was selected due to the excellent organic acids production and rock solubilization (Klaic et al., 2017; Klaic et al., 2018; Klaic et al., 2021; Lodi et al., 2021). The spores were germinated at 30°C in Erlenmeyer flasks containing 60 mL of potato dextrose agar (PDA), which were allowed to solidify tilted. The flasks were kept in a Biochemical Oxygen Demand (BOD) chamber (Model SL 200, Solab, Brazil) for 4 days at 30°C for inoculum growth. After that, the agar surface was gently scraped with distilled water to

obtain the spore suspension. The spore concentration was determined using a Neubauer chamber.

As solid substrates, the agro-industrial by-products sugarcane bagasse (SCB), wheat bran (WB) and soybean bran (SB) were used. These substrates were chosen for their low cost, high local availability and for providing favorable nutritional and structural conditions for the solid matrix (Casciatori et al., 2014; Zambom et al., 2001). The SCB was donated by Usina Itajobi (Marapoama, SP, Brazil) and the brans were acquired in local businesses (Agropecuária Claro, São Carlos, SP, Brazil). All by-products were dried in a stove (Model 035, Marconi, Brazil) at 60°C until constant mass and the SCB was sieved to remove powder and coarser fibers, passing through sieves with an opening of 5 × 5 mm and 4 × 2 mm, respectively. It is important to note that the by-products, used as substrates, did not undergo any additional pre-treatment or washing.

3.2.3. Solid-state fermentation

SSFs were carried out in polypropylene packages of 12 x 20 cm coupled with a 3.6 cm diameter polyvinyl chloride nozzle. In each package, 5 g of dry substrate (d.s.) and the spore suspension (1×10^7 spores g^{-1} d.s.) were added. The humidification of substrates was carried out by adding a saline solution at a proportion of 1.5 mL g^{-1} d.s. (7.5 mL in total), with the following composition: 0.25% $(NH_4)2SO_4$, 0.1% KH_2PO_4, 0.025% $MgSO_47H_2O$, and 0,004% $CuSO_4$ (Klaic et al., 2021). The substrates and the nutrient solution were autoclaved at 121°C for 20 min before all fermentations. Then, they were mixed and homogenized, together with the inoculum, inside a previously sterilized laminar flow chamber. In some fermentations it was evaluated the methanol addition, which was added after autoclaving and cooling the samples. The SSF were conducted at 30°C for 4 days, with the exception of the kinetics study which was conducted for 7 days, in BOD chamber. For each evaluated condition, a package without inoculum was also incubated under the same conditions as a control. At the end of the SSFs, solid-liquid extraction was performed by adding distilled water at a proportion of 15 mL g^{-1} d.s.. The water and fermented solids were manually stirred inside the packages for 10 min. After extraction, the samples were vacuum-filtered and centrifuged (Model 5810R, Eppendorf, Germany) for 20 min at 8000 rpm and 4°C. The supernatants were used to carry out the analytical determinations.

3.2.3.1. Oxalic acid optimization

Sequential experiments designs were performed aiming optimize the oxalic acid production. Initially, the substrates were defined through mixture design and the variables sucrose, methanol and saline solution pH were evaluated in a factorial design 2^3. After that, the optimal conditions were select in a Box-Behnken design and the P solubilization was evaluated in the three rocks (Bayóvar, Itafós and Registro). Fig. 3.1 summarizes the steps that was performed and more details are descripted in the next topics.

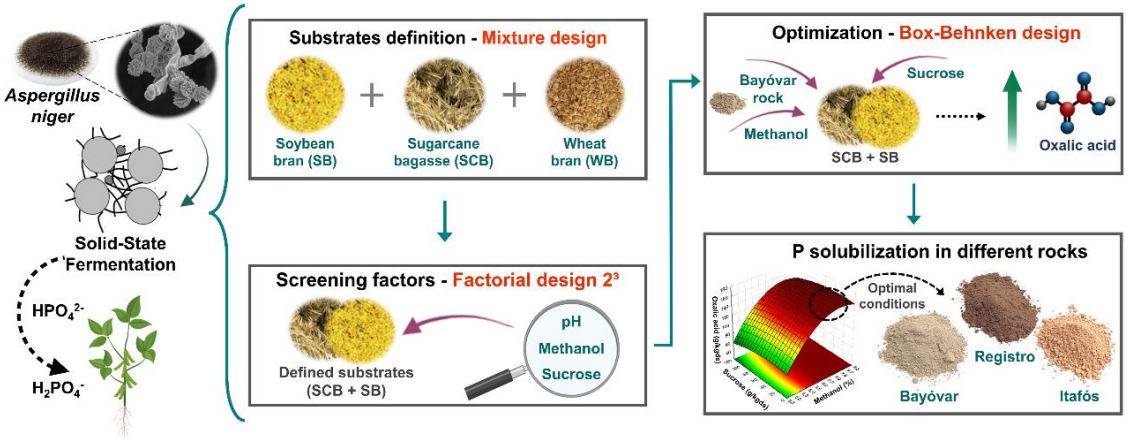

Fig. 3.1. Schematic illustration of oxalic acid optimization steps by solid-state fermentation using the microorganism *Aspergillus niger*.

3.2.3.1.1. Mixture design

In the mixture design experiments, SCB, WB and SB were mixed in the proportions shown in Table 3.2. The percentage of SCB was limited to at least 50%, so that the maximum proportions of WB and SB were 50%. This restriction was made to avoid overheating in a future scale-up. The moisture content was adjusted according to the maximum absorption of the solid matrix, which varied according to the combination of substrates. However, the added salt content per mass of dry substrate was the same in all combinations, so distilled water was also used to adjust the humidity. In these fermentations no supplementation with any other carbon source was carried out and no methanol was added. The responses analyzed were the pH variation and the production of organic acids. All treatments were performed in duplicate.

Table 3.2. Matrix and results of the mixture design carried to evaluate the influence of the composition of agro-industrial by-products sugarcane bagasse (SCB), soybean bran (SB) and wheat bran (WB) on the pH variation (%) and production of organic acids by *Aspergillus niger* C in solid-state fermentation at 30°C for 4 days.

Run	Independent variable			Dependent variable*		
	SCB	SB	WB	pH variation (%)	Oxalic acid (g kg^{-1} d.s.)	Gluconic acid (g kg^{-1} d.s.)
1	1.00	0.00	0.00	3.87 ± 0.89	0.00 ± 0.00	0.00 ± 0.00
2	0.50	0.50	0.00	-21.05 ± 0.43	49.04 ± 3.06	0.00 ± 0.00
3	0.50	0.00	0.50	-4.29 ± 0.76	4.31 ± 0.56	16.10 ± 2.23
4	0.68	0.17	0.17	-16.37 ± 0.48	15.46 ± 1.63	0.48 ± 0.03
5	0.75	0.25	0.00	-12.04 ± 0.55	24.48 ± 1.69	0.00 ± 0.00
6	0.75	0.00	0.25	-9.50 ± 6.53	0.00 ± 0.00	6.53 ± 1.08
7	0.83	0.08	0.08	3.11 ± 0.60	7.41 ± 0.94	0.75 ± 0.02
8	0.50	0.25	0.25	-11.29 ± 0.73	27.01 ± 4.67	5.75 ± 0.36
9	0.58	0.33	0.08	-17.59 ± 0.13	35.58 ± 4.23	0.00 ± 0.00
10	0.58	0.08	0.33	-12.96 ± 0.61	12.50 ± 0.47	5.79 ± 0.05

*Citric, succinic and malic organic acids were quantified but were not detected at relevant contents.
g kg^{-1} d.s. means g per kg of dry substrate.

3.2.3.1.2. Factor design 2^3

Aiming identifying significant variables for improve the oxalic acid production, a factorial design 2^3 using the substrates defined in mixture design was performed. The following factors were evaluated in +1 and -1 levels: sucrose (5 and 100 g kg^{-1} d.s.), methanol (1 and 6% in mass) and pH of the saline solution (2 and 7), as shown in Table 3.3, totalizing 8 treatments, all of them were performed in duplicate. The responses analyzed were the pH variation, soluble proteins and organic acids production.

Table 3.3. Matrix and results of the factorial design 2^3 carried out to evaluate the influence of methanol (Met), sucrose (Suc) and initial pH of the saline solution (pH of SS) on the final pH of the liquid extract (Final pH), oxalic acid production (OA) and soluble proteins (SP).

Run	Independent variable			Dependent variable		
	Met (%)	Suc (g kg^{-1} d.s.)	pH of SS	Final pH	OA (g kg^{-1} d.s.)	SP (mg kg^{-1} d.s.)
1	1 (-1)	5 (-1)	2 (-1)	6.82 ± 0.03	64.61 ± 0.30	7.92 ± 0.22
2	1	5	7 (+1)	6.62 ± 0.01	68.67 ± 0.32	8.14 ± 0.85
3	1	100 (+1)	2	6.43 ± 0.16	60.16 ± 0,08	8.31 ± 0.67
4	1	100	7	6.59 ± 0.12	57.83 ± 1.16	8.63 ± 0.15
5	6 (+1)	5	2	4.41 ± 0.08	121.06 ± 4.76	3.93 ± 0.30
6	6	5	7	4.36 ± 0.16	121.72 ± 8.30	3.91 ± 0.09
7	6	100	2	4.91 ± 0.03	90.84 ± 6.56	4.48 ± 0.48
8	6	100	7	4.66 ± 0.03	102.91 ± 4.79	4.54 ± 0.17

Solid-state fermentations were carried out at 30°C for 4 days using sugarcane bagasse (SCB) and soybean bran (SB) (1:1 weight ratio) as solid substrates and *Aspegillus niger* C as microorganism.
g kg^{-1} d.s. means g per kg of dry substrate.

3.2.3.1.3. Box-Behnken design

A Box-Behnken design with the significant variables and Bayóvar rock was performed aiming finding the optimal conditions for oxalic acid production. The variables evaluated at levels -1, 0 and +1 were sucrose (5, 52.5 and 100 g kg^{-1} d.s.), methanol (4, 6 and 8% in mass) and Bayóvar rock (5, 10 and 15 g kg^{-1} d.s.), as shown in Table 3.4, totalizing 8 treatments of them were performed in duplicate. The responses analyzed were the final pH of liquid extract, oxalic acid production and solubilized P.

Table 3.4. Matrix and results of the Box-Behnken design carried out to evaluate the influence of methanol (Met), sucrose (Suc) and Bayóvar rock (BR) on the final pH of the liquid extract, oxalic acid production (OA) and solubilized P (P exp and P pred).

Run	Independent variables			Dependent variables			
	Met (%)	Suc (g kg^{-1} d.s.)	BR (g kg^{-1} d.s.)	Final pH	OA (g kg^{-1} d.s.)	P exp[1] (g kg^{-1} d.s.)	P pred[2] (g kg^{-1} d.s.)
1	4 (-1)	5 (-1)	10 (0)	5.55 ± 0.04	81.59 ± 4.08	2.86 ± 0.09	2.75
2	8 (+1)	5	10	3.36 ± 0.01	175.45 ± 2.07	3.25 ± 0.06	3.18
3	4	100 (+1)	10	6.00 ± 0.16	89.63 ± 7.89	2.69 ± 0.22	2.65
4	8	100	10	3.41 ± 0.05	145.61 ± 2.01	3.18 ± 0.04	3.08
5	4	52.5 (0)	5 (-1)	5.75 ± 0.01	100.87 ± 8.92	2.29 ± 0.23	2.19
6	8	52.5	5	3.47 ± 0.06	155.23 ± 14.14	2.69 ± 0.16	2.62
7	4	52.5	15 (+1)	5.27 ± 0.01	97.90 ± 0.19	2.95 ± 0.00	3.21
8	8	52.5	15	3.39 ± 0.11	161.51 ± 0.54	3.39 ± 0.10	3.64
9	6 (0)	5	5	3.56 ± 0.01	137.28 ± 14.59	2.02 ± 0.22	2.15
10	6	100	5	3.81 ± 0.04	126.59 ± 0.68	1.82 ± 0.11	2.05
11	6	5	15	3.58 ± 0.01	163.67 ± 5.43	3.24 ± 0.11	3.16
12	6	100	15	3.65 ± 0.02	163.30 ± 18.89	3.30 ± 0.32	3.07
13	6	52.5	10	3.55 ± 0.11	151.31 ± 26.18	2.64 ± 0.45	2.61
OC*	7	5	15	3.34 ± 0.06	161.07 ± 2.90	3.38 ± 0.12	3.35

Solid-state fermentations were carried out at 30°C for 4 days using sugarcane bagasse (SCB) and soybean bran (SB) (1:1 weight ratio) as solid substrates and *Aspegillus niger* C as microorganism.
g kg^{-1} d.s. means g per kg of dry substrate.
[1]P exp corresponds to the value of solubilized P obtained experimentally.
[2]P pred corresponds to the solubilized P value obtained according to the following fitted regression equation: $P = 3{,}745 - 0{,}808Met - 0{,}000099\ Suc + 0{,}1017BR + 0{,}0763Met^2$
*OC means optimized condition.

3.2.3.1.4. P solubilization of different types and contents of phosphate rocks

The solubilization of Bayóvar, Itafós and Registro rocks was analyzed under optimized sucrose and methanol conditions (determined in the Box-Behnken design) at the following levels: 15, 30, 60 and 120 g kg^{-1} d.s.. The responses analyzed were the final pH of liquid extract, oxalic acid production, solubilized P and P solubilization efficiency.

3.2.4. Comparative study on the action of the microorganism in phosphorus release

In order to verify the impact of other actions of the microorganism beyond oxalic acid production on the release of total P contained in the system, a comparative study was performed in the optimized condition. Two conditions were evaluated: firstly, the optimized condition without *A. niger* spore inoculation but with 161 g kg^{-1} d.s. of abiotic oxalic acid (treatment 1), corresponding to the final amount of acid produced in the optimal condition; secondly, the conventional optimized condition with spore inoculation (treatment 2). The P solubilization efficiency was calculated according to Eq. (3.1), considering the total amount of P initially present.

3.2.5. Analytic determinations

3.2.5.1. Soluble proteins

The concentration of soluble proteins was analyzed by the modified Bradford method, in which 20 µL of extract samples were reacted with 1 mL of Bradford reagent for 5 minutes at room temperature. Protein concentration was determined by spectrophotometry (Ultrospec 2100 pro, Amersham, UK) at 595 nm, using a Bradford reagent standard curve with bovine serum albumin solution (Bradford, 1976).

3.2.5.2. Organic acids

The concentrations of citric, oxalic, gluconic, malic and succinic acids were determined using a Waters Model 410 HPLC (high-performance liquid chromatography) equipped with a UV detector (210 nm) and an Aminex HPX87-H column maintained at 55°C. The eluent was 5 mM sulfuric acid in Milli-Q water at a flow rate of 0.6 mL min^{-1}. All samples were filtered using a 0.22 µm filter previously to be injected into the equipment.

3.2.5.3. Soluble phosphorus

The soluble P content was determined using a colorimetric method adapted from the work of Murphy and Riley (1962). A 5 mL volume of the clear supernatant sample was reacted with 2 mL of ascorbic acid solution (0.4 mol L^{-1}), 0.2 mL of citric acid (0.03 mol L^{-1}), and 2 mL of a reagent composed of 25 mL of a sulfuric acid solution (4.7 mol L^{-1}), 5.5 mL of ammonium molybdate solution (0.08 L^{-1}), and 0.6 mL of an

antimony and potassium tartrate solution (0.05 mol L^{-1}). This mixture was reacted at 50°C for 15 min in thermostatic bath, forming a blue phosphoantimonylmolybdenum complex at the end of the reaction. The concentration of the complex was determined by spectrophotometry (Ultrospec 2100 pro, Amersham, UK) at 880 nm, using a KH_2PO_4 standard curve at concentrations from 5 to 70 µmol L^{-1}.

3.2.5.4. Total phosphorus

The total P content of the substrates was determined by the company Ciência em Solo Laboratório de Análises e Consultoria Agrícola. The method applied was nitro-perchloric digestion and determination by UV-vis spectroscopy with ammonium molybdate. The values obtained was 3.9 and 1.7 g kg^{-1} d.s. of total P for SB and SCB, respectively.

3.2.5.5. Phosphorus solubilization efficiency

To measure the efficiency with which the P contained in the medium was solubilized, it was considerate the total amount of P initially present. This includes the amount added from the rock and the amount present in the substrates, as shown by Eq. (3.1).

$$\text{P solubilization efficiency}(\%) = \frac{\text{Solubilized P}}{\text{Initial Total P}} \times 100 \quad (3.1)$$

3.2.5.6. Enzymatic assays

Acid phosphatase activity was measured according to Tabatabai and Bremner (1969). One unit (U) of acid phosphatase activity was defined as 1 µmol of p-nitrophenol released per hour under the assay conditions.

The determination of endoglucanase and β-glucosidase activity were based on Ghose (1987). One unit (U) of enzyme activity was defined as the amount of enzyme needed to release 1 µmol of reducing sugars per minute of reaction per mL of enzyme.

3.2.6. Statistical analyzes

Minitab® 16 software (Minitab Inc., State College, USA) was used to perform analysis of variance (ANOVA) and comparisons between means by Tukey test, with a confidence level of 95%. Contour plots were also performed using Minitab®.

3.3. Results and discussion

3.3.1 Effect of the combination of agro-industrial by-products on the production of oxalic acid by *Aspergillus niger*

The composition of the substrates can influence the formation of bioproducts by SSF, both by the nutritional and structural properties of the solid matrix (Casciatori et al., 2014; Behera and Ray, 2016). Thus, aiming to maximize the oxalic acid production by *A. niger* to solubilize PRs, the agro-industrial by-products sugarcane bagasse (SCB), soybean bran (SB) and wheat bran (WB) were investigated. Among these substrates, SCB also functions as a bulking agent, which is particularly important for large-scale SSF bioprocesses (Casciatori et al., 2014).

It is well established that one of the main bottlenecks in large-scale SSF processes is the poor removal of metabolite heat, particularly in packed-bed bioreactors (PBBs). To minimize this problem, it is crucial for the bed to have adequate porosity, allowing proper air percolation and efficient transfer of respiratory gases. Using SCB as a substrate and bulking agent has shown promising results for this purpose. Typically, smaller particle sizes are more susceptible to compaction. On the other hand, larger particle sizes allow for better aeration due to the void spaces between the particles. The bran used had a shape more similar to spheres approximately 0.5 mm in diameter, while the SCB had a shape more similar to cylinders approximately 0.5 mm in diameter and 15 mm in length. Rodrigues et al. (2022) and Casciatori et al. (2023) reported that bed overheating during SSF bioprocesses in PBBs was below 3°C when using a 70% SCB ratio. On the other hand, Casciatori et al. (2023) demonstrated that using SCB in a proportion of only 30% caused a temperature increase of around 9°C. Thus, aiming to avoid an overheating in a future scale-up, the percentage of SCB was fixed at $\geq 50\%$.

Fig. 3.2 and Table 3.2 present the results of the cultivation assays planned according to the mixture design. The adjusted coefficients of determination (R^2 adj) of the quadratic models used in the construction of the contour plots were 74.3, 97.8 and 92.5% for the pH variation, oxalic acid and gluconic acid, respectively, indicating that the models explain the responses.

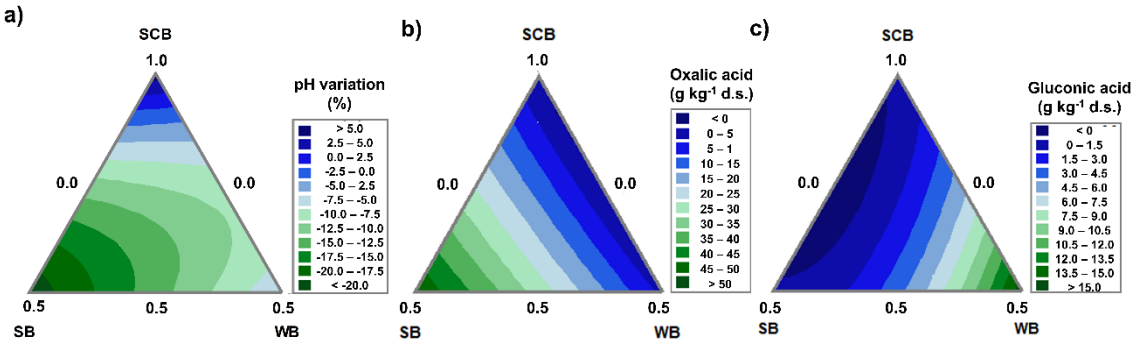

Fig. 3.2. Results from the mixture design experiments: a) contour plots showing the influence of the composition of wastes sugarcane bagasse (SCB), soybean bran (SB) and wheat bran (WB) on the pH variation (%) and b) production of oxalic and c) gluconic acids in g per kilogram of dry substrate (g kg^{-1} d.s.). Solid-state fermentations were carried out at 30°C for 4 days using *Aspegillus niger* C as microorganism.

In general, compositions with a higher proportion of SCB showed a lower production of organic acids, as can be seen in Fig. 3.2a, which shows the contour plot of the pH variation in relation to the control (without inoculum). The pH is related to the organic acids production, but since the pH varies according to the substrate composition, it was necessary to express in terms of pH variation. Negative values of pH variation indicate that the pH decreased and positive values indicate that the pH increased after fermentation in relation to the control. Therefore, the SCB:SB:WB 0.5:0.5:0 composition showed the greatest pH drop (< -20%), indicating that a higher amount of organic acids was produced in this combination, while compositions with SCB close to 100% showed a positive pH variation, indicating an unfavorable composition for the production of organic acids.

As mentioned previously, in addition to serving as a substrate, SCB functions as a crucial bulking agent. Consequently, media with a higher proportion of SCB exhibit greater porosity and, therefore, greater oxygen availability (Casciatori et al., 2014). However, despite these favorable structural characteristics, SCB is nutritionally poorer compared to the brans. SCB contains higher concentrations of lignin, cellulose and hemicellulose and lower concentrations of starch, proteins and minerals. These characteristics make it less suitable as a sole source of carbon and hinder proper

development and metabolism of the microorganism, affecting the production of acids (Zambom et al., 2001; Rodríguez-Zúñiga et al., 2011; Szczerbowski et al., 2014).

Regarding the quantified organic acids (citric, oxalic, gluconic, malic, and succinic acid), oxalic acid was produced in higher quantities, followed by gluconic acid, as shown in the contour plots in Fig. 3.2b and 1c, respectively. According to Fig. 3.2b, the composition that provided the highest production of oxalic acid (> 50 g kg^{-1} d.s.) was SCB:SB:WB 0.5:0.5:0, the same composition in which the greatest drop in pH was observed. This suggests that oxalic acid was likely the main organic acid responsible for this drop. In turn, the highest production of gluconic acid (> 15 g kg^{-1} d.s.) occurred in the composition SCB:SB:WB 0.5:0:0.5, as shown in Fig. 3.2c.

Aspergillus niger is well-known for its ability to efficiently produce organic acids, especially citric acid (Yang, Lubeck and Lubeck, 2017). As a result, it is responsible for almost all commercial citric acid production through submerged fermentation (SF) (Soccol et al., 2006). The type of acid produced during fungal metabolism depends on the process conditions, with the pH of the culture medium and the type and concentration of the carbon source being determining factors. Citric acid synthesis by *A. niger* occurs via primary metabolism, forming in the Krebs cycle. High concentrations (120 – 250 g L^{-1}) of easily metabolizable sugars, such as glucose and sucrose, maintenance of low pH values (1.7 – 2.0), and the presence of trace metal ions are reported to be necessary conditions to achieve high yields and production rates of citric acid (Yang, Lubeck and Lubeck, 2017; Carvalho et al., 2005). On the other hand, neutral pH values favor the production of oxalic and gluconic acids over citric acid (Yang, Lubeck and Lubeck, 2017). This explains the formation of non-significant amounts of citric acid, since no supplementation with easily metabolizable sugars was performed in this mixture design and the initial pH of the saline solution was adjusted to pH 6.

In contrast, the synthesis of oxalic acid by *A. niger* does not involve mitochondrial metabolism. Instead, it occurs through the hydrolysis of oxaloacetate, which is formed from pyruvate after glycolysis, by the enzyme oxaloacetate hydrolase (Yang, Lubeck and Lubeck, 2017). Oxalic acid is secreted when the pH of the medium is close to neutrality, with an optimum at pH 6. Some studies also suggest that enriching the medium with significant amounts of N and P is favorable for increasing the production of oxalic acid (Cameselle et al., 1998; Walaszczyk et al., 2018).

Furthermore, according to Walaszczyk et al. (2017), the selectivity, yield and rate of oxalic acid production by *A. niger* are favored at lower sugar concentrations (< 100 g L^{-1}), since the production of gluconic and citric acids are impaired under these conditions.

Gluconic acid, on the other hand, is directly produced through the action of the enzyme glucose oxidase present in the cell wall of *A. niger*. The enzyme is stable at pH values between 4 and 6, with an optimum around 5.5, and is induced in the presence of high levels of glucose (130 – 150 g L^{-1}) and oxygen (Yang, Lubeck and Lubeck, 2017; Carvalho et al., 2005; Ramachandran et al., 2006). According to Roehr et al., (1996), to produce gluconic acid, the cultivation medium must be limited in terms of N and P and present sufficient concentrations of trace elements.

These facts are consisted with the results obtained here, since WB has a higher starch content compared to SB, which implies in a greater amount of glucose available, since amylase is one of the several enzymes produced by *A. niger* (Bellaouchi et al., 2021). As a result, the production of gluconic acid is favored over oxalic acid when WB is used. On the other hand, SB has lower available glucose content and a higher level N than WB (Generoso et al., 2008), which favors the production of oxalic acid (Cameselle et al., 1998). In view of the presented findings, further tests were carried out to maximize organic acid production and optimize PR solubilization using a composition of agro-industrial by-products containing only SCB and SB in a 1:1 weight ratio. This choice was made because this composition resulted in the greatest pH drop and the highest production of oxalic acid, which has been shown to be one of the most promising acids to the solubilization of PRs by biotechnological route (Mendes et al, 2020).

3.3.2 Factor screening in oxalic acid production

In addition to the pH of the culture medium and the concentration of sugars, another variable that can influence on the production of organic acids is the addition of small concentrations of low molecular weight alcohols, such as ethanol and methanol (Anwar et al., 2009). Thus, a 2^3 factorial design was used to investigate the influence of sucrose concentration, pH of the saline solution for humidification of solid substrates and methanol concentration on oxalic acid production. Fig. 3.3 and Table 3.3 present the results that were obtained in this experimental design.

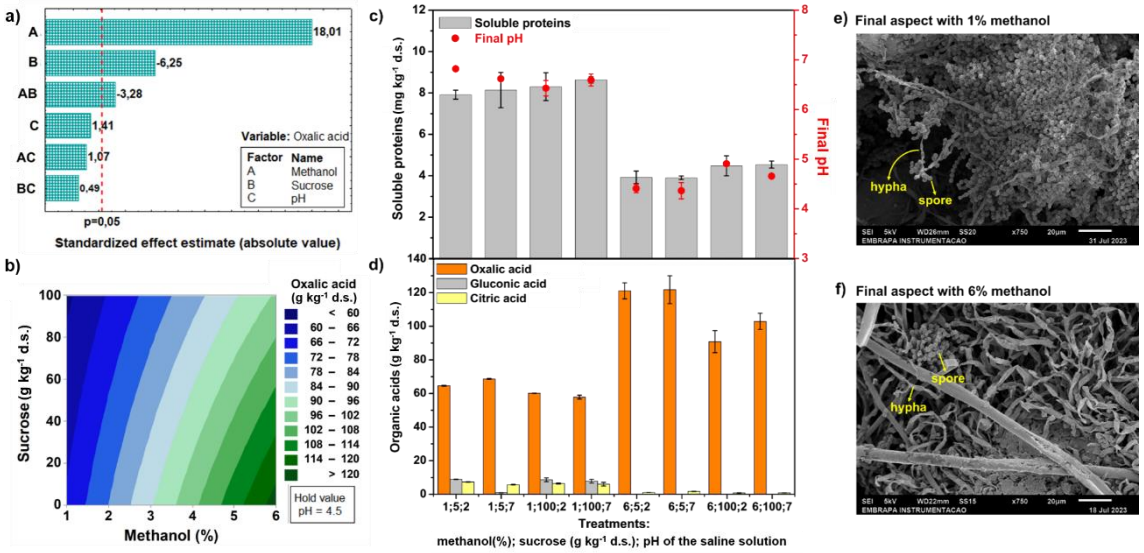

Fig. 3.3. Results from the factorial design experiments: influence of the variables methanol, sucrose and pH of the saline solution. a) Pareto plot showing the effect of analyzed variables on the oxalic acid production. b) Contour plot showing the influence of the methanol and sucrose levels on oxalic acid production. c) Soluble proteins concentration in mg per kilogram of dry substrate (mg kg^{-1} d.s.) and final pH of liquid extract. d) Production of organic acids (g kg^{-1} d.s.). Electron microscopy of the final aspect of the fermented solids with e) 1% and f) 6% methanol addition. Solid-state fermentations were carried out at 30°C for 4 days using sugarcane bagasse and soybean bran (1:1 weight ratio) as solid substrates and *Aspegillus niger* C as microorganism.

When evaluating the effect of the three variables on the oxalic acid production, only pH and interactions with pH did not show a significant effect, while methanol and sucrose, as well as the interaction between methanol and sucrose, showed significant effects, as shown in Fig. 3.3a, which presents the Pareto chart of the variables analyzed for the oxalic acid as response variable. As previously mentioned, in SF studies, the medium pH has an important influence on oxalic acid production, with an optimum around 6. However, in SSF it does not seem to have the same effect, which is probably related to H^+ ions are not dissolved in the culture medium, as occurs in SF, being only adsorbed on the solid matrix (Behera and Ray, 2016). On the other hand, methanol showed a positive and sucrose a negative significant effect on oxalic acid production, with a predicted production > 130 g kg^{-1} d.s. in the region with the lowest sucrose level (5 g kg^{-1} d.s.) and highest methanol level (6%), as shown in Fig. 3.3b, which shows the

contour plot for the oxalic acid production. The R^2 adj of the linear model used to build the contour plot was 96.3%.

According to the data presented in Table 3.3, in runs 2 and 6, where 1% and 6% methanol were added, respectively, there was an increase of 1.4 and 2.5 times in the production of oxalic acid, respectively, in relation to the production where the addition of methanol was not performed (run 2, Table 3.2). These two conditions also had the lowest sucrose supplementation (5 g kg^{-1} d.s.). As previously mentioned, lower concentrations of sugar seem to be more favorable to produce oxalic acid by *A. niger*, since the selectivity to produce oxalic acid increases in relation to citric and gluconic acids (Walaszczyk et a., 2017).

The role of methanol in the induction of oxalic acid is not yet well established in the literature; however, its role in the induction of citric acid production has been more explored. Some of the effects observed in citric acid production are also applicable to the production of oxalic acid, as both are produced inside the cell. According to Usami and Taketomi (1961), methanol can suppress the synthesis of cell wall proteins in the initial stages of culture, making the cell membrane more permeable and thereby enhancing the ability to secrete acids. Fungal morphology also appears to be affected by methanol, which promotes pellet formation rather than mycelial growth, which inhibits sporulation and increases the acid yield of fermentation (Anwar et al., 2009). Indeed, in the tests where 1% methanol was added, the sporulation was expressive, while in the tests with 6% methanol, mainly hyphae formation was observed, with practically no spore production, as shown in Fig. 3.3c and d, respectively.

The methanol effect in biomass formation also can be seen in the final soluble protein concentration, shown in Fig. 3.3e, together with the final pH of the liquid extract. Soluble protein concentration is an indirect measure to the biomass since it is not possible to perform this measurement directly in the SSF. In treatments where 6% methanol was added, the concentration of soluble proteins was significantly lower than that obtained with 1% methanol, indicating that the greater addition of methanol impaired the growth of the microorganism. Furthermore, in treatments with a higher methanol addition, the final pH values of the liquid extract were significantly lower than those obtained with 1% methanol, likely due to the significant increase in oxalic acid production (2.5 times), as discussed earlier. In fact, the decrease in pH can be attributed to both oxalic acid, as well as gluconic and citric acids. Nevertheless, the increase in

methanol concentration appears to enhance the selectivity for oxalic acid production, as evidenced by the quantification of the other acids, which exhibited a reduction in production in assays with higher methanol additions (Fig. 3.3f). The individual response of acids to methanol is likely linked to the tolerance and stimulation of the enzymes involved in their synthesis.

Thus, in order to optimize the production of oxalic acid and, consequently, the potential use of the approach to solubilization of PR, the variables methanol concentration, sucrose concentration and Bayóvar rock concentration were evaluated using a Box-Behnken design. Although sucrose had a negative effect on the production of oxalic acid, it was maintained in the optimization study due to the addition of the Bayóvar rock in the design, which is a variable that has a hitherto unknown effect in this study. It is important to note that the pH of the saline solution was set at 6, which is the optimal value reported for oxalic acid production (Walaszczyk et al., 2018).

3.3.3 Optimization of oxalic acid production and Bayóvar rock solubilization

Fig. 3.4 presents the results of the experiments from the Box-Behnken design. According to Fig. 3.4a and 3.4b, which show the contour plots of the oxalic acid production and the final pH of the liquid extract, respectively, sucrose had the same effect observed in the factorial design. That is, lower concentrations of sucrose were more favorable to produce oxalic acid and reduce the medium pH. As for methanol, the optimal region was around 7% to 8% for these two response variables, slightly higher than the concentration used at the high level of the factorial design (6%). The influence of PR on the production of oxalic acid and the final pH of the liquid extract seems to have been favorable, as the optimal regions encompass the maximum addition of rock. This may be related to the greater availability of P as the rock was being solubilized. As previously mentioned, high concentrations of P in the medium seem to be favorable to produce oxalic acid (Cameselle et al., 1998).

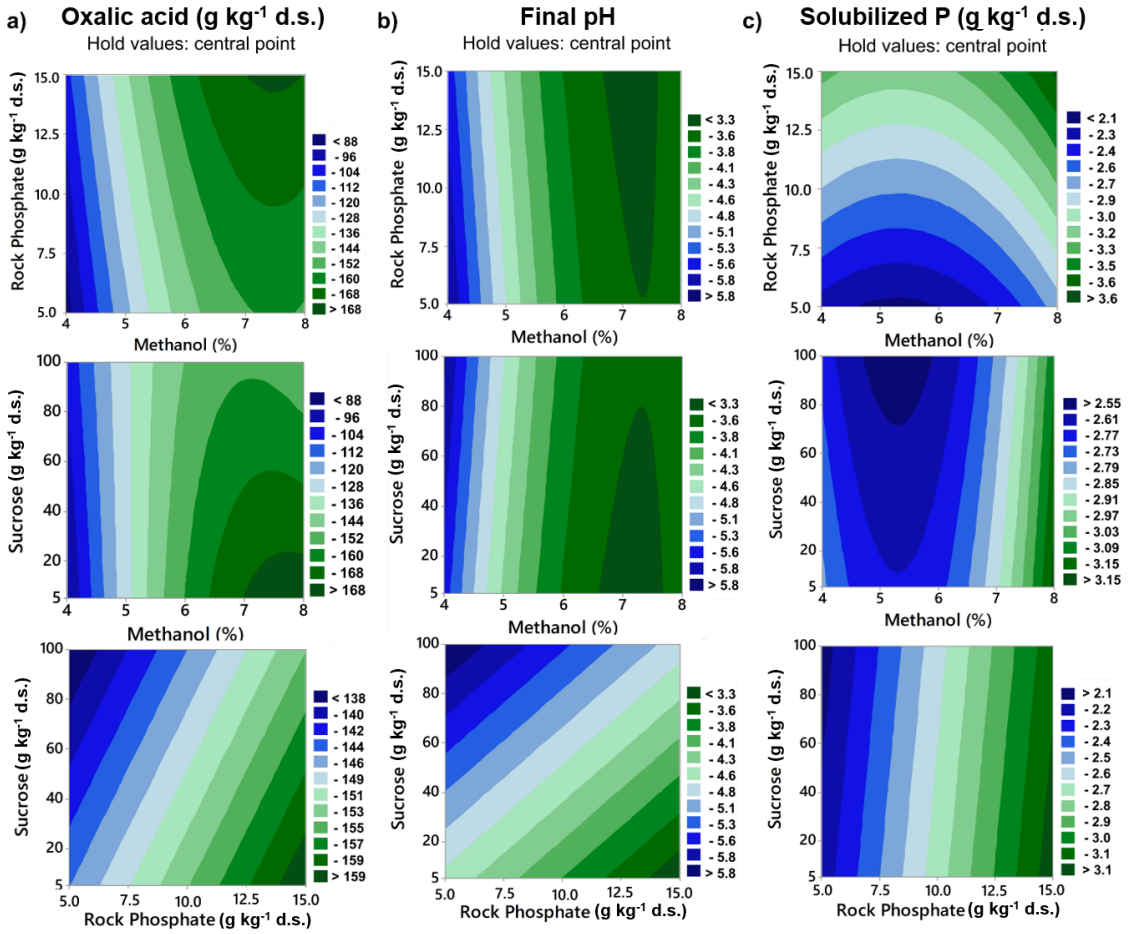

Fig. 3.4. Contour plots, resulting from the Box-Behnken design experiments, showing the influence of methanol, sucrose and rock phosphate concentrations on a) oxalic acid production in g per kg of dry substrate (g kg^{-1} d.s.), b) final pH of the liquid extract and c) solubilized P from the Bayóvar rock. Solid-state fermentations were carried out at 30°C for 4 days using sugarcane bagasse and soybean bran (1:1 weight ratio) as solid substrates and *Aspegillus niger* C as microorganism.

For the contour plots of solubilized P (Fig. 3.4c), the PR concentration had a similar influence, resulting in the highest values of solubilized P observed in regions with the maximum addition of PR. Likewise, for methanol, the optimal region for rock solubilization was predicted to be above 8%, in the maximal addition. On the other hand, the influence of sucrose seems to be less significant compared to that observed in the production of oxalic acid and the final pH of the liquid extract.

The models obtained for oxalic acid, final pH and solubilized P, excluding non-significant quadratic terms and interactions, are presented by Eq. (3.2) (R^2 = 85.23%),

(3.3) (R^2 = 98.47%) and (3.4) (R^2 = 79.81%), respectively. The optimized conditions for each of the 3 evaluated responses resulted in a minimum addition of sucrose (5 g kg^{-1} d.s.) and maximum of PR (15 g kg^{-1} d.s.), differing slightly only for the optimal addition of methanol, which was 7.9, 7.03 and 8.00% for oxalic acid production, final pH and solubilized P, respectively. It is interesting to note that the optimized conditions to produce oxalic acid and solubilize P are practically the same, showing a strong relationship between these two variables. However, it was observed that the addition of 8% methanol is a critical concentration, so that at slightly higher concentrations, acid production practically ceases (data not shown). Thus, it was decided to continue the work with 7% methanol, which was considered the ideal working concentration. Table 3.4 presents the responses obtained for all Box-Behnken combinations as well as the predicted responses considering the solubilized P model (Eq. (3.4)).

$$\mathrm{OA} = -196.7 + 89met + 0.51suc + 1.675PR - 5.59met^2 - 0.0997(met)(suc) \quad (3.2)$$

$$\text{Final pH} = 15.421 - 3.304met + 0.00837suc - 0.0802PR + 0.2247met^2 - 0.0010(met)(suc) + 0.0105(met)(PR) \quad (3.3)$$

$$\mathrm{P} = 3.745 - 0.808met - 0.00099suc + 0.1017PR + 0.0763met^2 \quad (3.4)$$

where OA, P, *met*, *suc* and *PR* represent the production of oxalic acid in g per kg of dry substrate (g kg^{-1} d.s.), solubilized P (g kg^{-1} d.s.), methanol content (%), sucrose content (g kg^{-1} d.s.) and PR content (g kg^{-1} d.s.), respectively.

As a result of the optimization, the production of oxalic acid was 161 g kg^{-1} d.s., which is equivalent to 119.3 mM or 10.7 g L^{-1} when considering the amount of distillated water that was used in the solid-liquid extraction (15 mL g^{-1} d.s.). This production corresponds to an increase of 3.3 and 1.3 times in relation to the values obtained previously in the mixture design (Table 3.2, run 2) and in the factorial design (Table 3.3, run 6), respectively, which can be mainly attributed to the higher addition of methanol and the higher P content in the medium.

There are few studies that have explored the production of oxalic acid by SSF. Leangon et al. (1999) used sweet potato as a culture medium, without adding other nutrients, and produced 26.4 g kg^{-1} d.s. of oxalic acid, an amount lower than the

produced in the present work. This difference may be related to the lack of nutrients, as P and N, and to the difficulty in excreting the acid in the extracellular medium, since alcohol was not added. A higher production, of 123 g kg^{-1} d.s., however, but still lower than that obtained in the present study, was reported by Mai et al. (2016), who used corncob as a carbon source and a methanol-resistant mutant strain of *A. niger* in a semi-solid-state fermentation process. An oxalic acid production higher than that of the present work, by SSF, was obtained by Amenaghawon and Agbedor (2021), who used ground sweet potato peel as a substrate. The authors optimized the concentrations of KH_2PO_4, $NaNO_3$ and $MgSO_4$ and reached 29 g L^{-1} of oxalic acid. However, these authors did not use the HPLC method to quantify oxalic acid, but a catalytic kinetic spectrophotometric method, which makes comparison difficult.

Given that the objective of the present work is to optimize oxalic acid production to solubilize PRs by SSF, the obtained production is quite promising. It surpasses the yield reported by Amaro et al. (2022), which was 71 mM through submerged fermentation (SF). According to the authors, this quantity was sufficient to solubilize 100% of the P contained in a low solubility ore that was added at a concentration of 10 g L^{-1}. Furthermore, according to Mendes et al. (2022), who investigated the extraction of phosphate from PRs by oxalic acid, the reaction between oxalic acid and PR is fast and efficient. They observed that 75% of the P was released in the first hour and that it was not necessary to use an excess of oxalic acid.

When comparing with other studies that investigated the solubilization of PRs by SSF in a similar PR range, it was found that the value of solubilized P reached in the optimized condition, of 3.38 g kg^{-1} d.s., equivalent to 225.3 mg L^{-1}, is superior to the reported by the literature. Klaic et al. (2017) evaluated the solubilization of PR Bayóvar using ground SCB supplemented with glucose and reported a maximum solubilized P value of 125 mg L^{-1}, corresponding to a solubilization efficiency of 36%. Klaic et al. (2021) investigated the solubilization of PR Itafós using ground SCB and wheat bran in a 3:1 ratio by mass with addition of sucrose and reported a maximum solubilized P value of 2.72 g kg^{-1} d.s..

In fact, upon evaluating the amount of solubilized P in the present study in relation to the amount that was added, it was observed that the solubilized P exceeded the initially added amount in all combinations. According to the characterization of the rock Bayóvar (Table 3.1), the highest amount of P added was 2.01 g kg^{-1} d.s.,

corresponding to 15 g kg^{-1} d.s. of Bayóvar rock. Thus, there was probably release of P from the agro-industrial by-products, since the SB and SCB used presented 3.9 and 1.7 g kg^{-1} d.s. of P, respectively, totalizing 2.8 g kg^{-1} d.s. of P, since each was utilized in a proportion of 50% in terms of dry matter.

Plants contain P in both organic and inorganic forms. Organic P is present mainly as phospholipids, nucleic acids and phytate, whereas inorganic P is available as phosphate from minerals and also as insoluble components attached to the cell wall (Dai et al., 2010; Ingelmann et al., 2020). Wang et al. (2022) explored the mechanisms of wheat straw degradation and P release by phosphate solubilizing fungi. Their study demonstrated that more than 92% of the total P contained in wheat straw was released after incubation with *A. niger*. According to the authors, the release of organic P occurred mainly due to the action of multiple enzymes that were produced, such as cellulases, phosphatases and phytases, while the inorganic P was released mainly by the excretion of oxalic acid. Thus, the process studied here has the potential to solubilize P from PRs and to provide additional P through the release of organic and inorganic P present in the SB. Therefore, the release of P from secondary resources, such as agro-industrial residues, can decrease the reliance on P from mineral reserves.

Fig. 3.5 illustrates the results of the comparative study on the action of the microorganism in P release. It is important to highlight that the total amount of P present considered in the calculation of solubilization efficiency (Eq. (3.1)) was 4.81 g kg^{-1} d.s. (2.01 g kg^{-1} d.s. from the rock and 2.8 g kg^{-1} d.s. from the substrates). In treatment 1, the efficiency was 33.5%, releasing 1.61 g kg^{-1} d.s. of P. This amount is less than the quantity added from the PR (2.01 g kg^{-1} d.s.). In contrast, in treatment 2, the efficiency was 70.2%, releasing 3.38 g kg^{-1} d.s. of P, which exceeds the amount of P added from the PR. This suggests that both organic and inorganic phosphorus are likely being released from the rock and substrates, highlighting the multiple actions of *A. niger* in releasing P. Inorganic P is primarily released through oxalic acid production, while organic P is released through enzyme production. It was found that, under the studied conditions, endoglucanase, β-glucosidase, and acid phosphatases were produced (data not shown). The endoglucanase and β-glucosidase enzymes belong to the cellulase group, playing a crucial role in digesting cellulose and separating organic phosphorus (P) from cells. Subsequently, phosphatases can release P in the form of ions that are absorbable by plants (Wan et al., 2020).

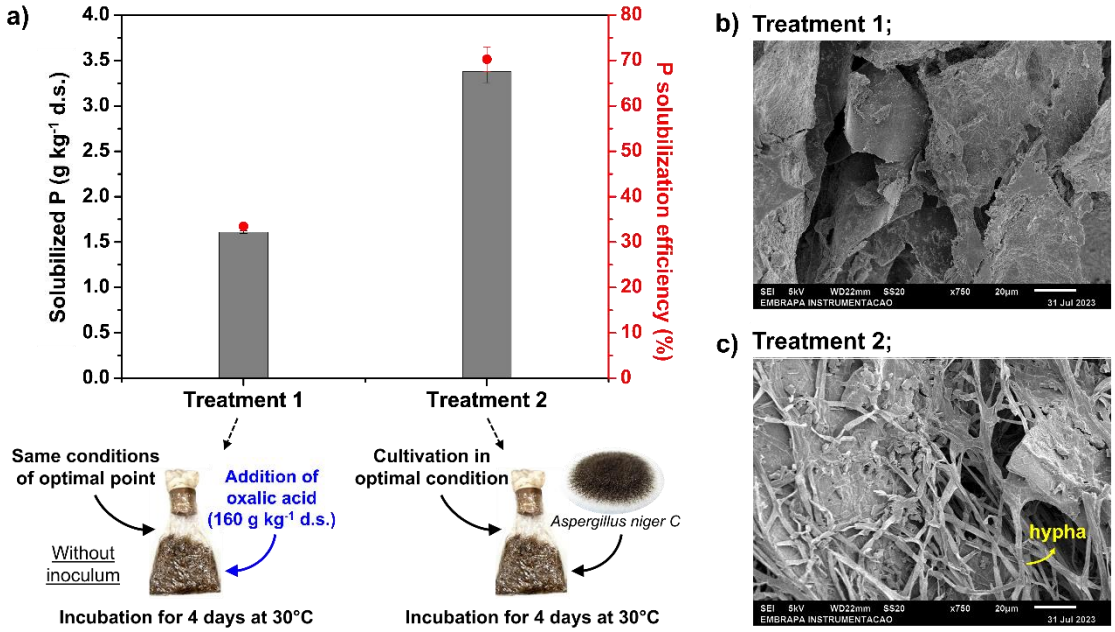

Fig. 3.5. a) Solubilization of Bayóvar phosphate rock in a medium under optimal conditions of fermentation determined by Box-Behnken design (sugarcane bagasse and wheat bran in a weight proportion 1:1, 5 g per kg of dry substrate (g kg^{-1} d.s.) of sucrose, 7% of methanol and 15 g kg^{-1} d.s. of rock) under different treatments: addition of 161 g kg^{-1} d.s. of abiotic oxalic acid (treatment 1) and solid-state fermentation by microorganism *Aspergillus niger* C (1×10^7 spores g^{-1} d.s.) (treatment 2). Electron microscopy of the solids at the end of incubation of treatments b) 1 c) and 2.

Furthermore, the superior results observed in treatment 2 may be attributed to a physical interaction between the mineral and the microorganisms. This interaction is illustrated in Fig. 3.5b and 3.5c, which depict electron microscopy images of the solids in treatments 1 and 2, respectively. In particular, Fig. 3.5c (treatment 2) shows the contact between fungal hyphae and substrates. Lodi et al. (2021) investigated the biological solubilization of a potassium mineral (K-feldspar) and also observed greater solubilization in the inoculum treatment. This positive effect caused by the interaction between microorganism and mineral seems to be related to the generation of physical forces capable of fragmenting parts of the mineral, creating more reactive surfaces. Another possible mechanism is related to the secretion of extracellular polymeric substances, such as polysaccharides, which could create a microenvironment in which

the organic acids became concentrated, facilitating the adhesion of fungal hyphae to the mineral surface (Lian et al., 2008).

3.3.3.1 Time profiles of the P solubilization process in the optimized conditions

In view of the promising results of the solubilization of the Bayóvar rock, the time profiles of the bioprocess under optimized conditions were evaluated to determine the ideal period for the fermentation process and the behavior of the responses analyzed over time, as shown in Fig. 3.6.

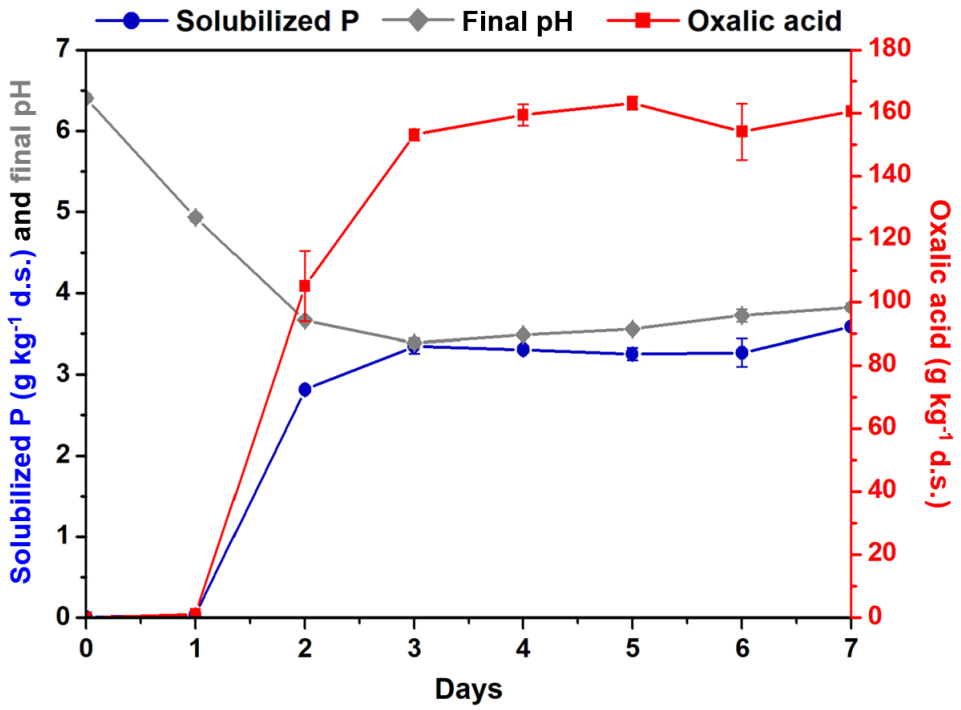

Fig. 3.6. Time profiles for solubilized P, oxalic acid production in g per kg of dry substrate (g kg^{-1} d.s.) and final pH of the liquid extract during solid-state fermentation of *Aspergillus niger* C in the optimized condition: sugarcane bagasse and soybean bran in a weight proportion 1:1, 5 g kg^{-1} d.s. of sucrose, 7% methanol and 15 g kg^{-1} d.s. of Bayóvar rock.

According to the profile of solubilized P, practically in 3 days the maximum value (3.58 g kg^{-1} d.s.) was reached. On the 3rd day, the greatest drop in pH (3.39) was also observed and oxalic acid reached more than 95% of the maximum production (163 g kg^{-1} d.s.) that occurred on the 5th day. All profiles were stable in the last 4 days of

fermentation, indicating that it can be interrupted in 3 days and that the production of oxalic acid was strongly related to the drop in pH and the release of P. Klaic et al. (2017), who also evaluated the solubilization of the Bayóvar rock, observed similar profiles for solubilized P and pH, with process stabilization in 3 days, both by SSF and by SF. This finding aligns with Mendes et al. (2022), who reported that the reaction between oxalic acid and PR is rapid and efficient.

As for oxalic acid, most studies report longer incubation times to reach maximum oxalic acid production, up to 40 days (Walaszczyk et al., 2017; Walaszczyk et al., 2018; Amaro et al., 2022). Thus, the rapid production of oxalic acid obtained here may be related to the addition of methanol and the low soluble sugar content, which provides greater selectivity to produce oxalic acid, as demonstrated and discussed in the present work. Klaic et al. (2018), who evaluated the biological solubilization of PR Itafós by *A. niger*, also reported a rapid production of oxalic acid, but after 24 h the profile began to decline. The authors attributed this decrease to the formation of calcium oxalate. According to Mendes et al. (2022), calcium oxalate is readily formed as soon as Ca is released from apatite by the action of oxalic acid. The absence of a decrease in oxalic acid accumulation in the current profile times is likely related to the fact that, under the conditions employed to conduct the fermentations, there is an excess of oxalic acid in relation to calcium (14.3 mol of oxalic acid/mol of Ca). Furthermore, in the presence of low concentrations of soluble sugar, other acids eventually formed, such as citric and gluconic acid, can also be used as a carbon source to produce oxalic acid (Walaszczyk et al., 2017; Walaszczyk et al., 2018).

3.3.4. Evaluation of phosphorus solubilization in different types and contents of phosphate rocks

Considering that the amount of oxalic acid produced appears capable of promoting the solubilization of most of the inorganic phosphorus present, the addition of higher contents of rock, including other types of PRs (specifically, Itafós and Registro rocks), was evaluated. The assays were performed under optimal conditions of sucrose (5 g kg^{-1} d.s.) and methanol (7%). Additions of 15, 30, 60 and 120 g kg^{-1} d.s. of Bayóvar, Itafós and Registro rocks were evaluated, the results are shown in Fig. 3.7. Similarly, to calculate the solubilization efficiency, the amount of P released was considered in relation to the amount added from the rocks, according to the

characterizations presented in Table 3.1, and according to amount present in the substrates (2.8 g kg^{-1} d.s.).

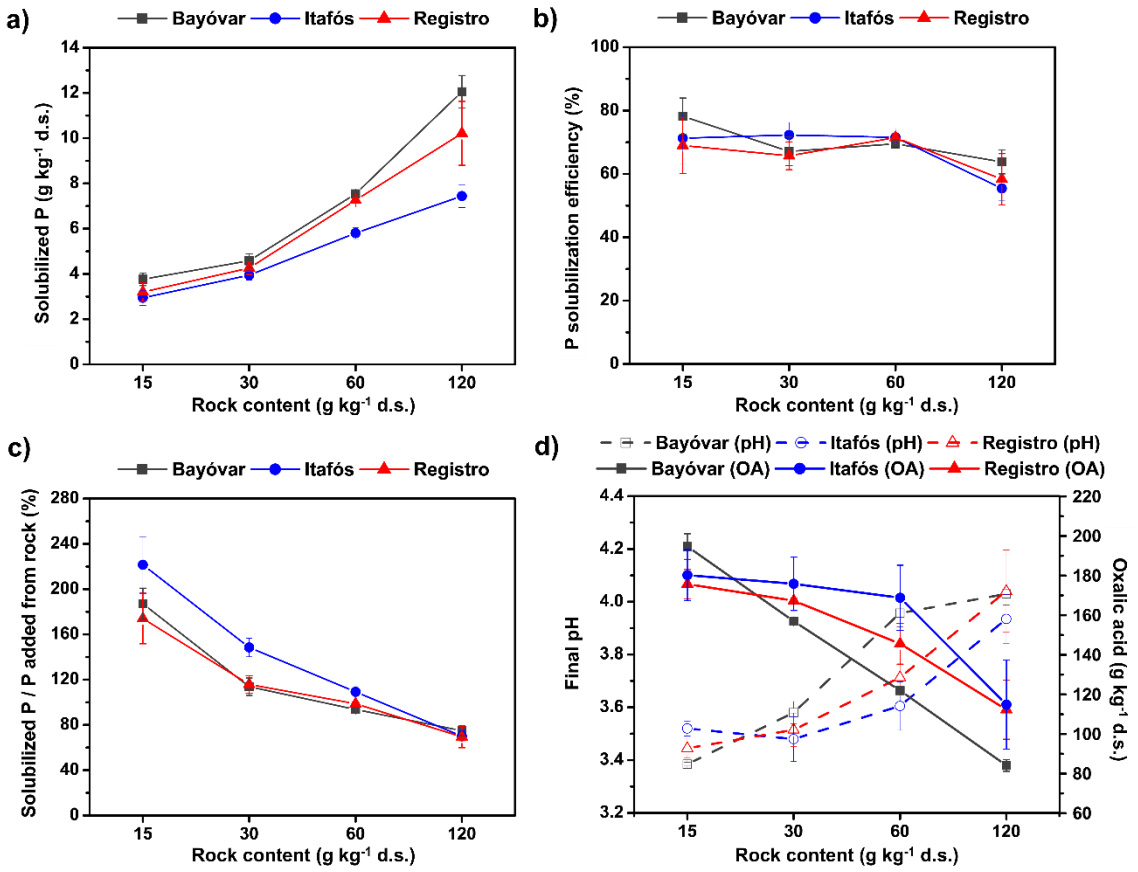

Fig. 3.7. Solubilization of different levels of Bayóvar, Itafós and Registro phosphate rocks by solid-state fermentation of *Aspergillus niger* C under the following conditions: sugarcane bagasse and soybean bran in a weight proportion 1:1, 5 g per kg of dry substrate (g kg^{-1} d.s.) of sucrose and 7% of methanol. Results for a) solubilized P (g kg^{-1} d.s.), b) P solubilization efficiency (%), c) Ratio between solubilized P and P added from rock and d) final pH of liquid extract and oxalic acid production (g kg^{-1} d.s.).

According to Fig. 3.7a, the solubilized P increased with the rise in rock content for all types of rocks. Bayóvar and Registro exhibited similar behaviors, while Itafós rock presented significantly lower solubilized P values at rock levels of 60 and 120 g kg^{-1} d.s.. This difference is related to several factors, such as P content, rock type (sedimentary or igneous), and composition of phosphate phases. The Bayóvar rock used is of sedimentary origin, while the rocks Itafós and Registro are of igneous origin.

Sedimentary rocks generally are more easily solubilized because their composition results in a more porous and less resistant crystal compared to igneous ones. According to X-ray diffraction characterizations of the rocks used, the phosphate phases correspond to 75%, 66%, and 41% (by mass) of the Bayóvar, Registro, and Itafós rocks, respectively (Klaic et al., 2017; Klaic et al., 2018; Favaro et al., 2022). These characteristics favor the solubilization of the Bayóvar rock more, followed by Registro and Itafós. Regarding the P_2O_5 content, the Bayóvar and Registro rocks have similar values, 30.73% and 28.08%, respectively. In contrast, the Itafós rock has a lower P_2O_5 content, 20.29%, as shown in Table 3.1.

Despite the physico-chemical differences among the rocks used, considering the P solubilization efficiency, showed by Fig. 3.7b, there was no significant difference between the rocks for all rock contents. It is worth noting that, for calculating solubilization efficiency, the total P present in both rocks and substrates was considered (Eq. (3.4)). The values remained at around 70% efficiency until the addition of 60 g kg^{-1} d.s. of rock, but decreased to approximately 60% with the addition of 120 g kg^{-1} d.s.. However, this decrease was significant only for the Itafós rock. In addition to having a lower phosphate phase, as mentioned earlier, the Itafós rock contains a large amount of crystalline quartz phase, as characterized by Klaic et al. (2018), further hindering access to the crystal by microorganisms.

The ratio between solubilized P and the added P from the rocks also was analyzed. The profiles exhibited a decline with an increase in rock content, as illustrated in Fig. 3.7c. For rocks Bayóvar and Registro, this ratio exceeded 100% up to a rock addition of 30 g kg^{-1} d.s.. In the case of rock Itafós, this ratio exceeded 100% up to a rock addition of 60 g kg^{-1} d.s.. It is important to emphasize that ratios greater than 100% do not signify that all P from the rock was solubilized, as there is no way to distinguish how much P was solubilized from the rock versus the substrates.

This decrease in the ratio between solubilized P and the added P from the rocks is probably related to the inhibitory effects on the metabolism of microorganisms, mainly caused by the release of certain components present in the rocks, such as F, Al, and Fe (Mendes et al., 2013; Silva et al., 2014; Klaic et al., 2018). These inhibitory effects impair the acid production, as can be seen in Fig. 3.7d, which shows the oxalic acid production with the rock content. Another possible explanation is that calcium oxalate formation occurred, which is a reaction that happens readily, as mentioned in

section 3.3.3.1. For all rocks, oxalic acid production decreases with the rock content, especially for Bayóvar rock, which can be related to its higher content of F.

Consequently, the final pH of the liquid extract increased with the rock content for all types of rocks, as shown in Fig. 3.7d. Klaic et al. (2018) also reported a decrease in the solubilization efficiency of PR Itafós, as well as lower biomass formation and lower acid production with increasing rock content.

Despite the inhibitory effects, the P-solubilization results are very promising, with efficiencies around 60% and ratio around 70% in the addition of 120 g kg^{-1} d.s. of rock. The best P-solubilization result was obtained with the Bayóvar rock, achieving an efficiency of 63.8% on the higher addition of rock, 120 g kg^{-1} d.s., resulting in a P release of 12.1 g kg^{-1} d.s.. This value corresponds to 806.7 mg L^{-1} of P when considering the proportion of distilled water to perform the extraction (15 mL g^{-1} d.s.). The superior results for the Bayóvar rock are likely related to its higher phosphate phase content and the fact that it is a sedimentary rock, as previously mentioned.

Klaic et al. (2017) reported that the P-solubilization of the Bayóvar rock, reached 450 mg L^{-1} by SF and 138 mg L^{-1} by SSF, with efficiencies of 65 and 40%, respectively. Mendes et al. (2015) evaluated the addition of biochar in an optimization study of the solubilization of Araxá rock by SSF to minimize the toxic effects caused by the release of some rock components. However, the efficiency was only 25.7%, with a maximum reported solubilization of 8.6 g kg^{-1} d.s.. Regarding the other rocks, at the maximum addition of rock (120 g kg^{-1} d.s.), a P release of 7.4 g kg^{-1} d.s. (496.1 mg L^{-1}) was achieved for the Itafós rock and 10.2 g kg^{-1} d.s. (681.0 mg L^{-1}) for the Registro rock, with efficiencies of 55.4% and 58.3%, respectively. Klaic et al. (2018) achieved solubilization of Itafós rock at approximately 120 mg L^{-1} (61% efficiency) and 355 mg L^{-1} (41% efficiency) using SSF and SF, respectively. Favaro et al. (2022) reported Registro rock solubilization by SF at approximately 250 mg L^{-1}, with an efficiency of 30%. Given that Itafós and Registro rocks are significantly less reactive than Bayóvar rocks due to their igneous origin, the results obtained here through the optimization of oxalic acid production by SSF are quite promising. and could pave the way for further exploration of biotechnological solubilization of low reactive PRs. Although the values of soluble P are significantly lower compared to commercial fertilizers, this product can be used in combination, contributing to the reduced use of chemical phosphate fertilizers. Moreover, microbial action in the soil can continue to solubilize part of the

unsolubilized rock, promoting slow release, which is particularly desirable after the initial stages of plant growth.

3.4. Conclusions

In this study, oxalic acid production was optimized via SSF using *Aspergillus niger* to enhance the solubilization of phosphate rocks. The findings revealed that a 1:1 ratio of sugarcane bagasse and soybean bran significantly improved oxalic acid production. The addition of 7% methanol and 5 g kg^{-1} d.s. sucrose tripled oxalic acid yields. Under these optimized conditions, even low reactive igneous rocks showed notable solubilization. Additionally, the solid-state fermentation process effectively released organic phosphorus from the substrates. This approach has the potential to support the development of environmentally sustainable and cost-effective phosphorus biofertilizers.

References

Amaro, J. K. C., Xavier, L. V., Ribeiro, M. M. A. D. C., Vieira, B. S., Mendes, G. D. O., 2022. Optimization of oxalic acid production by fungi for biotechnological solubilization of rock phosphate. Sci. Agric. 80, e20210076.

Amenaghawon, N. A., Agbedor, M., 2021. A multilayer full feed forward neural network for modelling and optimizing nutrient medium composition for oxalic acid production from sweet potato peels. ATBU J. Sci. Educ. 9, 44-53.

Anwar, S., Ali, S., and Sardar, A. A, 2009. Citric acid fermentation of hydrolysed raw starch by *Aspergillus niger* IIB-A6 in stationary culture. Sindh Univ. Res. J. (Sci. Ser.), 41, 1–8.

Behera, S. S.; Ray, R. C., 2016. Solid-state fermentation for production of microbial cellulases: recent advances and improvement strategies. Int. J. Biol. Macromol. 86, 656–669.

Bellaouchi, R., Abouloifa, H., Rokni, Y., Hasnaoui, A., Ghabbour, N., Hakkou, A., Bechchari, A., Asehraou, A., 2021. Characterization and optimization of extracellular enzymes production by *Aspergillus niger* strains isolated from date by-products. J. Genet. Eng. Biotechnol. 19, 50.

Bradford, M. M., 1976. A rapid and sensitive method for the quantitation of microgram quantities of protein utilizing the principle of protein-dye binding. Anal. Biochem. 72, 248-254.

Cameselle, C., Bohlmann, J. T., Nunez, M. J., Lema, J. M., 1998. Oxalic acid production by *Aspergillus niger*: Part I: Influence of sucrose and milk whey as carbon source. Bioprocess Eng. 19, 247-252.

Carvalho, W., Silva, D. D. V., Canilha, L., Mancilha, I. M., 2005. Food additives produced by fermentation part I: organic acids. Rev. Anal. 18, 70-76.

Casciatori, F. P., Laurentino, C. L., Taboga, S. R., Casciatori, P. A., Thomeo, J. C., 2014. Structural properties of beds packed with agro-industrial solid by-products

applicable for solid-state fermentation: experimental data and effects on process performance. Chem. Eng. J. 255, 214-224.

Casciatori, F. P., Mafra, N. S. C., Rodrigues, N. A., Sales, E. H., Maia, M. M. S., Dias, A. C. P., Grajales, L. M., 2024. Flow configuration and Packing Density of Sugarcane Bagasse and Wheat Bran Affecting Enzymes Production by Solid-State Fermentation. Bioenergy Res. 17, 187-197.

Dai, Z., Lu, J., Li, X., Lu, M., Yang, W., Gao, X., 2010. Nutrient release characteristic of different crop straws manure. Trans. Chin. Soc. Agric. Eng. 26, 272-276.

FAO. Food and Agriculture Organization of the United Nations, 2024. FAOSTAT. Database. Available from: https://www.fao.org/faostat/en/#data/RFN. [Accessed on: June 2024].

Farinas, C. S., 2015. Developments in solid-state fermentation for the production of biomass-degrading enzymes for the bioenergy sector. Renew. Sustain. Energy Rev. 52, 179–188.

Favaro, C. P., Klaic, R., Bettiol, W., Ribeiro, C., Farinas, C. S., 2022. Bio-based composite granules with simultaneous biocontrol and phosphorus fertilization roles: Outcomes from a lab-scale in vitro assessment. Biotechnol. Prog. 38, e3242.

Generoso, R. A. R., Gomes, P. C., Rostagno, H. S., Albino, L. F. T., Barreto, S. L. D. T., Brumano, G., 2008. Chemical and energetic composition of some foods for broiler chickens at two ages. Rev. Bras. Zootec. 37, 1251-1256.

Ghose, T. K., 1987. Measurement of cellulase activities. Pure Appl. Chem., 59, 257-268.

Ingelmann, C. J., Witzig, M., Möhring, J., Schollenberger, M., Kühn, I., Rodehutscord, M., 2018. Effect of supplemental phytase and xylanase in wheat-based diets on prececal phosphorus digestibility and phytate degradation in young turkeys. Poult. Sci. 97, 2011-2020.

Jain, R., Saxena, J., Sharma, V., 2010. The evaluation of free and encapsulated *Aspergillus awamori* for phosphate solubilization in fermentation and soil–plant system. Appl. Soil Ecol. 46, 90-94.

Klaic, R., Gava Junior, M., Florencio, C., Ribeiro, C., Farinas, C. S., 2021. Biological solubilization of phosphate rock by solid-state cultivation to produce eco-friendly fertilizers. Pesqui. Agropecu. Bras. 56, e01441.

Klaic, R., Plotegher, F., Ribeiro, C., Zangirolami, T. C., Farinas, C. S., 2018. A fed-batch strategy integrated with mechanical activation improves the solubilization of phosphate rock by *Aspergillus niger*. ACS Sustain. Chem. Eng. 6, 11326-11334.

Klaic, R., Plotegher, F., Ribeiro, C., Zangirolami, T. C., Farinas, C. S., 2017. A novel combined mechanical-biological approach to improve rock phosphate solubilization. Int. J. Miner. Process. 161, 50-58.

Leangon, S., Maddox, I. S., Brooks, J. D., 1999. Influence of the glycolytic rate on production of citric acid and oxalic acid by *Aspergillus niger* in solid-state fermentation. World J. Microbiol. Biotechnol. 15, 493-495.

Lian, B., Wang, B., Pan, M., Liu, C., Teng, H. H., 2008. Microbial release of potassium from K-bearing minerals by thermophilic fungus *Aspergillus fumigatus*. Geochim. Cosmochim. Acta. 72, 87-98.

Lodi, L. A., Klaic, R., Ribeiro, C., Farinas, C. S., 2021. A green K-fertilizer using mechanical activation to improve the solubilization of a low-reactivity potassium mineral by *Aspergillus niger*. Bioresour. Technol. Rep. 15, 100711.

Mai, H. T. N., Lee, K. M., Choi, S. S., 2016. Enhanced oxalic acid production from corncob by a methanol-resistant strain of *Aspergillus niger* using semi solid-sate fermentation. Process Biochem. 51, 9-15.

Mendes, G. D. O., Vassilev, N. B., Bonduki, V. H. A., da Silva, I. R., Ribeiro Jr, J. I., Costa, M. D., 2013. Inhibition of *Aspergillus niger* phosphate solubilization by fluoride released from rock phosphate. Appl. Environ. Microbiol. 79, 4906-4913.

Mendes, G., Moreira de Freitas, A. L., Liparini Pereira, O., Ribeiro da Silva, I., Bojkov Vassilev, N., Dutra Costa, M., 2014. Mechanisms of phosphate solubilization by fungal isolates when exposed to different P sources. Ann. Microbiol. 64, 239-249.

Mendes, G. D. O., da Silva, N. M. R. M., Anastácio, T. C., Vassilev, N. B., Ribeiro Jr, J. I., da Silva, I. R., Costa, M. D., 2015. Optimization of *Aspergillus niger* rock phosphate solubilization in solid-state fermentation and use of the resulting product as a P fertilizer. Microb. Biotechnol. 8, 930-939.

Mendes, O. G., Murta, H. M., Valadares, R. V., da Silveira, W. B., da Silva, I. R., Costa, M. D., 2020. Oxalic acid is more efficient than sulfuric acid for rock phosphate solubilization. Miner. Eng. 155, 106458.

Mendes, G. D. O., Dyer, T., Csetenyi, L., Gadd, G. M., 2022. Rock phosphate solubilization by abiotic and fungal-produced oxalic acid: reaction parameters and bioleaching potential. Microb. Biotechnol. 15, 1189-1202.

Murphy, J. A. M. E. S., Riley, J. P., 1962. A modified single solution method for the determination of phosphate in natural waters. Anal. Chim. Acta. 27, 31-36.

Penn, C. J., Camberato, J. J., 2019. A critical review on soil chemical processes that control how soil pH affects phosphorus availability to plants. Agriculture, 9, 120.

Ramachandran, S., Fontanille, P., Pandey, A., Larroche, C., 2006. Gluconic acid: properties, applications and microbial production. Food Technol. Biotechnol. 44, 185-195.

Rodrigues, N. A., Katayama, E. T., Casciatori, F. P., 2022. Alternative strategies to perform solid-state cultivation in a multilayer packed-bed bioreactor: Continuous and cyclic operations. Chem. Eng. J. 448, 137726.

Roehr, M., Kubicek, C. P., Komínek, J., 1996. Gluconic acid, in: Rehm, H. J., Reed, G. (Eds.), Biotechnology: Products of Primary Metabolism, Verlag Chemie, Weinheim, pp. 347–362.

Silva, U. D. C., Mendes, G. D. O., Silva, N. M. R., Duarte, J. L., Silva, I. R., Totola, M. R., Costa, M. D., 2014. Fluoride-tolerant mutants of *Aspergillus niger* show enhanced phosphate solubilization capacity. PLoS One. 9, e110246.

Soccol, C. R., Vandenberghe, L. P., Rodrigues, C., Pandey, A., 2006. New perspectives for citric acid production and application. Food Technol. Biotechnol. 44, 141-149.

Szczerbowski, D., Pitarelo, A. P., Zandoná Filho, A., Ramos, L. P., 2014. Sugarcane biomass for biorefineries: comparative composition of carbohydrate and non-carbohydrate components of bagasse and straw. Carbohydr. Polym. 114, 95-101.

Tabatabai, M. A., Bremner, J. M., 1969. Use of p-nitrophenyl phosphate for assay of soil phosphatase activity. Soil biology and biochemistry, 1, 301-307.

Usami, S., Taketomi, N., 1961. Use of methyl alcohol as a promotive agent in citric acid fermentation. Hakko-Kyokaishi. 19, 435–442.

Vassilev, N., Medina, A., Azcon, R., Vassileva, M., 2006. Microbial solubilization of rock phosphate on media containing agro-industrial wastes and effect of the resulting products on plant growth and P uptake. Plant Soil. 287, 77–84.

Vassilev, N., Mendes, G., Costa, M., Vassileva, M., 2014. Biotechnological tools for enhancing microbial solubilization of insoluble inorganic phosphates. Geomicrobiol. J. 31, 751-763.

Walaszczyk, E., Gasiorek, E., Podgórski, W., 2017. Effect of sucrose concentration on oxalic acid biosynthesis by *Aspergillus niger*. Zesz. Probl. Post. Nauk Roln. 588, 129–138.

Walaszczyk, E., Podgórski, W., Janczar-Smuga, M., Dymarska, E., 2018. Effect of medium pH on chemical selectivity of oxalic acid biosynthesis by *Aspergillus niger* W78C in submerged batch cultures with sucrose as a carbon source. Chem. Pap. 72, 1089-1093.

Wan, W. J., Wang, Y., Tan, J. D., Qin, Y., Zuo, W. L., Wu, H. Q., He, H. M., He, D. L, 2020. Alkaline phosphatase-harboring bacterial community and multiple enzyme activity contribute to phosphorus transformation during vegetable waste and chicken manure composting. Bioresour. Technol. 297, 122406.

Wang, L., Guan, H., Hu, J., Feng, Y., Li, X., Yusef, K. K., Gao, H., Tian, D., 2022. *Aspergillus niger*. Enhances Organic and Inorganic Phosphorus Release from Wheat Straw by Secretion of Degrading Enzymes and Oxalic Acid. J. Agric. Food Chem, 70, 10738-10746.

Xiao, C. Q., Chi, R. A., Huang, X. H., Zhang, W. X., Qiu, G. Z., Wang, D. Z., 2008. Optimization for rock phosphate solubilization by phosphate-solubilizing fungi isolated from phosphate mines. Ecol. Eng. 33, 187-193.

Yang, L., Lübeck, M., Lübeck, P. S., 2017. *Aspergillus* as a versatile cell factory for organic acid production. Fungal Biol. Rev. 31, 33-49.

Zambom, M. A., Santos, G. T., Modesto, E. C., Alcalde, C. R., Gonçalves, G. D., Silva, D. C., Silva, K. T., Faustino, J. O., 2001. Nutritional value of soybean hull, soybean meal, ground corn, and wheat bran for cattle. Acta Sci. Anim. Sci. 23, 937-943.

Chapter 4

4. Bioconversion of phosphate rock by *Aspergillus niger* in packed bed bioreactors: toward scalable biofertilizer production for agricultural use

ABSTRACT

This study evaluated the solubilization of phosphate rock (PR) from Registro (São Paulo, Brazil) by solid-state fermentation (SSF) using *Aspergillus niger* in a multilayer packed-bed bioreactor (PBB). Preliminary lab-scale experiments demonstrated that the omission of sucrose and mineral salts from the culture medium did not impair oxalic acid production or PR solubilization. Ethanol was also tested as a substitute for methanol (a modulator for oxalic acid synthesis). Although it induced acid production, it was less effective at equivalent concentrations of methanol. In the bench-scale using PBB, phosphate release efficiency declined - likely due to methanol evaporation - reaching a maximum of 24.6%. Methanol supplementation via the air humidification system was explored as a strategy to overcome this problem, but did not recover lab-scale performance. Despite this, in situ drying within the PBB effectively preserved microbial viability and acid phosphatase activity for 34 days. Greenhouse tests using biofertilizers produced on a lab-scale showed that replacing 50% of the chemical fertilizer with biofertilizers promoted plant performance equivalent to the control, in which only chemical fertilizer was added. These findings underscore both the potential and challenges of scaling up PR solubilization via SSF in aerated bioreactors, highlighting the need for further optimization to match lab-scale efficiencies.

Keywords: Phosphorus, Solid-state fermentation, Organic acids, Sustainable agriculture, Phosphate-solubilizing microorganisms.

4.1. Introduction

The solubilization of phosphate rocks (PRs) through biotechnological approaches, particularly using phosphate-solubilizing microorganisms (PSMs), has emerged as a promising strategy for producing phosphate biofertilizers and reducing reliance on conventional chemical fertilizers (Rawat et al., 2021). Among the known mechanisms, the production of organic acids - leading to acidification of the medium -

is widely recognized as the primary process responsible for the solubilization of inorganic P (Mendes et al., 2020).

In this context, this strategy has been studied mainly with the use of the filamentous fungus *Aspergillus niger*, both by submerged fermentation (SmF) and solid-state fermentation (SSF), due to its remarkable capacity to produce large quantities of organic acids such as citric, oxalic, gluconic, and malic acids (Mendes et al., 2015; Klaic et al., 2017; Klaic et al., 2018). Furthermore, *A. niger* is known for its strong enzymatic profile, including the production of phosphatases, which have an important contribution to the mineralization of organic P present in the soil, which is mainly in the form of phytate (Laothanachareon et al., 2022).

Significant advances have been made in optimizing this biotechnological route. Klaic et al. (2017, 2018) demonstrated that mechanical pretreatment of PRs substantially enhances solubilization yields and that a batch-fed operation mode can further improve efficiency. Complementing these findings, Mendes et al. (2020) evaluated the solubilization capacity of various organic acids and identified oxalic acid as the most effective. Building upon this knowledge, Rodrigues et al. (2024) successfully optimized oxalic acid production by *A. niger* under SSF conditions and reported that methanol acts as a potent metabolic modulator, tripling oxalic acid production compared to control conditions. Under these optimized conditions, up to 12 g of soluble P per kg of dry substrate was achieved, corresponding to a solubilization efficiency of 64%.

Despite the promising outcomes of these studies, they remain restricted to lab-scale systems. However, due to the urgent need to transition to more sustainable agriculture, it is important that these processes also be investigated on a larger scale (Díaz-Rodríguez et al., 2025). In particular, scaling up is quite challenging for SSF processes, since significant gradients in temperature, humidity, and oxygen availability are usually observed (Perez et al., 2021; Casciatori et al., 2024). Nonetheless, SSF offers advantages in the context of sustainable agriculture, including the potential to utilize agro-industrial residues as substrates, thus aligning with circular economy principles.

Considering the advances reported by Rodrigues et al. (2024), the present study aimed to investigate the solubilization of Registro PR via SSF using *A. niger* in a multilayer packed-bed bioreactor (PBB). To our knowledge, this is the first time that the

phosphate rock solubilization process through SSF has been evaluated in a PBB. In addition to evaluating the viability of this process, the study explored the potential for in-situ drying of the fermented solids within the bioreactor itself - a downstream strategy intended to preserve both microbial viability and enzymatic activity. To complement the bioprocess development, greenhouse trials with lettuce were conducted using biofertilizers produced at lab-scale, offering preliminary insights into their agronomic potential under controlled conditions.

4.2. Material and methods

4.2.1. Characterization of mineral rocks

In the solubilization experiments, the Registro PR, which was kindly donated by Nutrisafra Fertilizantes Ltda. (Cosmopolis, SP, Brazil) was used. The rock was dried in a stove (Model 035, Marconi, Brazil) at 110ºC for 48 hours to reduce humidity content and stored in dry boxes at room temperature for further use in the experiments. The characterization of the the was carried out by Favaro et al. (2022) and the results are presented in Table 4.1.

Table 4.1. Physicochemical analysis of the Registro phosphate rock (Favaro et al., 2022).

Oxide species	Registro rock (mass %)
SiO_2	2.21
Al_2O_3	3.91
Fe_2O_3	14.1
CaO	34.9
MgO	0.36
TiO_2	0.63
P_2O_5	28.08
Na_2O	0.51
K_2O	0.08
MnO	1.69
Loss on ignition	6.54
Total	93.01
F	1.18

Analyzes consisted of X-ray diffraction (XRD) and X-ray fluorescence (XRF) to determine the 10 most common oxides found in the ores and specific ion analysis to determine fluorine (F). After that, the rock was submitted to mechanical treatment for 20 min aiming to improve the solubilization process, as reported by Klaic et al. (2017), in an orbital mill (Model CT-251, Servitec) consisting of a porcelain jar and alumina balls.

4.2.2. Microorganism and substrates

The filamentous fungus *Aspergillus niger* C (BRMCTAA 82) was obtained from the Embrapa Food Agroindustry collection (Rio de Janeiro, Brazil). This strain was selected due its excellent organic acids production (Klaic et al., 2017; Rodrigues et al., 2024). The spores were germinated in Erlenmeyer flasks containing 60 mL of potato dextrose agar (PDA), which were allowed to solidify tilted. The flasks were kept in a Biochemical Oxygen Demand (BOD) chamber (Model SL 200, Solab, Brazil) at 30°C for at least 5 days. After that, the agar surface was gently scraped with distilled water to obtain the spore suspension which was used as inoculum in the cultivations. The spore concentration was determined using a Neubauer chamber.

As solid substrates, the agro-industrial by-products sugarcane bagasse (SCB) and soybean bran (SB) were used in a proportion of 1:1 (w:w). These substrates were chosen because they provided a good production of oxalic acid by the same strain used in this study, as reported by Rodrigues et al. (2024). The SCB was donated by Usina Itajobi (Marapoama, SP, Brazil) and the SB was acquired in local businesses (Agropecuária Claro, São Carlos, SP, Brazil). All by-products were dried in a stove (Model 035, Marconi, Brazil) at 60°C until constant mass and the SCB was sieved to remove powder and coarser fibers, passing through sieves with an opening of 5 × 5 mm and 4 × 2 mm, respectively. It is important to note that the by-products, used as substrates, did not undergo any additional pre-treatment or washing.

4.2.3. Solid-state fermentation

The SSF processes were conducted at the lab-scale using 12 × 20 cm polypropylene packages fitted with a 3.6 cm diameter polyvinyl chloride nozzle, and at the bench scale using a multilayer packed bed bioreactor (PBB). Registro rock was added at a quantity of 120 g per kg of dry substrate (d.s.) in all cultivations at both

scales. This value was chosen based on Rodrigues et al. (2024), who reported a P release efficiency of approximately 60% at this concentration. High PR loadings per kg of dry substrate are essential for biofertilizers to significantly reduce the reliance on synthetic fertilizers. Further details about the cultivations are presented in the following sections.

4.2.3.1. Lab-scale experiments

For SSF carried out in polypropylene packages, 5 g of dry substrate - composed of 2.5 g of SCB and 2.5 g of SB - was used per package. Moisture content was adjusted to 70% (wet basis) for all treatments. Both the substrates and the humidifying solution were autoclaved at 121 °C for 20 minutes before fermentation. After cooling, they were mixed and homogenized with the inoculum inside a previously sterilized laminar flow chamber. The inoculum was prepared to provide an initial concentration of 1×10^7 spores g^{-1} d.s.

In treatments involving methanol or ethanol, these compounds were added only after the autoclaved substrates had cooled. All laboratory-scale fermentations were carried out at 30 °C for 3 days in a BOD chamber. This incubation period was selected based on the findings of Rodrigues et al. (2024), who observed that P release and oxalic acid production peaked and stabilized after 72 hours. For each condition evaluated, a non-inoculated package was incubated in parallel as a control.

4.2.3.1.1. Effect of sucrose and mineral salt addition to the cultivation medium

In a previous study, Rodrigues et al. (2024) optimized oxalic acid production and PR solubilization in SSF using a 1:1 (w:w) mixture of SCB and SB as substrates and *A. niger* as the microbial agent. In that study, the authors employed a saline solution to humidify the substrate and supplemented the medium with sucrose. The composition of the saline solution was as follows: 0.25% $(NH_4)_2SO_4$, 0.1% KH_2PO_4, 0.025% $MgSO_4 \cdot 7H_2O$, and 0.004% $CuSO_4$. Based on the optimization results, the ideal sucrose addition was determined to be 5 g kg^{-1} d.s.

Considering the aim of evaluating the feasibility of larger-scale production, the current work investigated whether the culture medium could be simplified by excluding sucrose and mineral salt supplementation. Three treatments were evaluated: (1) addition of both saline solution and sucrose, following the optimized conditions reported by

Rodrigues et al. (2024); (2) addition of saline solution without sucrose; and (3) no addition of saline solution or sucrose, with substrates moistened using distilled water only.

4.2.3.1.2. Effect of ethanol in the solubilization process of phosphate rock

To further simplify and improve the process for potential large-scale application, the replacement of methanol with ethanol in the culture medium was evaluated, given that ethanol is a renewable compound with lower toxicity. According to the optimization study conducted by Rodrigues et al. (2024), the addition of 7% methanol (w w^{-1}) resulted in a threefold increase in oxalic acid production. Based on this, ethanol was tested at concentrations of 6, 9, and 12% (w w^{-1}) as a substitute for methanol. The experimental conditions were defined based on the evaluation described in section 4.2.3.1.1.

4.2.3.2. Experiments at bench scale

Figure 4.1 provides an overview of the experimental setup using the multilayer PBB. Compressed air was first filtered and then directed sequentially through a flow meter and two humidifiers - one maintained at ambient temperature and the other thermally regulated at the process temperature. Each humidifier was filled with glass beads, and the interstitial spaces were saturated with distilled water to ensure complete humidification of the incoming air. Upon exiting the PBB, the air passed through a dehumidification system consisting of a trap, in which the condensed water was collected in a flask and then passed through a silica column (5.2 cm in diameter and 39 cm tall). This system reduced the air's relative humidity to below 15%, allowing accurate real-time CO_2 measurement using a VAISALA Analog Output Transmitter Indigo 201 sensor.

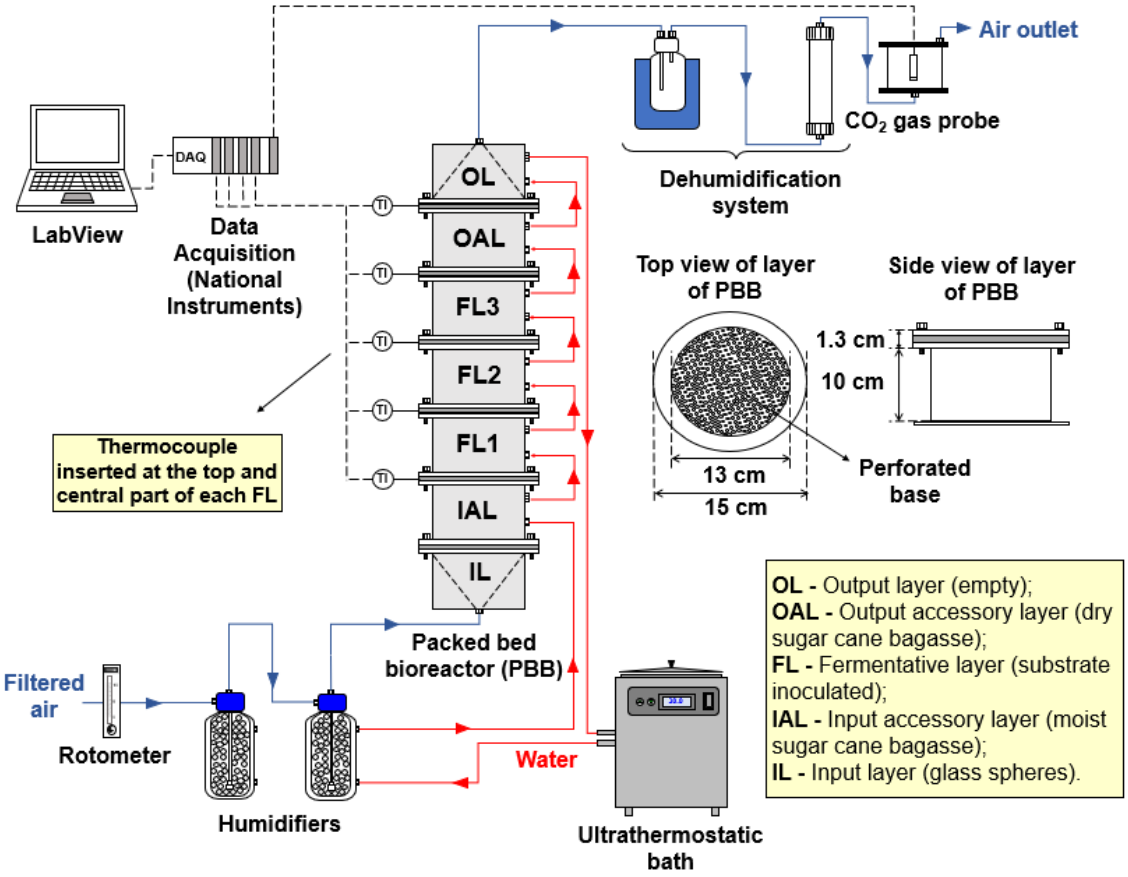

Fig. 4.1. Schematic representation of the experimental apparatus at bench scale using a multilayer packed-bed bioreactor. Figure extracted and adapted from Rodrigues et al. (2022).

The bioreactor configuration is the same to that used in the studies by Rodrigues et al. (2022). It is a PBB composed of cylindrical stainless-steel layers with a perforated bottom that are 10 cm high, 13 cm internal diameter and 15 cm external diameter. The annular space was used as a jacket for water circulation to maintain the ideal process temperature (30°C).

To ensure uniform air distribution, glass spheres were placed in the inlet layer (IL). The inlet accessory layer (IAL) was packed with moist SCB to ensure air saturation when entering the bed. At the opposite end, the outlet accessory layer (OAL) was packed with dry SCB to capture any moisture that might condense, while the outlet layer (OL) remained empty. The intermediate fermentative layers (FLs) were filled with moist substrate inoculated with fungal spores. Between each layer, a flange (1.3 cm thick) was placed, together with a rubber ring, to ensure the sealing of the equipment. T-

type thermocouples were inserted through these flanges, extending to the central top area of each layer for real-time temperature monitoring.

Prior to inoculation and packing, the layers were sanitized with 70% ethanol and exposed to ultraviolet light for 15 minutes. The packing technique used was loose packing proposed by Casciatori et al. (2014), in which the substrates are smoothly accommodated without causing bed compression. All procedures were performed under sterile conditions.

Three batches were performed, each containing three fermentative layers (FL1, FL2, and FL3). Batches 1 and 2 included the addition of 7% methanol (w w^{-1}) to the solid matrix. In Batch 2, methanol was also added to the humidifiers at the same concentration. Batch 3 was conducted without methanol addition. In all batches, the airflow was maintained at 250 L h^{-1}, slightly lower than the rate used by Rodrigues et al. (2022), (350 L h^{-1}) in order to minimize methanol loss.

4.2.3.2.1 Drying process of the fermented solids

At the end of the SSF process for Batch 1, the fermentative layer FL1 - containing fermented solids - was repositioned within the bioreactor, placed directly above the inlet layer (IL) and below the outlet layer (OL), as shown in in Fig. 4.2a and 4.2b, which provide a schematic illustration of the experimental apparatus and a real image, respectively. Filtered air, previously passed through a silica column to reduce humidity, was then percolated through the packed bed at a flow rate of 700 L h^{-1}. The ultrathermostatic bath responsible for circulating water through the bioreactor's jackets, as well as through the silica column, was maintained at 30 °C.

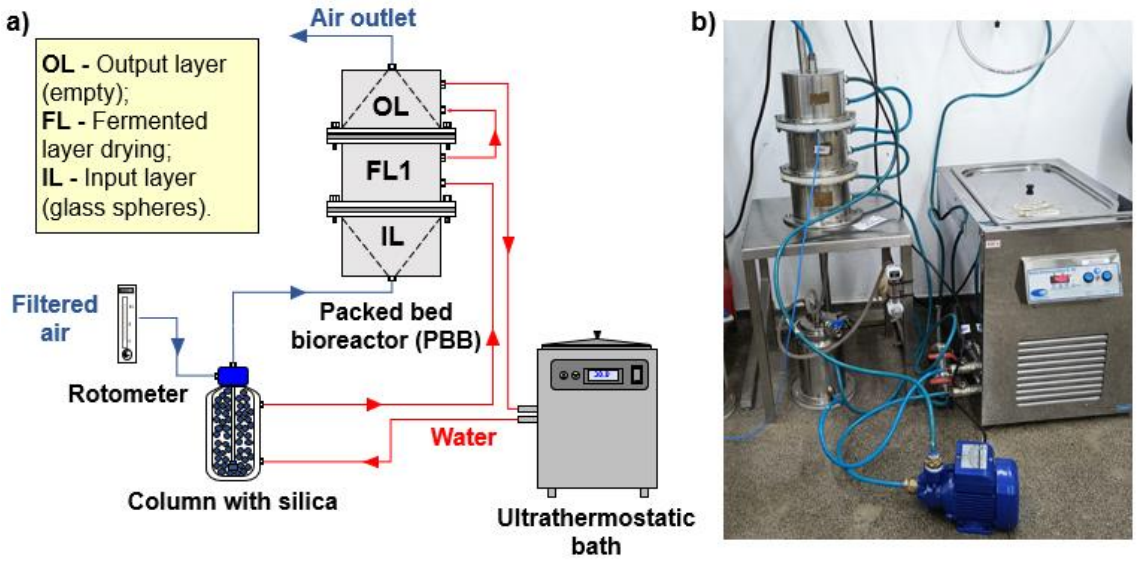

Fig. 4.2. a) Schematic representation and b) real image of the experimental setup used for drying fermented solids using the multilayer packed-bed bioreactor itself.

Drying was carried out until the relative humidity of the outlet air decreased to ≤ 5%. After completion of the drying process, the moisture content of the fermented solids was measured, and the dried material was stored at 4°C. Microbial viability as well as acid phosphatase (ACP) activity were monitored during 34 days of storage.

4.2.4. Application of biofertilizers in soil-plant system

To assess the agronomic potential of the biofertilizers developed through the SSF processes described in this study, a greenhouse trial was conducted at ParcTec (São Carlos, São Paulo, Brazil) in collaboration with Ikove Agro Bioinsumos Agrícolas Ltda. Lettuce was selected as the test crop due to its short growth cycle. The cultivation was carried out in pots (Fig. 4.3a) for 30 days, using sphagnum peat as an inert substrate. Throughout the experimental period, plants were irrigated daily using an automatic system to ensure consistent water supply.

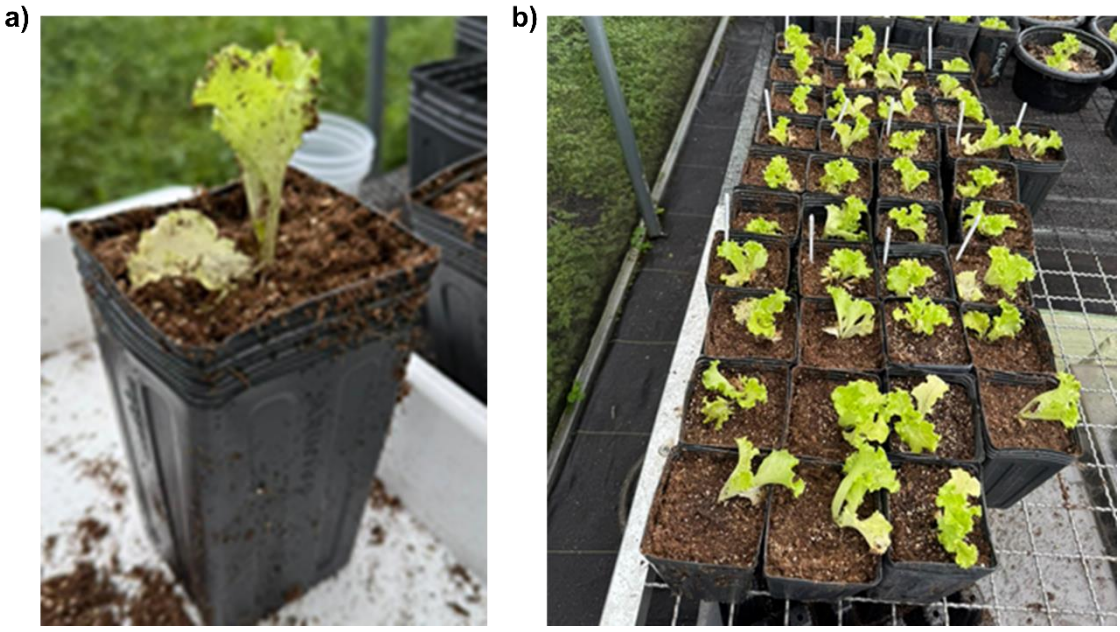

Fig. 4.3. a) Experimental pots prepared for lettuce cultivation; b) Overview of the greenhouse setup at the beginning of the trial.

Biofertilizers were produced at the lab-scale using polypropylene packages, and three different treatments involving the biofertilizers were compared with a control. Each treatment included 9 replicates (Fig. 4.3b). In all treatments, the P dose was standardized to 60 mg per pot (Van Raiji et al., 1997). In the control treatment, the entire P dose was provided by a commercial synthetic fertilizer (Maxgreen). In the other treatments, 50% of the P was supplied by the synthetic fertilizer, while the remaining 50% was replaced with biofertilizers derived from the SSF process.

The first treatment consisted of applying fermented solids produced by SSF with 7% methanol and 120 g kg^{-1} d.s. of Registro rock incorporated into the matrix. The second treatment involved fermented solids produced under the same conditions but without the addition of methanol. In the third treatment, a liquid extract - free of cells and insoluble particles - was applied. This extract was obtained from fermented solids produced with 7% methanol and the same concentration of Registro rock. The control treatment involved the application of chemical fertilizer only, without any biofertilizer component.

4.2.5. Analytical procedures

At the end of the SSF process, solid-liquid extraction was performed by adding 15 mL of distilled water g^{-1} d.s. This process involved mixing the sample with the water, followed by agitation for 30 minutes at 25°C in an orbital shaking incubator. After extraction, the samples were centrifuged (Model 5810R, Eppendorf, Germany) for 20 min at 10000 rpm and 4°C and vacuum-filtered. The resulting supernatants were used for analytical determinations, except for microbial growth analysis, in which the crude extract was used directly.

4.2.5.1. Colony-forming unit counting

Microbial growth was estimated by counting colony-forming units (CFU), which indicate the number of viable cells capable of forming colonies. For this analysis, the distilled water used for extraction was previously sterilized. The resulting extracts were appropriately diluted and plated on potato dextrose agar (PDA) supplemented with 0.1 g L^{-1} of rose bengal. Plates were incubated at 30 °C for 2 days, after which colonies were counted. Rose bengal is a dye that inhibits bacterial growth and limits fungal colony expansion, enabling discrete colony formation for accurate counting. The CFU count was calculated according to Eq. 4.1

$$\mathrm{CFU} = \frac{\mathrm{CN} \times \mathrm{DF} \times \mathrm{EV}}{\mathrm{PV} \times \mathrm{SDM}} \tag{4.1}$$

where: CN is the colonies number; DF is the dilution factor of the plated sample; EV is the volume of the distilled water used for extraction; PV is the volume of the plated sample; SDM is the sample dry matter subjected to extraction.

4.2.5.2. Oxalic acid determination

The production of oxalic acid was determined using a Waters Model 410 HPLC (high-performance liquid chromatography) equipped with a UV detector (210 nm) and an Aminex HPX87-H column maintained at 55°C. The eluent was 5 mM sulfuric acid in Milli-Q water at a flow rate of 0.6 mL/min. All samples were filtered using a 0.22 μm filter previously to be injected into the equipment.

4.2.5.3. Soluble and total P determination

The soluble P content was determined using a colorimetric method adapted from the work of Murphy and Riley (1962). A 5 mL volume of the clear supernatant sample was reacted with 2 mL of ascorbic acid solution (0.4 mol L^{-1}), 0.2 mL of citric acid (0.03 mol L^{-1}), and 2 mL of a reagent composed of 25 mL of a sulfuric acid solution (4.7 mol L^{-1}), 5.5 mL of ammonium molybdate solution (0.08 mol L^{-1}), and 0.6 mL of an antimony and potassium tartrate solution (0.05 mol L^{-1}). This mixture was reacted at 50°C for 15 min in thermostatic bath, forming a blue phosphoantimonylmolybdenum complex at the end of the reaction. The concentration of the complex was determined by spectrophotometry (Ultrospec 2100 pro, Amersham, UK) at 880 nm, using a KH_2PO_4 standard curve at concentrations from 5 to 70 µmol L^{-1}.

The efficiency of P solubilization was calculated using Eq. (4.2), considering the total initial P present in the medium. This included both the P introduced from Registro rock and the P naturally present in the substrates.

$$\text{P solubilization efficiency}(\%) = \frac{\text{Solubilized P}}{\text{Initial Total P}} \times 100 \quad (4.2)$$

The total P content of the substrates was determined by the company Ciência em Solo Laboratório de Análises e Consultoria Agrícola. The method applied was nitro-perchloric digestion and determination by UV-vis spectroscopy with ammonium molybdate. The values obtained was 3.9 and 1.7 g kg^{-1} d.s. of total P for SB and SCB, respectively.

4.2.5.4. Phosphatase activity assays

Phosphatase activities were measured by quantifying the amount of p-nitrophenol released from 5 mM p-nitrophenyl phosphate (p-NPP) in the respective buffer at 37°C. The reaction was carried out for 10 minutes and was stopped by the addition of 1 mL of 0.1 M NaOH. The amount of p-nitrophenol released was measured at 410 nm, and its concentration was determined using a calibration curve made with concentrations of 10 – 60 µmol L^{-1} of p-nitrophenol. One unit (U) of acid phosphatase activity was defined as 1 µmol of p-nitrophenol released per hour under the assay conditions (Tabatabai and Bremner, 1969).

4.2.6. Statistical analyzes

Minitab® 16 software (Minitab Inc., State College, USA) was used to perform analysis of variance (ANOVA) and comparisons between means by Tukey test, with a confidence level of 95%. Contour plots were also performed using Minitab®.

4.3. Results and discussion

4.3.1. Effect of sucrose and mineral salt addition to the cultivation medium

To evaluate the solubilization process of the Registro PR in a multilayer PBB, preliminary experiments were first conducted at the lab-scale using polypropylene packages, based on the conditions previously optimized by Rodrigues et al. (2024), which included the addition of 7% methanol (w w^{-1}) and 5 g kg^{-1} d.s. of sucrose. These initial trials aimed to assess whether the humidification solution used to moisten the substrates could be simplified by excluding sucrose and mineral salts - an adjustment that could significantly reduce production costs at larger scales. The results of this comparison are presented in Fig. 4.4.

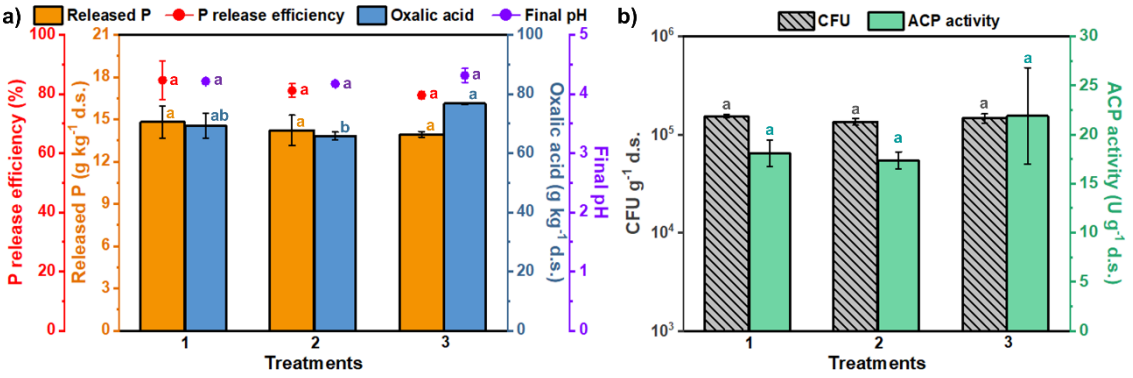

Fig. 4.4. Results of a) released P, P release efficiency, oxalic acid production, final pH, b) colony-forming units (CFU) and acid phosphatase (ACP) activity for the following treatments: (1) with sucrose and mineral salts, (2) without sucrose and with mineral salts, and (3) without sucrose and without mineral salts. All cultivations were carried out with the addition of 7% methanol (w w^{-1}) and 120 g kg^{-1} d.s. of Registro rock. Different letters indicate statistically significant differences between treatments ($\alpha \leq 0.05$), while the same letters indicate no significant difference.

According to Fig. 4.4a and 4.3b, a significant difference was observed only between treatments 2 (without sucrose, with salts) and 3 (without sucrose and salts) for oxalic acid production, with treatment 3 showing slightly higher levels. All other evaluated parameters did not differ significantly among the three treatments, indicating that the addition of sucrose or mineral salts to the solid matrix is unnecessary. Therefore, in subsequent experiments, the substrates were moistened only with water. These findings are likely related to the complex composition of the substrates used, which contain diverse types of carbohydrates, proteins, and mineral salts (Oviedo-Rondon et al., 2024), along with the robust enzymatic capacity of *A. niger* (Laothanachareon et al., 2022).

4.3.2. Effect of ethanol in the solubilization process of phosphate rock

In addition to assessing the feasibility of excluding sucrose and mineral salts from the cultivation medium, the potential to replace methanol with ethanol was also evaluated prior to initiating the bioreactor experiments, considering ethanol's renewable origin and lower toxicity (Pohanka, 2016). The results are presented in Fig. 4.5.

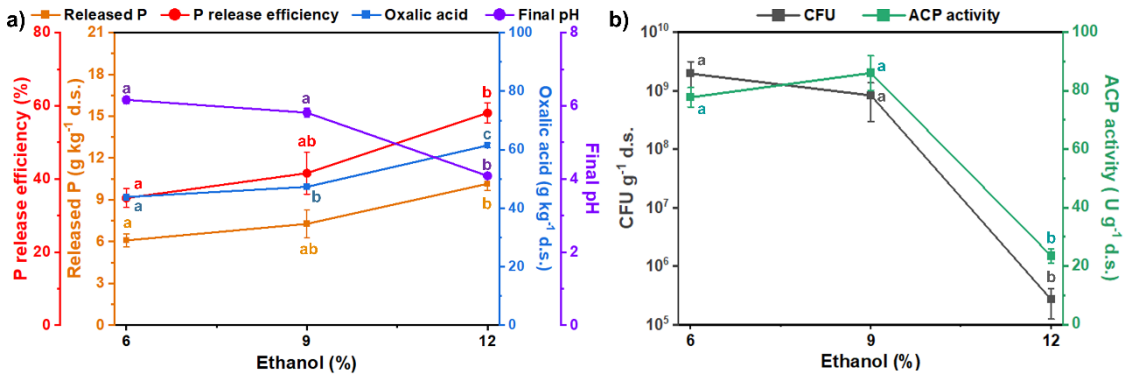

Fig. 4.5. Effect of adding 6, 9 and 12% of ethanol to the cultivation medium on the following responses: a) released P, P release efficiency, oxalic acid production, final pH, b) colony-forming units (CFU) and acid phosphatase (ACP) activity. All cultivations were carried out with the addition of 120 g kg^{-1} d.s. of Registro rock. Different letters indicate statistically significant differences between treatments ($\alpha \leq 0.05$), while the same letters indicate no significant difference.

In general, increasing the ethanol content resulted in higher oxalic acid production, which in turn lowered the final pH and enhanced P release. At 12% ethanol, all these parameters were significantly different compared to the 6% ethanol treatment, as shown in Fig. 4.5a. Additionally, microbial growth and ACP activity were significantly lower at 12% ethanol compared to 6%, as shown in Fig. 4.4b.

At 6% and 9% ethanol, microbial growth appeared to be less affected, reaching 2.0×10^9 CFU g^{-1} d.s. and 8.3×10^8 CFU g^{-1} d.s., respectively. In contrast, at 12% ethanol, the CFU count dropped to 2.7×10^5 g^{-1} d.s., representing a reduction of 3 - 4 orders of magnitude. ACP activity followed a similar trend: values at 6% and 9% ethanol were 77.7 and 86.0 U g^{-1} d.s., respectively, while at 12%, it decreased to 23.5 U g^{-1} d.s. - approximately three times lower. For comparison, in the treatments with 7% methanol (Fig. 4.4b), CFU and ACP activity averaged 1.5×10^5 CFU g^{-1} d.s. and 19 U g^{-1} d.s., respectively.

These results suggest that, similar to methanol, ethanol redirects metabolic activity toward oxalic acid accumulation rather than biomass formation. However, even at the highest ethanol content tested (12%) – which is 1.7 times higher than the optimized methanol level (7%) - the P release efficiency remained lower than that achieved with methanol. Specifically, the treatment with 7% methanol and no added sucrose or mineral salts (treatment 3) released 13.9 g P kg^{-1} d.s. (79.6% efficiency), while the 12% ethanol treatment released 10.2 g P kg^{-1} d.s. (58.0% efficiency).

In this way, the cultivations performed in the multilayer PBB aiming at the solubilization of the Registro rock were conduct adding 7% of methanol (w w^{-1}) in the solid matrix. Although this condition is not favorable for ACP production, the enzyme activity levels achieved (19 U g^{-1} d.s.) can contribute to the mineralization of organic P (Rodrigues et al., 2024). Studies specifically evaluating ACP production by *A. niger* under SSF are scarce, some research has reported phytase production by this species (Singh et al., 2024). Kumari and Bansal (2023), for example, optimized phytase production by *A. niger* in wheat bran and reported activities ranging from 20 to 520 U g^{-1} d.s. These results highlight the potential of *A. niger* to produce phosphatases under SSF.

4.3.3. Evaluation of the solubilization process of phosphate rock in the multilayer packed-bed bioreactor

Three batches were conducted in the multilayer PBB. Table 4.2 summarizes the process conditions and average responses (considering all layers) for each batch. Batch 1 was carried out using the same conditions previously identified as optimal in lab-scale experiments: addition of 7% methanol (w w^{-1}) to the solid matrix and no supplementation with sucrose or mineral salts. However, the performance observed in the bioreactor was substantially lower than in the lab-scale. The amount of released P reached only 4.3 g kg^{-1} d.s., corresponding to a P release efficiency of 24.6% - approximately three times lower than the value obtained in the lab-scale setup (13.9 g P kg^{-1} d.s.).

Table 4.2. Process conditions and average responses for the three batches conducted in the multilayer packed-bed bioreactor.

	Batch 1	Batch 2	Batch 3
Methanol in the solid matrix (% w w^{-1})	7	7	-
Methanol in air humidification solution (% w w^{-1})	-	7	-
Cultivation time (h)	72	96	96
Air flow (L h^{-1})	250	250	250
Peak CO_2 production (% v v^{-1})	0.40	0.56	0.48
Maximum CO_2 accumulation (mol)	172.07	254.01	231.72
Maximum temperature (°C)	34.71	35.71	35.79
Average temperature (°C)	32.97	32.66	32.64
Average CFU (CFU g^{-1} d.s.)	1.86×10^9	1.46×10^8	1.63×10^9
Average released P (g kg^{-1} d.s.)	4.30	4.04	1.59
Average P released efficiency (%)	24.57	23.09	9.07
Average final pH	5.34	6.28	6.80
Average ACP activity (U g^{-1} d.s.)	22.36	16.26	14.87
Average oxalic acid (g kg^{-1} d.s.)	49.38	50.80	40.52

This decline in performance was likely due to the loss of methanol from the solid matrix during the process, as it may have been carried away by the airflow due to thermodynamic equilibrium dynamics. Unlike in sealed polypropylene packages, the continuous flow of air in the bioreactor facilitates the evaporation and subsequent

removal of volatile compounds such as methanol (Zavec et al., 2020). As a result, its local concentration may have dropped below the threshold required to trigger the metabolic shift toward oxalic acid biosynthesis, which is crucial for phosphate rock solubilization (Klaic et al., 2021; Rodrigues et al., 2024).

Indeed, oxalic acid production in batch 1 (49.4 g kg^{-1} d.s.) was 1.6 times lower than the value obtained at lab-scale (76.7 g kg^{-1} d.s.). Furthermore, the growth in the batch 1 was 1.9×10^9 CFU g^{-1} d.s., 4 orders of magnitude higher than the value obtained at lab-scale (1.5×10^5 CFU g^{-1} d.s.), reinforcing the hypothesis that methanol depletion occurred during the bioreactor operation.

Nevertheless, although there was a pronounced growth, the average ACP activity was approximately 24.6 U g^{-1} d.s., slightly higher than the value obtained in the lab-scale (21.9 U g^{-1} d.s.). These results suggests that, despite favorable conditions for biomass formation, the metabolic environment in the bioreactor may not have supported high-level ACP production. Although the temperature profiles between the three layers were similar (4.6a), with a maximum overheat of only 4.7 °C (Fig. 4.6d), ACP activity was lower in the layers furthest from the air inlet (Fig. 4.7e). The same behavior was observed for released P: the closer the layer was to the air inlet, the better the performance. This suggests that factors other than temperature - possibly gradients of methanol, O_2, and CO_2 - may have created progressively less favorable environments for the induction of ACP synthesis, as well as for the P release.

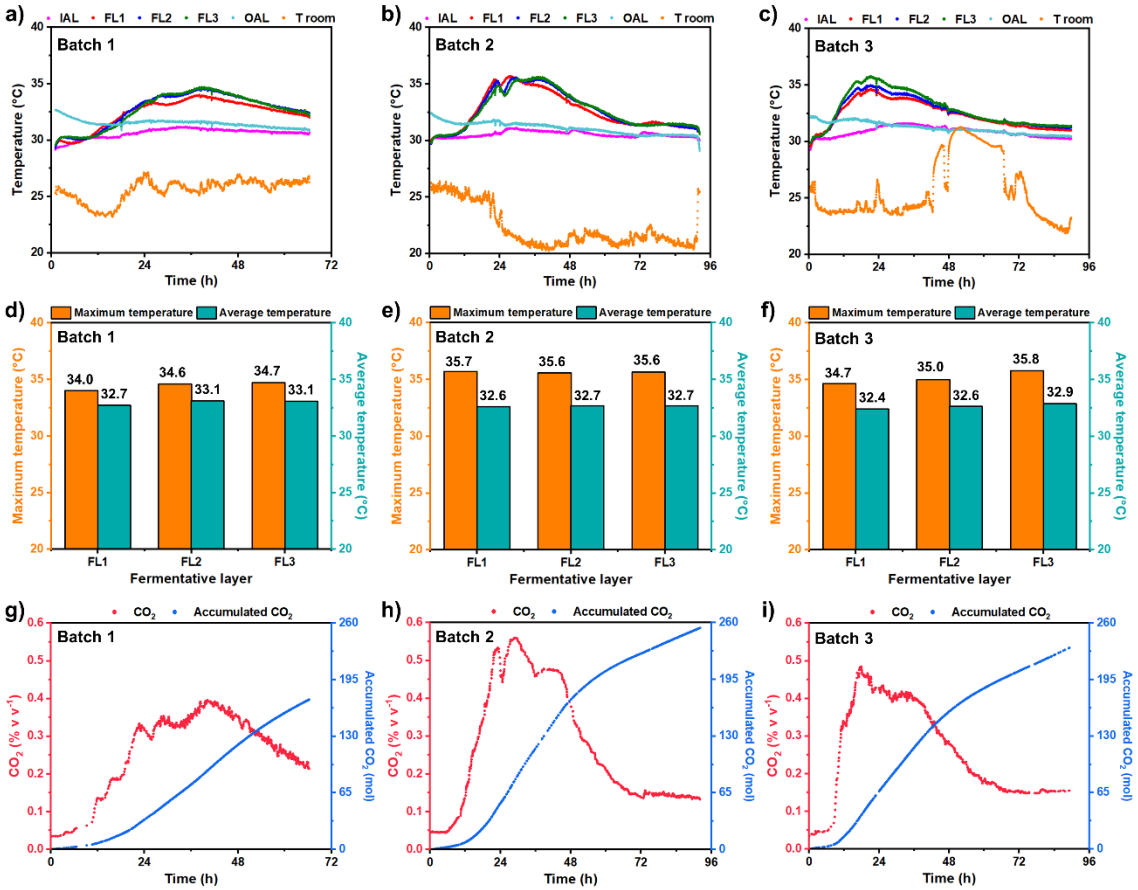

Fig. 4.6. Thermal behavior and CO_2 production in solid-state fermentation using a multilayer packed-bed bioreactor: temperature profiles of each layer for the batches a) 1, b) 2 e c) 3; maximum and average temperatures of each layer for the batches d) 1, e) 2 e f) 3; and CO_2 profiles and accumulated CO_2 for the batches g) 1, h) 2 e i) 3. FL1, FL2 and FLA3 mean fermentative layer 1, 2 and 3, respectively. FL1 - FL3 denote fermented layers 1 - 3 (FL1: closest to air inlet; FL3: furthest).

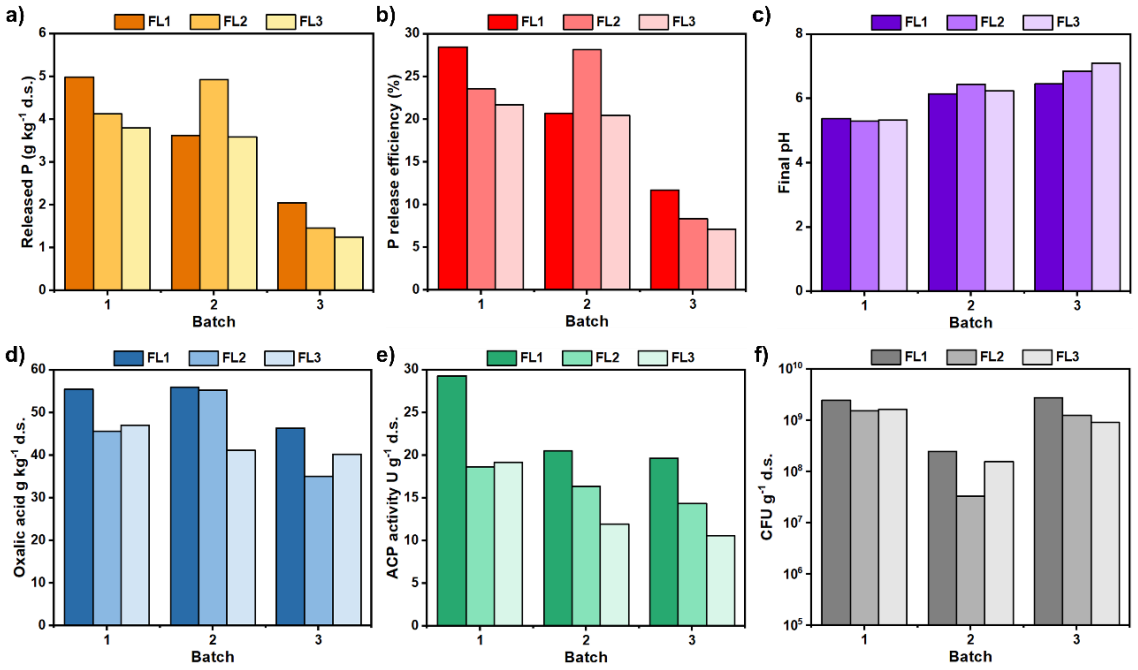

Fig. 4.7. Results of the solid-state fermentation using a multilayer packed-bed bioreactor for each layer and batch: a) released P; b) P release efficiency; c) Final pH; d) oxalic acid production; e) acid phosphatase (ACP); and f) colony-forming units (CFU). FL1, FL2 and FLA3 mean fermented layer 1, 2 and 3, respectively. FL1 - FL3 denote fermentative layers 1 - 3 (FL1: closest to air inlet; FL3: furthest).

Given the low released P observed in batch 1 and the hypothesis that this outcome was due to methanol loss from the solid matrix, a different strategy was employed in batch 2 to mitigate this issue. Specifically, methanol was added not only to the solid matrix but also to the air humidification solution at a concentration of 7% (w w^{-1}), as described in Section 4.2.3.2. Additionally, the cultivation period was extended by 24 hours. Although Rodrigues et al. (2024) reported that the P release and oxalic acid production reach their maximum values and stabilize after 72 hours, batch 1 exhibited a CO_2 production peak at approximately 40 hours (Fig. 4.6g) - a relatively late peak compared to that reported by Casciatori et al. (2024), who used the same strain and bioreactor configuration with sugarcane bagasse and wheat bran as substrates. Therefore, batch 2 was conducted for 96 hours to account for potentially delayed microbial metabolism.

Despite these adjustments, the results remained similar to those of batch 1, with a P release of 4.0 g kg^{-1} d.s. (23.1% efficiency) and oxalic acid production of 50.8 g

kg^{-1} d.s. The maximum temperature reached was only 1°C higher than in batch 1 (35.7°C). However, both growth and ACP activity were lower: 1.5×10^8 CFU g^{-1} d.s. and 16.3 U g^{-1} d.s., respectively, suggesting that although methanol supplementation via the humidifier likely increased its content in the solid matrix, it was insufficient to drive the metabolic shift toward greater oxalic acid production. These results highlight the difficulty in maintaining homogeneous conditions within PBBs in SSF processes, particularly when using volatile inducers. Further studies on methanol mass transfer within the PBB are needed to replicate lab-scale performance.

To further understand the role of methanol in this system, batch 3 was conducted without any methanol addition. The results showed a reduced oxalic acid production of 40.5 g kg^{-1} d.s. and a corresponding P release of only 1.59 g kg^{-1} d.s., leading to a P release efficiency of 9.1%. Thus, despite the suboptimal outcomes in batches 1 and 2, methanol clearly influenced P release. Microbial growth in batch 3 reached 1.6×10^9 CFU g^{-1} d.s., similar to batch 1 (1.9×10^9 CFU g^{-1} d.s.), while ACP activity was the lowest among all batches (14.9 U g^{-1} d.s.). Interestingly, considering that lab-scale tests using lower amounts of ethanol (6% and 9%) resulted in much higher ACP activity (77.7 and 86.0 U g^{-1} d.s., respectively) than methanol-based tests, it was expected that batch 3 would also exhibit greater ACP levels in the absence of methanol.

The factors that led to these results are not clear, but the main hypotheses suggest issues related to mass and energy transfers within the PBB - such as the difficulty in maintaining optimal temperature, as well as ensuring adequate O_2 supply and CO_2 removal - since ACP activity decreased in layers positioned farther from the air inlet across all three batches (Fig. 4.7e). Additionally, enzymatic activity may have declined over the course of cultivation. Vassilec et al. (2007) and Lei et al. (2017), who evaluated the production of phytase by *Aspergillus niger* and ACP by *Trichoderma asperellum*, respectively, also reported a decrease in the activity of these enzymes at the end of the cultivation. Phosphatase production is typically associated with active microbial growth, as this enzyme is linked to the carboxylic acid cycle. Therefore, its activity tends to be highest during the exponential growth phase, when nutrient demand is greatest (Mattey, 1992; Lill; Charvat, 1987). The decline in ACP activity during the stationary phase may result from several factors, including product inhibition or enzyme degradation for reuse as a nutrient source under starvation conditions (Barrios-Nolasco

et al., 2024). However, additional investigations are needed to confirm these hypotheses.

4.3.3.1. Bed drying using the multilayer packed-bed bioreactor itself

Drying fermented solids at low temperatures is a strategy widely recognized for increasing the shelf life of microbial bioinputs, as demonstrated by Mascarin et al. (2017), who reported that convective drying combined with active packaging effectively preserved the viability of *Beauveria bassiana* blastospores over time. Therefore, after the completion of batch 1, layer 1 (FL1) was kept in the multilayer PBB, and dry air was percolated through the bed, as described in section 4.2.3.2.1. According to Fig. 4.8a, which presents the relative humidity of the outlet air over time, the process began with air close to saturation (93%), gradually dropping to 4% after 22 hours of operation. As expected, the moisture content of the fermented solids at the end of drying reached 4.3% (wet basis), closely matching the relative humidity of the outlet air.

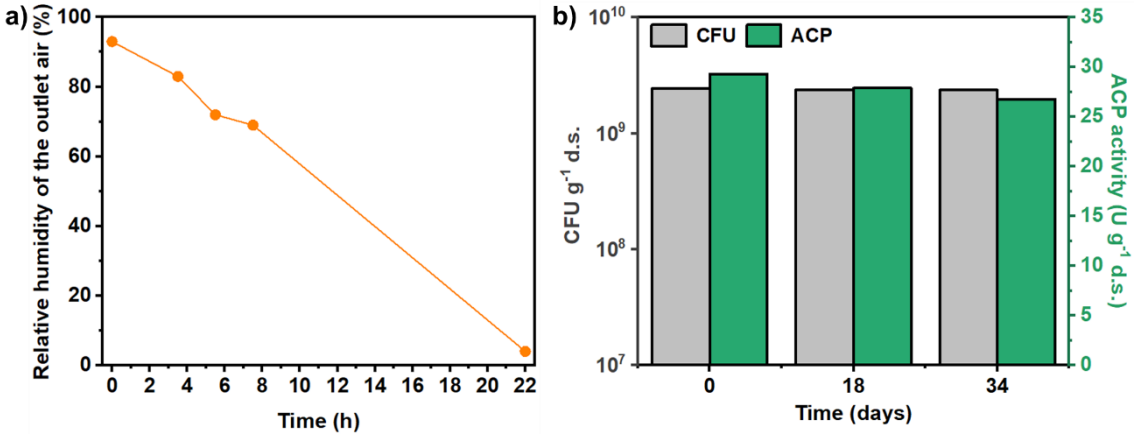

Fig. 4.8. Study of the drying of fermented solids after the solid-state fermentation process using the multilayer packed-bed bioreactor itself: a) relative humidity of the air leaving the drying system over time; b) CFU values and ACP activity of the dry fermented solids stored under refrigeration over 34 days.

Following drying, the fermented solids were stored in polypropylene package under refrigeration (4 °C), and their microbial viability and ACP activity were monitored for approximately one month (Fig. 4.8b). Over this period, the CFU count remained stable at approximately 2 × 10^9 CFU g^{-1} d.s., and ACP activity varied only

slightly (from 29.3 to 26.8 U g^{-1} d.s.), indicating that this downstream strategy was effective in preserving both viable spores and enzymatic functionality.

This result demonstrates that the multilayer PBB can be successfully used for in-situ drying, avoiding the need to transfer the biomass to separate drying equipment and thereby reducing operational complexity and contamination risks. This approach aligns with previous reports highlighting the benefits of in-situ drying in solid-state fermentation systems to simplify processing and reduce contamination risks (Gumbira-Sa'id et al., 1992). Future studies should assess long-term shelf stability and bioefficacy after storage to confirm the suitability of this method for large-scale production.

4.3.4. Application of biofertilizers in lettuce

To evaluate the effectiveness of the biofertilizers developed in this study, three different treatments were applied to lettuce plants, as described in section 4.2.4. The results are presented in Table 4.3.

Table 4.3. Effect of 50% replacement of chemical fertilizer with biofertilizers on lettuce growth parameters. The quantity of total P per plant pot was standardized to 60 mg.

Run	Number of leaves	Shoot length (cm)	Root length (cm)	Shoot fresh mass (g)	Root fresh mass (g)	Shoot dry mass (g)	Root dry mass (g)
A[1]	11.89 ± 5.06[a]	27.56 ± 5.66[a]	16.00 ± 10.01[a]	52.60 ± 35.05[a]	5.17 ± 4.04[a]	2.13 ± 1.43[a]	0.25 ± 0.19[ab]
B[2]	15.67 ± 6.53[a]	24.50 ± 2.59[a]	20.83 ± 2.14[a]	85.13 ± 43.54[a]	5.65 ± 2.83[a]	4.40 ± 2.49[a]	0.47 ± 0.25[a]
C[3]	15.33 ± 3.33[a]	24.33 ± 4.63[a]	16.00 ± 6.51[a]	81.13 ± 40.08[a]	6.43 ± 2.55[a]	3.34 ± 1.42[a]	0.44 ± 0.29[ab]
Control[4]	12.89 ± 4.08[a]	25.00 ± 4.33[a]	14.22 ± 6.65[a]	62.93 ± 31.26[a]	3.83 ± 2.54[a]	2.43 ± 1.20[a]	0.17 ± 0.09[b]

[1]: Treatment A - Application of fermented solids obtained by solid-state fermentation (SSF) with 7% methanol and 120 g kg^{-1} d.s. of Registro rock in the solid matrix;
[2]: Treatment B - Application of fermented solids obtained by SSF without methanol and with 120 g kg^{-1} d.s. of Registro rock in the solid matrix;
[3]: Treatment C - Application of the liquid extract (free of cells and insoluble particles) derived from fermented solids produced by SSF with 7% methanol and 120 g kg^{-1} d.s. of Registro rock in the solid matrix.
[4]: Control - Application of chemical fertilizer only.
Different letters indicate statistically significant differences between treatments ($\alpha \leq 0.05$), while the same letters indicate no significant difference.

As shown in Table 4.3, most growth parameters - including number of leaves, shoot and root length, shoot and root fresh mass, and shoot dry mass - did not differ significantly among treatments or compared to the control, which received 100% chemical phosphate fertilizer. These results are positive, as they indicate that replacing 50% of the chemical fertilizer with biofertilizers did not negatively affect lettuce growth. Moreover, treatment B resulted in a statistically significant increase in root dry weight compared to the control. P plays a central role in root formation and plant metabolism (Malhotra et al., 2018) and previous studies demonstrated that P application improves root biomass (Hansel et al., 2017; Tariq et al., 2017).

Treatment B involved the application of fermented solids from the SSF process without the addition of methanol and with the addition of rock in the solid matrix. This process favored microbial biomass accumulation over acid production, leading to lower concentrations of soluble P in the final product and high CFU values. Nonetheless, the superior performance of treatment B in promoting root growth may be related to the slower release of P, which could have stimulated more extensive root development over time.

A similar observation was reported by Mendes et al. (2015), who evaluated phosphate rock solubilization via SSF using sugarcane bagasse and sucrose as substrates and the fungus *A. niger* as a microbial agent. After optimizing the process, the fermented solids were subjected to drying at 70 °C or incineration at 350 °C and 500 °C. Although incineration reduced the water-soluble P content, plants fertilized with the solids incinerated at 500 °C showed greater dry matter accumulation and higher P and N uptake than those treated with solids dried at 70 °C, which retained higher soluble P levels. These findings suggest that P forms of intermediate solubility can be effectively assimilated by plants and may contribute to improved growth performance. Furthermore, as treatment B had a higher CFU count, the fungus *A. niger* may have contributed to the ongoing release of P.

4.4. Conclusions

This study explored the biological solubilization of Registro phosphate rock by *Aspergillus niger* through solid-state fermentation in a multilayer packed-bed bioreactor. Preliminary results in lab scale demonstrated that phosphate release can be achieved even in the absence of nutrient supplementation – such as sucrose and mineral

salts -, which may contribute to reducing process costs and complexity. However, scaling up the process in a packed-bed bioreactor presented important challenges. Methanol, although effective in inducing oxalic acid production, proved difficult to manage, probably due to its volatility, limiting P solubilization efficiency at bench scale. On the other hand, the implementation of in-situ drying directly within the bioreactor proved successful in preserving both microbial viability and acid phosphatase activity throughout the evaluated 34-day period. Although the agronomic tests were conducted with material produced at lab scale, they confirmed the potential of the product for partial replacement of chemical fertilizers. Overall, while the transition from lab to bench scale introduced important constraints, this study provides a valuable foundation for advancing solid-state fermentation of phosphate rock in bioreactors. The challenges associated with methanol volatility and retention suggest that this strategy may not be the most technically feasible for aerated systems. Future research should explore alternative metabolic modulation strategies to induce high organic acid production. Furthermore, efforts to optimize reactor configuration and process conditions to improve mass and heat transfer, along with long-term evaluations of biofertilizer performance under field conditions, will be essential to bring this technology closer to practical application.

References

Barrios-Nolasco, A., Castillo-Araiza, C.O., Huerta-Ochoa, S., Reyes-Arreozola, M.I., Buenrostro-Figueroa, J.J., Prado-Barragán, L.A., 2024. Evaluating the performance of *Yarrowia lipolytica* 2.2 ab in solid-state fermentation under bench-scale conditions in a packed-tray bioreactor. Fermentation 10, 344.

Casciatori, F.P., Laurentino, C.L., Taboga, S.R., Casciatori, P.A., Thomeo, J.C., 2014. Structural properties of beds packed with agro-industrial solid by-products applicable for solid-state fermentation: experimental data and effects on process performance. Chem. Eng. J. 255, 214–224.

Casciatori, F. P., Mafra, N. S. C., Rodrigues, N. A., Sales, E. H., Maia, M. M. S., Dias, A. C. P., Grajales, L. M., 2024. Flow configuration and Packing Density of Sugarcane Bagasse and Wheat Bran Affecting Enzymes Production by Solid-State Fermentation. Bioenergy Res. 17, 187-197.

Díaz-Rodríguez, A.M., Parra Cota, F.I., Cira Chávez, L.A., García Ortega, L.F., Alvarado, M.I.E., Santoyo, G., Santos-Villalobos, S., 2025. Microbial Inoculants in Sustainable Agriculture: Advancements, Challenges, and Future Directions. Plants, 14, 191.

Favaro, C.P., Klaic, R., Bettiol, W., Ribeiro, C., Farinas, C.S., 2022. Bio-based composite granules with simultaneous biocontrol and phosphorus fertilization roles: Outcomes from a lab-scale in vitro assessment. Biotechnol. Prog. 38, e3242.

Gumbira-Sa'id, E., Mitchell, D.A., Greenfield, P.F., Doelle, H.W., 1992. A packed bed solid-state cultivation system for the production of animal feed: Cultivation, drying and product quality. Biotechnol. Lett. 14, 623–628.

Hansel, F.D., Amado, T.J.C., Ruiz Diaz, D.A., Rosso, L.H.M., Nicoloso, F.T., Schorr, M., 2017. Phosphorus fertilizer placement and tillage affect soybean root growth and drought tolerance. Agron. J. 109, 2936–2944.

Klaic, R., Plotegher, F., Ribeiro, C., Zangirolami, T.C., Farinas, C.S., 2017. A novel combined mechanical-biological approach to improve rock phosphate solubilization. Int. J. Miner. Process. 161, 50–58.

Klaic, R., Plotegher, F., Ribeiro, C., Zangirolami, T. C., Farinas, C. S., 2018. A fed-batch strategy integrated with mechanical activation improves the solubilization of phosphate rock by *Aspergillus niger*. ACS Sustain. Chem. Eng. 6, 11326-11334.

Kumari, N., Bansal, S., 2023. Statistical modeling and optimization of microbial phytase production towards utilization as a feed supplement. Biomass Convers. Biorefin. 13, 8339–8349.

Laothanachareon, T., Bunterngsook, B., Champreda, V., 2022. Profiling multi-enzyme activities of *Aspergillus niger* strains growing on various agro-industrial residues. 3 Biotech 12, 17.

Lilly, W.W., Charvat, I., 1987. Activities and isoenzymes of acid phosphatase in *Schizophyllum commune*: a re-examination. Mycologia 79, 314–319.

Malhotra, H., Vandana, Sharma, S., Pandey, R., 2018. Phosphorus nutrition: plant growth in response to deficiency and excess. Plant Nutr. Abiotic Stress Toler. 171–190.

Mascarin, G.M., Jackson, M.A., Behle, R.W., Kobori, N.N., Júnior, Í.D., 2016. Improved shelf life of dried *Beauveria bassiana* blastospores using convective drying and active packaging processes. Appl. Microbiol. Biotechnol. 100, 8359–8370.

Mattey, M., 1992. The production of organic acids. Crit. Rev. Biotechnol. 12, 87–132.

Mendes, O. G., Murta, H. M., Valadares, R. V., da Silveira, W. B., da Silva, I. R., Costa, M. D., 2020. Oxalic acid is more efficient than sulfuric acid for rock phosphate solubilization. Miner. Eng. 155, 106458.

Mendes, G.D., da Silva, N., Anastacio, T.C., Vassilev, N.B., Ribeiro, J.I., da Silva, I.R., Costa, M.D., 2015. Optimization of *Aspergillus niger* rock phosphate solubilization in solid-state fermentation and use of the resulting product as a P fertilizer. Microb. Biotechnol. 8, 930–939.

Oviedo-Rondon, E.O., Toscan, A., Fagundes, N.S., Vidal, J.K., Barbi, J., Thiery, P., 2024. Soybean meal nutrient composition, amino acid digestibility, and energy content according to the country of origin and year of harvest evaluated via NIRS. J. Appl. Poult. Res. 33, 100448.

Perez, C.L., Casciatori, F.P., Thoméo, J.C., 2021. Improving enzyme production by solid-state cultivation in packed-bed bioreactors by changing bed porosity and airflow distribution. Bioprocess Biosyst. Eng. 44, 537-548.

Pohanka, M., 2016. Toxicology and the biological role of methanol and ethanol: Current view. Biomed. Pap. Med. Fac. Univ. Palacky Olomouc Czech Repub. 160, 35–45.

Rawat, P., Das, S., Shankhdhar, D., Shankhdhar, S.C., 2021. Phosphate-solubilizing microorganisms: mechanism and their role in phosphate solubilization and uptake. J. Soil Sci. Plant Nutr. 21, 49-68.

Rodrigues, N.A., Buffo, M.M., Casciatori, F.P., Farinas, C.S., 2024. New approaches for solubilization of phosphate rocks through solid-state fermentation by optimization of oxalic acid production. Bioresour. Technol. 408, 131165.

Rodrigues, N.A., Katayama, E.T., Casciatori, F.P., 2022. Alternative strategies to perform solid-state cultivation in a multilayer packed-bed bioreactor: Continuous and cyclic operations. Chem. Eng. J. 448, 137726.

Singh, B., Pragya, Tiwari, S.K., Singh, D., Kumar, S., Malik, V., 2024. Production of fungal phytases in solid state fermentation and potential biotechnological applications. World J. Microbiol. Biotechnol. 40, 22.

Tariq, A., Pan, K., Olatunji, O.A., Graciano, C., Li, Z., Sun, F., et al., 2017. Phosphorus application improves drought tolerance of *Phoebe zhennan*. Front. Plant Sci. 8, 1561.

Van Raij, B., Cantarella, H., Quaggio, J.A., Furlani, A.M.C., 1997. Recomendações de adubação e calagem para o Estado de São Paulo. Inst. Agron. Campinas, Boletim Técnico 100.

Vassilev, N., Vassileva, M., Bravo, V., Fernández-Serrano, M., Nikolaeva, I., 2007. Simultaneous phytase production and rock phosphate solubilization by *Aspergillus niger* grown on dry olive wastes. Ind. Crops Prod. 26, 332–336.

Zavec, D., Gasser, B., Mattanovich, D., 2020. Characterization of methanol utilization negative *Pichia pastoris* for secreted protein production: New cultivation strategies for current and future applications. Biotechnol. Bioeng. 117, 1394–1405.

Chapter 5

5. *Trichoderma harzianum* as a multifunctional microbial agent: optimizing solid-state fermentation in packed-bed bioreactors to produce essential metabolites for phosphorus availability

ABSTRACT

This study investigates the cultivation of *Trichoderma harzianum* using solid-state fermentation (SSF) in packed-bed bioreactors (PBBs) at lab and bench scales. The objective was to evaluate the strain's potential to enhance plant phosphorus (P) acquisition by promoting medium acidification and the production of phosphatases, indole derivatives, and flavonoids. Using beer draff (BD) and wheat straw (WS) as substrates, the optimized process in 0.5 L PBB enhanced multiple plant-growth traits, including high sporulation (1.08×10^{10} spores g^{-1} of dry mass, DM), acid phosphatase (ACP) activity (3.7 U g^{-1} DM), and phosphate mobilization. Additionally, the strain produced indole derivatives (511.3 μg g^{-1} DM) and total flavonoids (2.2 mg g^{-1} DM), compounds known to stimulate root development, enhance nutrient uptake, and activate plant defense mechanisms. Airflow and substrate ratio were the most significant factors, highlighting the crucial role of adequate O_2 supply and efficient CO_2 removal in SSF processes. However, bench-scale cultivation (22 L PBB) led to a 16.5°C temperature increase above the optimal level, significantly reducing metabolite production, particularly ACP and flavonoids, indicating the need for improved heat dissipation. Despite that, biomass formation occurred at the order of 1×10^9 spores g^{-1} DM and there was a good production of indole derivatives (688 and 498 μg g^{-1} DM for the batches 1 and 2, respectively). These findings can contribute to the development of multifunctional agricultural inputs for sustainable agricultural practices.

Keywords: Biofertilizer, Phosphorus solubilizing microorganisms, Phosphorus recycling and recovery, Sustainable agriculture, Biostimulants.

5.1. Introduction

Ensuring high levels of available phosphorus (P) in the soil is crucial for achieving high agricultural productivity and sustaining the growing demand for food

production (McDowell et al., 2024). However, P in soil is typically present in forms not readily assimilable by plants, necessitating extensive phosphatic fertilization (Urso and Gilbertson, 2018). Currently, commercial phosphate fertilizers are primarily derived from phosphate rocks, a finite resource, posing a threat to long-term global food security (IFA, 2023). Additionally, the high solubility of conventional mineral fertilizers results in substantial P losses through leaching, leading to eutrophication and negatively impacting local ecosystems and water quality (Chien et al., 2011). Therefore, improving the efficiency of P fertilizer use and exploring alternative P sources are crucial steps toward a more sustainable and circular agricultural system.

In this context, P-solubilizing microorganisms (PSMs) have gained attention for their ability to enhance P bioavailability in soil (Shi et al., 2024). These microorganisms facilitate P acquisition by plants through multiple mechanisms, including root growth stimulation (via mycorrhizal associations or hormonal regulation), modification of sorption equilibria to increase soluble orthophosphate concentrations, and enzymatic mineralization of organic P. Key metabolic processes include the production of organic acids, which solubilize inorganic P precipitates, and the secretion of phosphatases, cellulolytic enzymes, and siderophores, which contribute to P release from organic and inorganic sources (Richardson and Simpson, 2011).

Solid-state fermentation (SSF) offers a promising approach for cultivating these PSMs while simultaneously enabling the bioconversion of agro-industrial residues into valuable biofertilizers. SSF can promote P mineralization from organic waste by generating various hydrolytic enzymes (e.g., phosphatases, cellulases, and chitinases), which can be beneficial for soil application (Wang et al., 2022). Additionally, this process contributes to the sustainable management of agro-industrial byproducts. Filamentous fungi are particularly well-suited for SSF processes (Farinas, 2015). Among them, *Aspergillus niger* is widely recognized for its ability to produce high levels of organic acids and phosphatases, having proven efficient in solubilizing phosphate rocks (Klaic et al., 2017; Rodrigues et al., 2024). However, its direct application in agriculture remains limited. Conversely, *Trichoderma* species have been extensively used in agriculture, primarily as biocontrol agents, and have also shown potential to enhance plant P uptake (Porras et al., 2025). This occurs both directly, through the production of organic acids and phosphatases, and indirectly, via the synthesis of plant growth-promoting hormones such as indole-3-acetic acid, which

enhances root development and, therefore, P acquisition by plants (Richardson and Simpson, 2011). Given these capabilities, *Trichoderma* is a promising agent for the development of sustainable agricultural inputs with multiple functionalities, which is interesting from both an economic and environmental point of view.

In addition to its well-known role as a biocontrol agent and its production of enzymes directly involved in P acquisition, the fungus *T. harzianum* also synthesizes secondary metabolites that indirectly contribute to phosphorus mobilization, such as indole-3-acetic acid (IAA) and flavonoids. IAA, a key auxin, regulates various aspects of plant growth and development, particularly by stimulating adventitious root formation and increasing the number of lateral roots and root hairs (Prado et al., 2019a). These morphological changes expand the root surface area, thereby improving the plant's capacity to absorb phosphorus (Richardson and Simpson, 2011). Flavonoids, in turn, are phenolic compounds that function as signaling molecules in the rhizosphere, fostering interactions with beneficial microorganisms such as arbuscular mycorrhizal fungi and P-solubilizing bacteria. These interactions enhance P bioavailability either through solubilization of insoluble forms or by facilitating symbiotic nutrient uptake. Furthermore, flavonoids can influence root exudation profiles and act as chelating agents, contributing to the release of phosphorus from metal-phosphate complexes (Shah and Smith, 2020).

Despite the industrial relevance of *Trichoderma*, its large-scale production is still predominantly performed using SSF on rice substrates in plastic bags, a labor-intensive process that competes with food supply (Mascarin et al., 2019), highlighting the need for alternative substrates and more efficient and scalable fermentation technologies. However, SSF scale-up remains a challenge mainly due to difficulties in controlling metabolic heat accumulation, which limits the development of advanced bioreactor designs (Casciatori et al., 2024). Promising results have been reported by Sala et al. (2020) that demonstrated successful growth of *Trichoderma harzianum* in packed-bed bioreactors (PBBs) using beer draff as substrate, achieving spore yields of approximately 7×10^9 spores g^{-1} DM. Around 20 kg of wet beer draff are produced per 100 L of brewed beer, contributing to an estimated global production of 36.4 million tonnes per year (Nyhan et al., 2023). Given the strain's strong development on this abundant substrate, it is worth exploring its potential to produce essential metabolites involved in phosphorus cycling.

In light of these considerations, this study aimed to optimize the production of *T. harzianum* spores and P release efficiency in lab and bench scale PBBs using beer draff and wheat straw as substrates for SSF. The study comprehensively evaluated the microorganism's capacity to solubilize inorganic and organic P through direct mechanisms (organic acid and phosphatase production) and indirect mechanisms (indole derivative and flavonoid synthesis). The findings can contribute to expanding knowledge on *T. harzianum* and its applications, supporting the development of multifunctional inputs for sustainable agriculture.

5.2. Material and methods

5.2.1 Microorganisms and solid substrates

Trichoderma harzianum CECT 2929 was provided by the Spanish Type Culture Collection (CECT). The original strain was preserved at -80°C in sterile cryovials containing 10% glycerol, as recommended by the strain provider. For use, the fungus was cultivated on plates with malt extract agar (MEA) at 25°C for 6-8 days. A spore suspension was then obtained by scraping the surface of the agar after adding 10 mL of 0.1% (v v^{-1}) Tween 80. The spore concentration was determined using a Neubauer chamber.

The solid substrates used in the experiments were wheat straw (WS), obtained from the experimental farms of the Universitat Autònoma de Barcelona (UAB), and beer draff (BD), a solid byproduct from beer processing that was kindly provided by Cervesa del Montseny S.L. (Sant Miquel de Balenyà). BD from two different beer production batches were used in this study. For the experiments in Erlenmeyer flasks, BD from the first batch was utilized, while for the bioreactor experiments, BD from the second batch was employed. Additionally, the mixture with WS enhanced reactor's bed porosity and prevented compaction. For lab-scale cultivation, the WS was cut with scissors to a size of approximately 3 cm.

Wood chips (WC) were also used in the cultivations in bench scale as inert bulking agent. BD was stored frozen (-20°C), while WS and WC were kept at room temperature (20–25°C). Before use, both substrates and the WC were autoclaved twice at 121°C for 30 minutes.

Struvite ($MgNH_4PO_4 \cdot 6H_2O$), kindly provided by the Sostenipra Group (ICTA-UAB) from a wastewater treatment plant in Denmark, was also included in the solid

matrix as a source of low-solubility P in tests of inorganic P solubilization. Prior to utilization, the struvite was ground to enhance its surface area. The total P content of the struvite was 13.9% (w w^{-1}). Table 5.1 presents the characterization of the materials used.

Table 5.1. Characterization of materials employed in the SSF processes.

Parameter	BD[1]	BD[2]	WS	WC
MC (%)	73.70 ± 0.15	77.10 ± 0.20	8.66 ± 0.33	9.70 ± 0.30
OM (%)	96.95 ± 0.31	93.30 ± 0.30	96.81 ± 0.40	98.40 ± 0.60
pH	6.10 ± 0.01	6.60 ± 0.20	5.70 ± 0.02	5.10 ± 0.20
C (%)	45.62 ± 0.36	41.98 ± 0.16	42.10 ± 0.53	46.90 ± 0.60
H (%)	6.91 ± 0.28	6.51 ± 0.07	5.82 ± 0.44	9.70 ± 0.30
N (%)	3.20 ± 0.21	2.39 ± 0.07	0.57 ± 0.09	0.40 ± 0.20
S (%)	0.26 ± 0.06	0.23 ± 0.02	<0.1	<0.1
C/N ratio	14.27 ± 0.94	17.56 ± 0.54	73.74 ± 11.00	117.40 ± 13.6
Total P (%)	0.47 ± 0.01	0.54 ± 0.02	0.07 ± 0.00	-

MC: moisture content; OM: organic matter content; BD[1]: beer draff from the first batch of beer; BD[2]: beer draff from the second batch of beer; WS: wheat straw; WC: wood chips.

5.2.2 Solid-state fermentation

The SSF processes were conducted in Erlenmeyer flasks and packed-bed bioreactors (PBBs) at both lab and bench scales. Fig. 5.1 presents an overview of the experimental setup, with further details provided in the following sections.

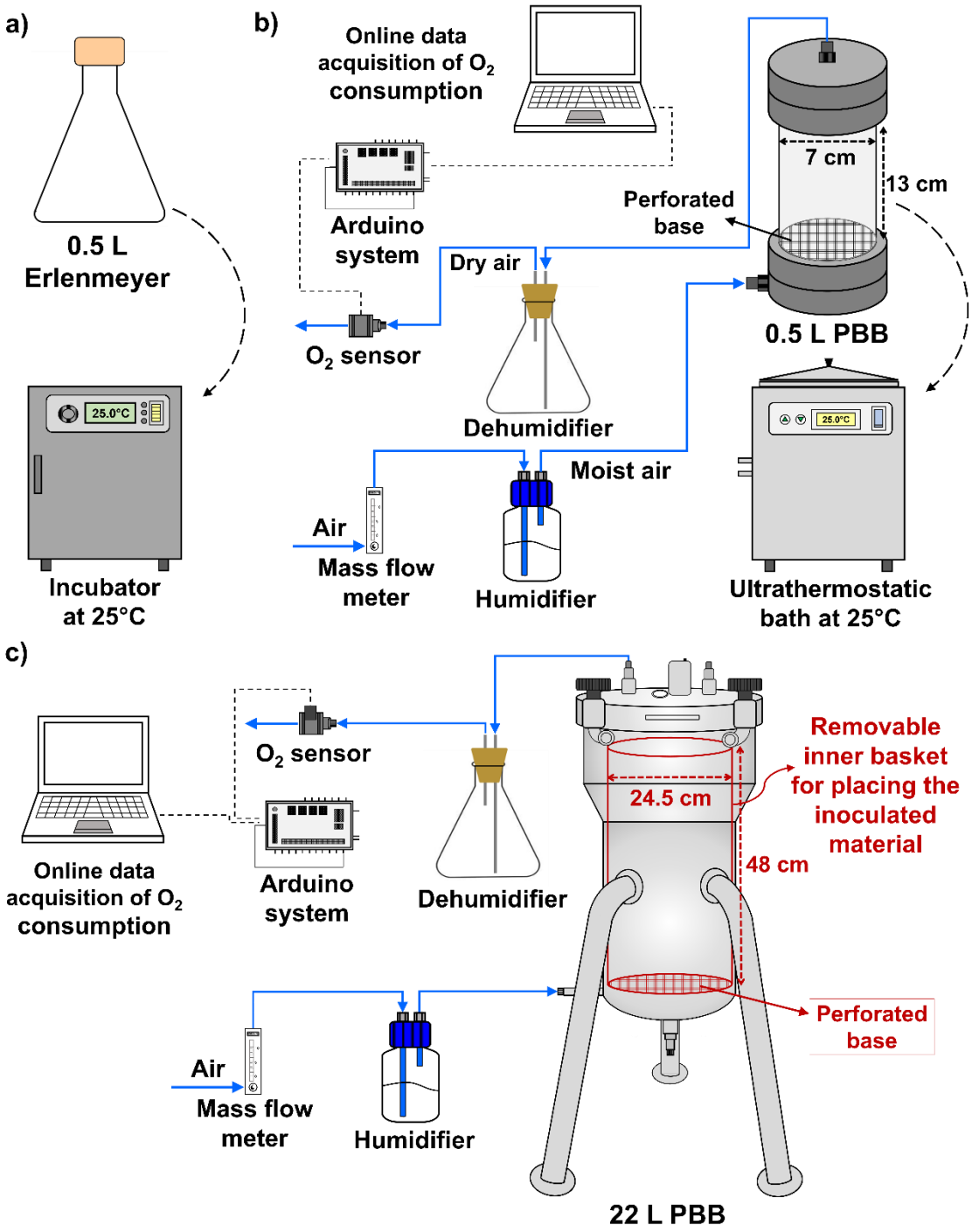

Fig. 5.1. Schematic representation of the experimental apparatus at lab and bench scales: (a) 0.5 L Erlenmeyer flask, (b) 0.5 L PBB and (c) 22 L PBB.

5.2.2.1 Evaluation of P release in flasks

To evaluate the microorganism's ability to solubilize P, a set of cultivations was carried out in 0.5 L Erlenmeyer flasks. In these experiments, the solubilization of both

organic and inorganic P through SSF was assessed. Struvite was used as the inorganic P source, added at a concentration of 3.5% (w w^{-1} on a dry basis, d.b.). Similar concentrations of phosphate rock have been used in other studies, which reported positive solubilization results through this process with the fungus *A. niger* (Klaic et al., 2021; Rodrigues et al., 2024). The organic P source was provided by the substrates themselves, which were employed in a BD:WS ratio of 7:3 (w w^{-1} on d.b.). This mixture resulted in a moisture content of 65%, ideal for promoting the growth of this strain (Sala et al., 2020), thus no additional water was added. The total dry mass (DM) of substrates packed in each Erlenmeyer flask was 12.5 g.

Based on the work of Rodrigues et al. (2024), the addition of low molecular weight alcohols to the culture medium was tested to enhance inorganic P solubilization. Methanol was added at concentrations of 3%, 6%, and 9% (w w^{-1} on d.b.), while ethanol was added at concentrations of 4%, 8%, and 12% (w w^{-1} on d.b.). SSF processes were conducted in duplicate in incubators set at 25 °C, the optimal temperature for sporulation of this strain (Sala et al., 2020). The spore suspension volume was adjusted to reach an initial concentration of 1×10^7 spores g^{-1} DM. After inoculation, the flasks were closed with filters to prevent contamination while allowing gas exchange. All procedures were performed under sterile conditions. The cultivation period for these tests was 4 days. Subsequently, a time-course experiment was performed in duplicate (48–120 hours), with samples taken every 24 hours. The sacrificial sampling method was used, meaning that two Erlenmeyer flasks were prepared for each time point. The evaluated responses included sporulation, final pH, acid phosphatase (ACP) activity, alkaline phosphatase (ALP) activity and P release.

5.2.2.2 Optimization of spore production in 0.5 L PBB

For the optimization of spore production, a Box-Behnken design was applied. The process parameters evaluated were airflow (10 – 100 mL min^{-1}), BD:WS ratio (2:8 – 8:2), and inoculum size (1×10^5 – 1×10^7 spores g^{-1} DM). The experiments were performed in 0.5 L PBBs, consisting of cylindrical Polyvinyl chloride (PVC) reactors 13 cm in height and 7 cm in diameter, corresponding to a working volume of 0.45 L and a total volume of 0.5 L. Before entering the bioreactor, the air was passed through a humidification system to ensure saturation and prevent bed drying, as shown in Fig. 5.1b.

Considering that the different BD:WS ratios in each treatment result in beds with varying bulk densities due to the specific physical properties of each particle, the bed volume inside the bioreactor was standardized instead of the mass (Casciatori et al., 2014). The bulk densities were calculated using Eq. (1). This approach was adopted because comparing beds with the same mass, but different heights would be inappropriate, given that the focus of this study is to analyze key variables for scale-up. Bed height, along with factors such as moisture content, affects bed porosity, as the weight of the upper layers can cause compaction in the lower layers (Casciatori et al., 2024).

$$\rho_{\text{bulk}} = \frac{m_{bed}}{V_{rec}} \quad (1)$$

where ρ_{bulk}, m_{bed} and V_{rec} represent the bulk density (g L^{-1}), bed mass (g) and the volume (L) occupied by the bed inside the bioreactor, respectively.

The moisture content of all treatments was adjusted to 70%, as this was the value obtained in the treatment with the highest proportion of BD (BD:WS ratio = 8:2), which is the more humid substrate. Prior to inoculation and packing, the bioreactors were sanitized with 70% ethanol and exposed to ultraviolet light for 15 minutes. The packing technique used was loose packing proposed by Casciatori et al. (2014), in which the substrates are smoothly accommodated without causing bed compression. All procedures were performed under sterile conditions. The bioreactors were then completely sealed, allowing only airflow in and out. Cultivation was carried out for 4 days, with temperature control maintained by immersing the bioreactors in a thermostatic water bath set to 25°C. Spore production was the response variable evaluated in this experiment.

5.2.2.3 Time course analysis under optimized conditions in 0.5 L PBB

Under the optimal conditions for sporulation, defined in the previous section (aeration, substrate ratio, and inoculum size), the production of metabolites of interest was evaluated over time. Cultivation was carried out in the 0.5 L PBBs for 6 days, with sampling every 24 hours. The point corresponding to 4 days of cultivation was performed in triplicate, and the standard deviation obtained at this point was used as an

error estimate for the other time points. The sacrificial sampling method was applied, meaning one bioreactor was sacrificed at each time point. The responses evaluated over time included O_2 consumption, spore production, ACP activity, P release, indole derivatives, and total flavonoids. The inoculation, packing, and temperature control procedures were performed as described in the previous section.

5.2.2.4 Process scale-up to a 22 L PBB

The experimental setup for the 22 L PBB is shown in Fig. 5.1b. The bioreactor consists of a cylindrical stainless-steel vessel with a removable basket of 48 cm height x 24.5 cm diameter, with a total volume of 22 L. In all fermentations, the working volume was approximately 90% of the reactor capacity. As in the 0.5 L PBB, the incoming air passed through a humidification system before entering the bioreactor. A loose packing technique was used to prevent bed compaction.

To monitor temperature distribution and detect potential gradients, temperature sensors (standard Thermochron iButton device, Maxim Integrated, U.S.) were placed at six different positions inside the bioreactor. The room temperature was also recorded.

Two batches were conducted, each lasting six days. In batch 1, the optimal process conditions established in the 0.5 L PBBs were maintained, with a substrate ratio of BD:WS 6:4 and an inoculum size of 1×10^5 spores g^{-1} DM. To scale the airflow while minimizing bed drying, the superficial air velocity was used as the scaling criterion, calculated using Eq. (2).

$$\upsilon_s = \frac{Q}{A_t} \tag{2}$$

where υ_s is the air superficial velocity (cm min^{-1}), Q is the volumetric air flow rate (cm^3 min^{-1}) and A_t is the cross-sectional area of the PBB (cm^2).

In batch 2, the airflow rate was increased by 1.3 times, and 20% WC was added as an inert bulking agent. The values used, along with other cultivation characteristics, are presented in Section 3.4.

Simultaneously to the 22 L PBB batches, three 0.5 L PBBs were packed with the same inoculated material to assess potential scale-up issues. The responses evaluated

included O_2 consumption, temperature profiles, spore production, ACP activity, indole derivatives, and total flavonoids.

5.2.2.5 Assessment of Oxygen Consumption

In the SSF processes conducted in the 0.5 L and 22 L PBBs, the flow rate was monitored using a mass flow meter (Mass-Stream D-6311, Bronkhorst, NL). The O_2 content in the outlet gases was assessed using an electrochemical O_2 sensor O_2-A_2 (Alphasense, UK). Data analysis was performed by a non-commercial tailor-made software Arduino® based that calculates the respiration rates.

The specific rate of O_2 consumption was calculated according to Eq. 3 using the data of the molar fraction of O_2 in the outlet gas stream collected online, as well as the process parameters. The cumulative O_2 consumption (COC) was also determined by calculating the area under the curve of the specific rate of O_2 consumed.

$$\mathrm{sOUR} = \mathrm{F} \times \left(0.209 - y_{O_2}\right) \times \frac{\mathrm{P} \times 32 \times 60 \times 10^3}{\mathrm{R} \times \mathrm{T} \times \mathrm{DW} \times 10^3} \quad (3)$$

where sOUR is the specific Oxygen Uptake Rate (g O_2 kg DM^{-1} h^{-1}); F is the airflow (mL min^{-1}); yO_2 is the oxygen molar fraction in the exhaust gases (mol O_2 mol^{-1}); P is the pressure of the system assumed constant at 101325 Pa; 32 is the oxygen molecular weight (g O_2 mol^{-1} O_2); 60 is due to the conversion factor from minute to hour; 10^3 is due to the conversion factor from mL to L; R is the ideal gas constant (8310 Pa L K^{-1} mol^{-1}); T is the temperature at which F is measured (K); DW is the initial dry weight of solids in the reactor (g); 10^3 is due to the conversion factor from g to mg.

5.2.3 Analytical procedures

At the end of the SSF processes, the fermented solids were subjected to solid-liquid extraction for specific analytical procedures. This process involved mixing the sample with the respective liquid, followed by agitation for 30 minutes at 25°C in an orbital shaking incubator. For analyses requiring the removal of suspended solids, the samples were centrifuged at 9000 rpm for 15 minutes at 4°C. The details of each analysis are provided in the following sections.

5.2.3.1 Spore counting

To determine spore production, the fermented solids were extracted with 0.1% Tween 80 (9 mL g^{-1}). The extracts were diluted and plated on potato dextrose agar (PDA) containing 0.1 g L^{-1} of rose bengal. After incubation at 30°C for 2 days, colonies were counted. Rose bengal is a dye that inhibits bacterial growth and restricts the growth of fungal colonies, allowing these colonies to grow separately and to be counted. The number of spores was calculated according to Eq. 4, where the number of colonies was considered equivalent to the number of spores. This was confirmed by tests conducted (data not shown), which demonstrated that the number of colonies on PDA plates with rose bengal is equal to the number of spores counted using a Neubauer chamber.

$$\text{Spores} = \frac{\text{CN} \times \text{DF} \times \text{EV}}{\text{PV} \times \text{SDM}} \quad (4)$$

where: CN is the colonies number; DF is the dilution factor of the plated sample; EV is the volume of 0.1% Tween 80 solution used for extraction; PV is the volume of the plated sample; SDM is the sample dry matter subjected to extraction.

5.2.3.2 Soluble and total P determination

To determine the soluble P, the fermented solids were extracted with distilled water (5 mL g^{-1}). After the extraction, the samples were centrifuged. The soluble P of the supernatant was measured using the equipment 115 VAC PHOSPHAX sc, Hach-Lange, which determines P in the form of PO_4 in a range of 0.05 - 15 mg L^{-1}.

In experiments with struvite, the efficiency of P solubilization was calculated using Eq. (5), considering the total initial P present in the medium. This included both the P introduced through struvite and the P naturally present in the substrates.

$$\text{P solubilization efficiency}(\%) = \frac{\text{Solubilized P}}{\text{Initial Total P}} \times 100 \quad (5)$$

Total P determination was performed by the chemical analysis service of UAB using Inductively Coupled Plasma Optical Emission Spectrometry (ICP-OES).

5.2.3.3 Phosphatase activity assays

The fermented solids were extracted with sodium acetate buffer pH 4.8 (15 mL g^{-1}) and with sodium citrate dihydrate buffer pH 9.0 (15 mL g^{-1}) to measure the ACP and ALP activities, respectively. After extraction, the samples were centrifuged, and the supernatants were used in the reaction. Phosphatase activities were measured by quantifying the amount of p-nitrophenol released from 5 mM p-nitrophenyl phosphate (p-NPP) in the respective buffer at 37°C. The reaction was carried out for 10 minutes and was stopped by the addition of 1 mL of 0.1 M NaOH. The amount of p-nitrophenol released was measured at 410 nm, and its concentration was determined using a calibration curve made with concentrations of 10 – 60 µmol L^{-1} of p-nitrophenol. One unit (U) of acid phosphatase activity was defined as 1 µmol of p-nitrophenol released per hour under the assay conditions (Tabatabai and Bremner, 1969).

5.2.3.4 Quantification of indole derivatives

To determine the production of indole derivatives, the fermented solids were extracted with distilled water (5 mL g^{-1}). The reaction was carried out by mixing 1 mL of extract with 4 mL of Salkowski reagent (2% $FeCl_3$ in 35% perchloric acid) and incubating for 30 minutes. After incubation, the samples were centrifuged, and the supernatants were analyzed by spectrophotometry at 535 nm. The concentration of indole derivatives was determined using a standard curve prepared with indole-3-acetic acid (IAA) (Bric et al., 1991).

5.2.3.5 Quantification of total flavonoids

To quantify the total flavonoid content, the fermented solids were extracted with acidified methanol (85% methanol solution at 70% and 15% acetic acid solution at 10%, v v^{-1}). Unlike the other extractions, this process was performed in an ultrasonic bath. Then, 1 mL of the extract was mixed with 250 µL of 5% aluminum chloride and incubated in the dark for 30 minutes. After incubation, the samples were centrifuged, and the supernatants were analyzed by spectrophotometry at 425 nm. The concentration of total flavonoids was determined using a standard curve prepared with quercetin (Santos; Blatt, 1998).

5.2.4 Statistical analysis

Statistical analyses were performed using STATISTICA software, version 7 (StatSoft, Inc., 2004). Analysis of variance (ANOVA) was conducted, followed by mean comparisons using Tukey's test, with a confidence level of 95%. The software was also used for the design of experiments (DoE) and the construction of surface plots.

5.3. Results and discussion

5.3.1 Effect of the addition of alcohols on P release

The presence of low molecular weight alcohols in small concentrations in the cultivation medium can enhance the permeability of microbial cell membranes, thereby increasing the excretion of metabolites into the extracellular medium. This strategy has proven effective to produce organic acids by *A. niger* (Anwar et al., 2009). Rodrigues et al. (2024) reported a threefold increase in oxalic acid production after adding 7% methanol to the culture medium in SSF process. This approach allowed reaching an effective solubilization of P from phosphate rocks by green route aiming to produce phosphate fertilizers. However, the extent of this effect may vary depending on the microorganism and the culture conditions.

Several studies have demonstrated that certain strains of *T. harzianum* can produce organic acids and solubilize P, including citric, malic, oxalic, tartaric, succinic, and lactic acids (Zhang et al., 2014; Li et al., 2015; Bader et al., 2020). However, the potential of the strain studied here for these purposes was unknown; therefore, we sought to evaluate the effect of adding different concentrations of methanol and ethanol on the culture medium containing 3.5% of struvite (source of low solubility inorganic P), as explained in section 2.2.1. The advantage of using struvite, is that it is a byproduct obtained during the treatment of urban wastewater under alkaline conditions. Its recovery contributes to both sustainable agriculture and the prevention of P returning to water bodies, thereby avoiding environmental damage (Ahmed et al., 2018).

According to Fig. 5.2a, which presents the results of sporulation and the final pH after 4 days of incubation at different types and concentrations of alcohol, a reduction in spore production was observed as the alcohol concentration increased, being completely interrupted in the presence of 12% ethanol, where the spore count was lower than that of the inoculum (1×10^7 spores g^{-1} DM). In all conditions where alcohol was added, sporulation was significantly lower compared to the control condition without alcohol

(9.8×10^9 spores g^{-1} DM). This effect can also be observed in Fig. 5.2b, which shows the final appearance of the fermented solids without addition of alcohol and with the maximum addition of methanol and ethanol where sporulation occurred (9% methanol and 8% ethanol). In the control condition, where no alcohol was added, the microbial biomass exhibited a dark green color, characteristic of *T. harzianum* spore.

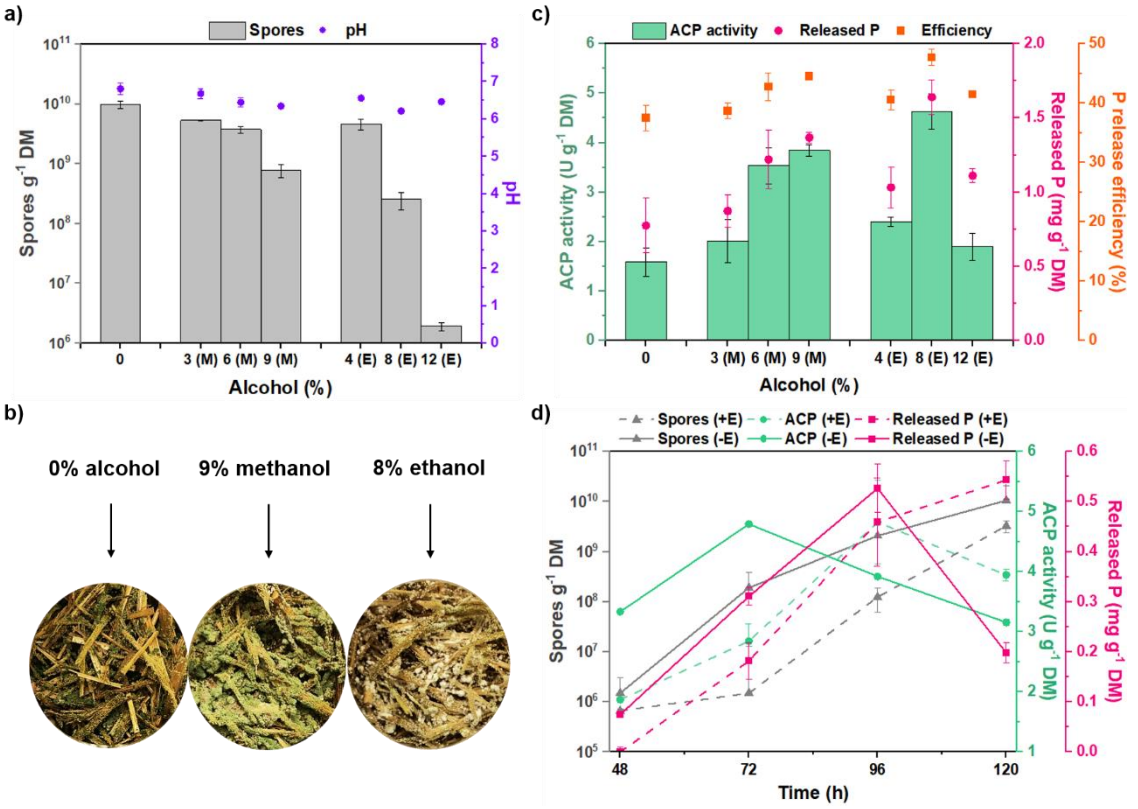

Fig. 5.2. Effect of different methanol and ethanol concentrations on *Trichoderma harzianum* SSF using beer draff:wheat straw 7:3 as substrates and 3.5% of struvite as inorganic P source. The evaluated responses include: a) spore production and final pH; b) phenotypic aspect of the fermented solids; c) Acid phosphatase (ACP) activity, released P, and P solubilization efficiency and d) time-course analysis (without struvite) comparing 8% ethanol addition versus no ethanol. SSF was conducted at 25°C for 4 days in Erlenmeyer flasks.

On the other hand, with the addition of 9% methanol, a lighter greenish color was observed, while the addition of 8% ethanol resulted in a whitish appearance. During its growth stages, *T. harzianum* typically initiates colony development with white

mycelium. As development proceeds, conidiophores are formed, which are responsible for generating and dispersing conidia, characterized by their green coloration (Meyer et al., 2019).

A lower sporulation with the addition of alcohol was also observed by Rodrigues et al. (2024). According to Anwar et al. (2009), the addition of methanol to the culture medium can reduce sporulation whilepotentially enhancing the yield of fermentation metabolites. However, the presence of alcohol does not seem to have stimulated higher acid production, as the final pH remained between 6 and 7, close to the initial pH (6.9) (Fig. 5.2a). Consequently, the P solubilization efficiency was less than 50% in all evaluated conditions, as shown in Fig. 5.2c, which shows the ACP activity, released P and the P solubilization efficiency for each condition. Li et al. (2015) investigated the ability of the strain *T. harzianum* SQR-T037 to solubilize several minerals and phytate. The authors reported that the strain could solubilize phytate, Fe_2O_3, CuO, and metallic Zn, but was unable to solubilize $Ca_3(PO_4)_2$. The authors reported that, even though different organic acids were detected, the pH remained high. Therefore, the decrease in pH appears to be a crucial factor for the solubilization of inorganic P.

On the other hand, a higher acid phosphatase (ACP) activity was observed in the treatments with alcohol, as evidenced in Fig. 5.2c. Comparing the values of ACP activity between the conditions where alcohol was added and the control condition, significantly higher values were obtained with the addition of 6% and 9% of methanol, and 8% of ethanol, while no significant difference was observed in the other conditions. The alkaline phosphatase activity (ALP) was also quantified, but the value was close to zero U g^{-1} DM. Regarding released P, only the values corresponding to the addition of 9% methanol and 8% ethanol were significantly higher than those of the control. However, the released P values followed the same trend as ACP activity, suggesting that the released P was primarily derived from organic sources through enzymatic action. It's important to note that in calculating released P, the soluble P initially present in the sample was discounted.

In this regard, the addition of 6% and 9% methanol, as well as 8% ethanol, appears to favor higher ACP excretion, with a value of 4.6 U g^{-1} DM. There are few studies in the literature about the production of phosphatases by *T. harzianum*, especially through SSF. Some studies have investigated phosphatase production by other *Trichoderma* species and different conditions. Busato et al. (2020) investigated

ACP production during a vermicomposting process enriched with phosphate rock, observing a maximum production of 3 U g^{-1} of vermicompost when simultaneously inoculating *Trichoderma asperellum* and *Trichoderma virens*. Mercl et al. (2020) studied soil P availability following inoculation with *Penicillium* sp. and *T. harzianum*, reporting an increase in ACP activity in the soil by *T. harzianum*, with a maximum value of 2.4 U g^{-1} DM. Lima et al. (2022) evaluated ACP production by different *Trichoderma* species through submerged fermentation using soybean molasses as a culture medium, achieving a maximum activity of 2.5 U mL^{-1} with *T. harzianum* as inoculum. In this context, the ACP activity values obtained here demonstrate the significant potential of the studied strain to release organic P.

Given that the strain did not exhibit significant potential for organic acid production, and therefore for solubilizing inorganic P, the next experiments were conducted without the addition of struvite. To better understand the influence of ethanol and evaluate the responses over time, two time-course experiments were conducted. Considering that the highest ACP activity was obtained with the addition of 8% ethanol, a cultivation with 8% ethanol was compared with a control without ethanol, as shown in Fig. 5.2d.

The ACP activity profiles exhibit a distinct peak, followed by a decline in activity (Fig. 5.2d). The decline may be attributed to enzymatic inactivation, possibly caused by product inhibition, or to enzymatic degradation, which could result from protease production REF. The peaks occurred at 96 hours and 72 hours of cultivation for treatments with and without ethanol, respectively, both reaching a maximum value of 4.8 U g^{-1} DM. In the cultivation without ethanol, the released P profile showed a decrease after 96 hours, possibly due to the formation of new P complexes or to the consumption of P by the microorganism itself.

Regarding the production of spores, the maximum values obtained were 3.3×10^9 spores g^{-1} DM and 1.1×10^{10} spores g^{-1} DM with 120 hours of cultivation for treatments with and without ethanol, respectively (Fig. 5.2d). Furthermore, the spore production profile for the treatment without ethanol increased faster than the treatment with 8% ethanol. These findings, combined with the phenotypic characteristics of the different treatments (Fig. 5.2b), suggest that the addition of alcohol only delayed strain development without altering the metabolic pathways or enhancing metabolite excretion.

Based on these results, the addition of ethanol did not provide significant advantages. Nevertheless, the strain exhibited efficiency in producing ACP and mobilizing organic P. Furthermore, the combination of BD and WS supported high spore production, achieving levels on the order of 1×10^{10} spores g^{-1} DM. In view of this, subsequent experiments focused on optimizing spore production by investigating critical scale-up factors, as detailed in the next section.

5.3.2 Optimization of spore production in 0.5 L PBB

A Box-Behnken design was employed using 0.5 L PBBs to optimize spore production. The variables evaluated were the BD:WS substrate ratio, inoculum size, and aeration, with a process time of 4 days. The results from all experimental combinations are presented in Fig. 5.3, which shows surface and contour plots of spore production, and in Table 5.2, which provides the design matrix, experimental responses, and predicted values from the regression model (R^2 adj = 68.26%) described in Eq. (6). Among the linear parameters, only inoculum size showed no significant effect. The model showed insignificant lack of fit (p-value = 0.490) and was simplified by excluding non-significant quadratic terms and interactions.

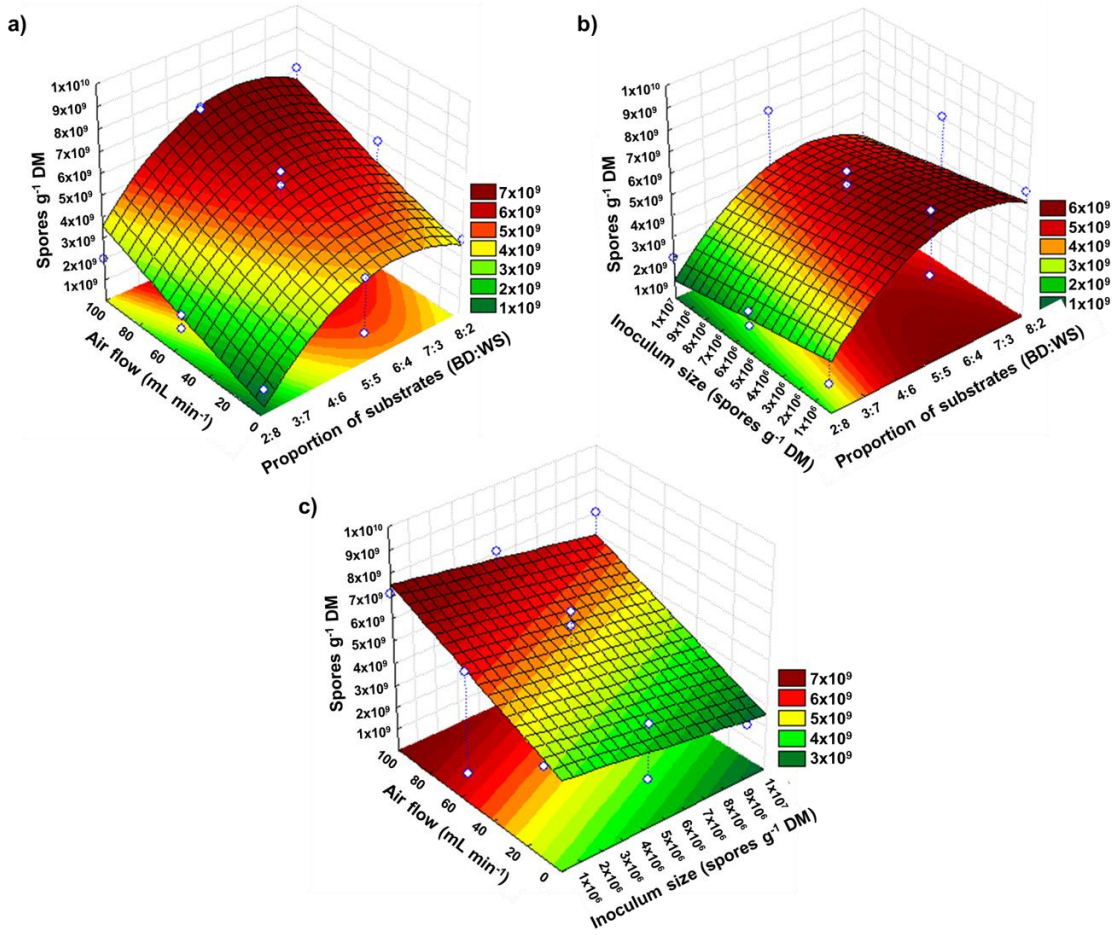

Fig. 5.3. Surface plots, resulting from the Box-Behnken design experiments, showing the influence of airflow, proportion of beer draff (BD) and wheat straw (WS) and inoculum size on sporulation. a) Inoculum size fixed in 5.05 × 10^6 spores g^{-1} DM. b) Air flow fixed in 55 mL min^{-1}. c) Proportion of substrates fixed in 5:5 BD:WS. SSF were carried out at 25ºC for 4 days in 0.5 L packed-bed bioreactors.

$$\text{Spores} = -4090142778 + 277112934(P_{BD}) - 155{,}8(IS) + 34357712(AF) - 2269941(PS)^2 \quad (6)$$

where P_{BD}, IS and AF represent the proportion of BD (%), inoculum size (spores g^{-1} DM) and air flow (mL min^{-1}), respectively.

Table 5.2. Matrix and results of the Box-Behnken design carried out to evaluate the influence of air flow, proportion of beer draff (BD):wheat straw (WS) and inoculum size on the sporulation by *Trichoderma harzianum* in 0.5 L packed-bed bioreactors.

Run	Bulk density (g L^{-1})	Independent variables			Dependent variables	
		Air flow (mL min^{-1})	BD:WS (C/N ratio)	Inoculum size (spores g^{-1} DM)	Spores exp[1] (g^{-1} DM)	Spores pred[2] (g^{-1} DM)
1	122	55	2:8 (45)	1.00×10^5	1.34×10^9	2.42×10^9
2	233	55	8:2 (21)	1.00×10^5	5.91×10^9	5.43×10^9
3	122	55	2:8 (45)	1.00×10^7	1.97×10^9	8.76×10^8
4	233	55	8:2 (21)	1.00×10^7	1.82×10^9	3.88×10^9
5	122	10	2:8 (45)	5.05×10^6	1.29×10^9	1.01×10^8
6	233	10	8:2 (21)	5.05×10^6	3.79×10^9	3.11×10^9
7	122	100	2:8 (45)	5.05×10^6	1.99×10^9	3.19×10^9
8	233	100	8:2 (21)	5.05×10^6	7.09×10^9	6.20×10^9
9	133	10	5:5 (28)	1.00×10^5	4.14×10^9	4.42×10^9
10	133	10	5:5 (28)	1.00×10^7	1.56×10^9	2.88×10^9
11	133	100	5:5 (28)	1.00×10^5	7.11×10^9	7.51×10^9
12	133	100	5:5 (28)	1.00×10^7	6.97×10^9	5.97×10^9
13	133	55	5:5 (28)	5.05×10^6	5.86×10^9	5.19×10^9
14	133	55	5:5 (28)	5.05×10^6	4.25×10^9	5.19×10^9
15	133	55	5:5 (28)	5.05×10^6	6.46×10^9	5.19×10^9
OC*	156	100	6:4 (25)	1.00×10^5	$1.08 \times 10^{10**}$	7.78×10^9

[1] Spores exp corresponds to the value of spores obtained experimentally.
[2] Spores pred corresponds to the value of spores obtained according to the fitted regression equation.
* OC means optimized condition.
** The value corresponds to cultivation performed under optimal conditions for a duration of 96 hours.

According to Fig. 5.3, the highest spore production values (1.08×10^{10} spores g^{-1} DM) were achieved at the maximum air flow tested (100 mL min^{-1}), a BD:WS proportion of approximately 6:4, and the smallest inoculum size evaluated ($1x10^5$ spores g^{-1} DM). By maximizing the response (spore production) using the model (Eq. (6)), these same conditions were determined as the optimal parameters.

Aeration is a key factor in SSF within PBBs, as it directly influences O_2 supply, CO_2 removal, and the dissipation of metabolic heat. Proper aeration rates are critical for supporting aerobic metabolism and ensuring optimal growth of microorganisms.

Conversely, excessively high rates can lead to substrate dehydration, reducing the moisture necessary for growth and spore formation (Mitchell et al., 2023). In this study, no adverse effect on substrate moisture was observed at the maximum airflow evaluated (100 mL min^{-1}), as the final moisture values remained similar to the initial level (70%). Under similar conditions, Sala et al. (2020) investigated aeration rates ranging from 20 to 60 mL min^{-1} during the cultivation of the same strain of *T. harzianum*. However, the authors reported that aeration was not a significant parameter, likely due to the restricted range of aeration rates evaluated.

Along with aeration, substrate proportion significantly impacts bioprocess yield. As previously discussed, altering the ratio of BD to WS results in beds with different bulk densities and porosities (Casciatori et al., 2014). These structural changes directly affect heat dissipation, air distribution, and ultimately bioprocess efficiency (Perez et al., 2021). Beyond these physical factors, substrate composition also varies with the proportions used, leading to changes in the C/N ratio, as shown in Table 5.2.

The optimal C/N ratio values for *Trichoderma* species vary widely in the literature, ranging from 6 to 160 (Gao et al., 2007; Dorta-Vásquez et al., 2019). For *T. harzianum* in submerged culture, ratios between 14 and 24 have been reported as optimal (Agosin et al., 1997; Said, 2007). However, carbon sources in liquid media are typically readily assimilable, such as glucose and sucrose. In contrast, complex solid substrates undergo gradual enzymatic degradation, releasing nutrients progressively. This suggests that the initial C:N ratio may not accurately reflect the ratio available over time, with degradation kinetics being an additional factor to consider. Therefore, the C:N ratio of 25, at which the highest sporulation was observed in the present study, may have facilitated a more balanced nutrient release throughout the process, promoting sporulation of *T. harzianum* (Gao et al., 2007).

As previously mentioned, the inoculum size was not a significant factor in the model; however, the highest spore production was observed at the smallest inoculum size evaluated (1×10^5 spores g^{-1} DM). This result is particularly advantageous for process scaling, as inoculum preparation often represents a significant fraction of production costs. Ideally, the inoculum should be sufficient to ensure homogeneous and rapid colonization of the substrate, but this does not necessarily require high inoculum levels ($> 1 \times 10^7$ spores g^{-1} DM), as excessive amounts could reduce spore production due to nutrient depletion. The lack of significance of this parameter in the model may be

attributed to the fast and abundant growth characteristic of *Trichoderma* species, as reported by other studies that also found no significant differences in sporulation when varying inoculum size (Valencia; Castro, 2004; Dorta-Vásquez et al., 2019; Li et al., 2022).

5.3.3 Time-course analysis of sporulation and associated metabolic responses in 0.5 L PBBs

Time is another crucial factor in process scaling, as longer cultivation times increase costs. Therefore, after establishing the optimal aeration conditions, substrate proportion, and inoculum size, we aimed to evaluate O_2 consumption and sporulation profiles over 144 hours of cultivation, along with other relevant parameters within the scope of this study, including ACP activity, released P, indole derivatives, and total flavonoids. Monitoring O_2 consumption provides crucial insights into the performance of aerobic microorganisms, particularly in SSF, where direct biomass quantification is not straightforward.

Fig. 5.4a presents the profiles of the specific O_2 consumption rate (sOUR) and cumulative O_2 consumption (COC) over time. The COC value at the end of the time course was 307.58 g O_2 kg^{-1} DM and the maximum sOUR value was 4.67 g O_2 kg^{-1} DM h^{-1} at approximately 43 hours, followed by a smaller secondary peak around 65 hours, possibly indicating diauxic growth. This phenomenon occurs when microorganisms utilize different carbon sources sequentially, prioritizing the most readily assimilable. In an SSF process with a mixture of BD and WS, such behavior is expected, as the substrate blend contains carbon sources with varying complexities. Although BD and WS have similar total carbon contents (Table 5.1), BD is more easily assimilated due to its lower cellulose and hemicellulose levels. Additionally, BD may retain starch residues and partially solubilized sugars from the beer production process (Massardi et al., 2020; Sun; Tomkinson, 2002).

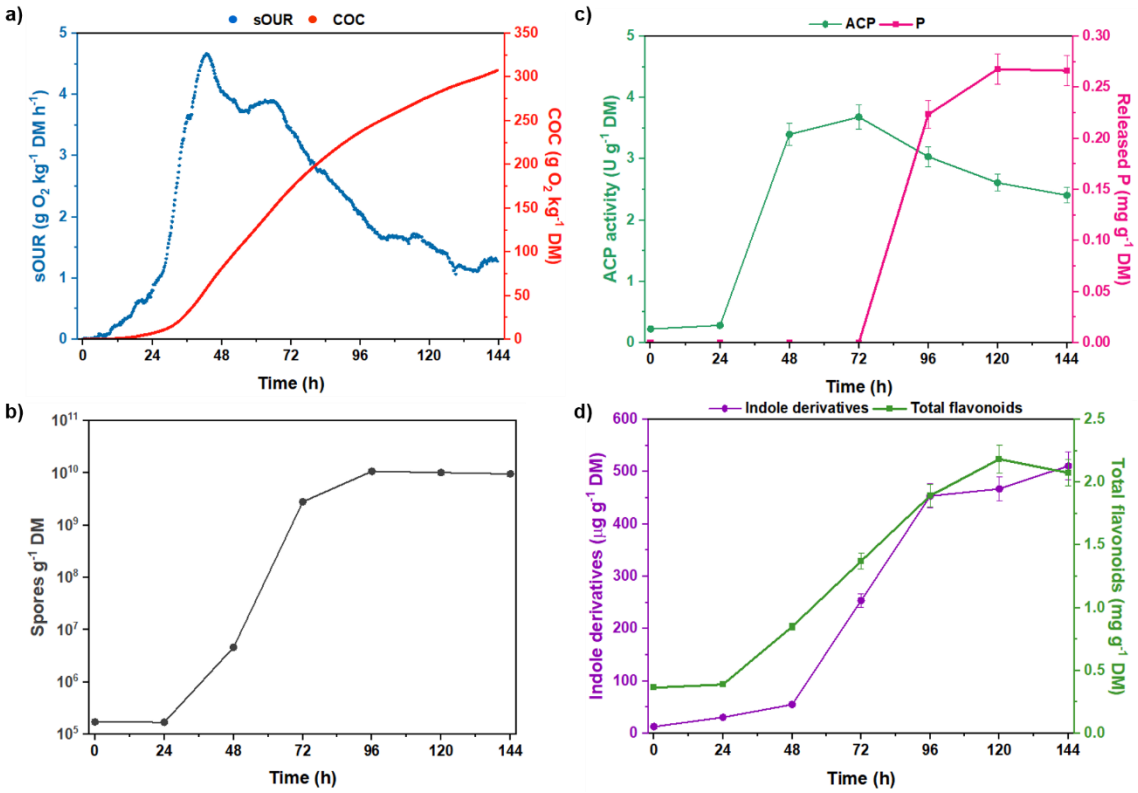

Fig. 5.4. Time course analysis under optimized conditions in 0.5 L PBBs. Profiles of a) Specific oxygen uptake rate (sOUR) and Cumulative Oxygen Consumption (COC), b) spores, c) Acid phosphatase (ACP) activity and released P, and d) indole derivatives and total flavonoids. SSF was conducted at 25°C in 0.5 L packed-bed bioreactors.

The sOUR values obtained in this study were higher than those reported in the literature for similar cultivations. Sala et al. (2021a) evaluated SSF of the same *T. harzianum* strain in a 0.5 L PBB using only BD as a substrate and reported a maximum sOUR of approximately 2.2 g O_2 kg^{-1} DM h^{-1}. In a 1.5 L PBB using 70% of BD and 30% of WC, Sala et al. (2021b) recorded a peak of 2.5 g O_2 kg^{-1} DM h^{-1}. Additionally, Ghoreishi et al. (2023), when evaluating grass clippings and pruning waste as substrates, reported maximum sOUR values below 1.5 g O_2 kg^{-1} DM h^{-1}. The higher sOUR values observed in this study suggest intensified metabolic activity of *T. harzianum* under the tested conditions, potentially linked to adequate nutrient availability and favorable aeration. Although Sala et al. (2021a) used only BD, which is a nutritionally rich medium, it results in lower porosity. These findings underscore the importance of bed porosity in SSF processes.

Since O_2 availability and metabolic activity are closely linked to spore formation, it is essential to examine how these factors influenced *T. harzianum* sporulation over time. The spore production profile under optimized conditions is presented in Fig. 5.4b, which shows that sporulation reaches its maximum value at 96 hours. Beyond this point, the number of spores remains constant, suggesting that extending the process past 96 hours does not lead to further spore production, as previously observed (Sala et al., 2022).

The maximum spore production achieved in this study, 1.08×10^{10} spores g^{-1} DM, is quite promising, particularly considering that no supplementation was used and the initial concentration was in the order of 1×10^5 spores g^{-1} DM. This represents a 60,000-fold increase in spore numbers. Zhang and Yang (2015) optimized the cultivation of a *T. harzianum* strain in straw and wheat bran using Erlenmeyer flasks and obtained a sporulation of 1.49×10^{10} CFUs g^{-1} DM, using an inoculum size of 1×10^7 CFU per bottle; however, their process required eight days of cultivation and supplementation with ammonium persulfate. Under conditions similar to those of the present study, Sala et al. (2021a) reported a maximum sporulation of 5×10^9 spores g^{-1} DM, while Ghoreishi et al. (2023) observed a peak sporulation of 3.03×10^9 spores g^{-1} DM. Both studies used an inoculum size f 1×10^7 spores g^{-1} DM.

The results for ACP activity and phosphorus release are presented in Fig. 5.4c. The maximum ACP activity obtained was 3.7 U g^{-1} DM after 72 hours of cultivation. After this peak, activity decreased over time to 2.4 U g^{-1} DM after 144 hours. This result is lower than the 4.8 U g^{-1} DM observed in Erlenmeyer flasks without ethanol addition. However, the trend was similar: a peak after 72 hours followed by a decline, which may be attributed to enzyme degradation or inhibition, as previously discussed.

The higher ACP activity observed in the Erlenmeyer flask cultivation was likely due to the medium composition, which had a higher proportion of BD (BD:WS 7:3) and, consequently, greater N and P content (Table 5.1). This medium may have better supported microorganism growth, leading to increased ACP production. Despite the lower proportion of structural substrate (WS), compaction was not an issue, as each Erlenmeyer flask contained only 10 g of material. Additionally, the higher P content may have stimulated greater ACP production and secretion, since this P is not readily available but is present in organic molecules such as nucleic acids and phospholipids (Wang et al., 2022).

As a result of ACP activity, the released P profile increased after 72 hours of cultivation, reaching a maximum of 0.27 mg P g^{-1} DM. It is important to emphasize that the quantified released P is in the form of P_2O_5. This value is also lower than that previously obtained in Erlenmeyer flasks, likely due to the factors discussed.

The profiles of indole derivatives and total flavonoids were evaluated and are presented in Fig. 5.4d. It is well known that one of the main pathways microorganisms use to produce IAA and related molecules is derived from tryptophan; however, *T. harzianum* also can synthesize IAA and its derivatives from naturally occurring compounds in the substrates, particularly in BD, which is rich in proteins and phenolic compounds (Ikram et al., 2017). Studies have shown that process conditions and substrate composition influence IAA production in *Trichoderma* and other microorganisms, suggesting the existence of alternative biosynthetic pathways beyond direct tryptophan utilization (Nieto-Jacobo et al., 2017; Prado et al., 2019a). In this study, aiming to reduce costs and simplify the process, tryptophan was not added.

Both profiles increased over time and began to stabilize after 96 hours of cultivation. The production of indole derivatives reached a maximum of 511.3 μg g^{-1} DM at 144 hours, equivalent to 32.7 μg mL^{-1} when considering the proportion of distilled water to dry matter used in the solid-liquid extraction. Napitupulu et al. (2019), who optimized process conditions for IAA production by *T. harzianum* in submerged fermentation using flasks, reported that after 96 hours of incubation under optimized conditions (with the addition of 1% tryptophan), IAA concentration also reached equilibrium, with a maximum of 10.1 μg mL^{-1}. In contrast, Ghoreishi et al. (2023), who evaluated the IAA production profile in grass and pruning waste with the addition of 0.45% tryptophan by *T. harzianum* in a 0.5 L PBB over 10 days, reported a maximum production of 101.46 μg g^{-1} DM on the third day, followed by a decline. This decline was likely due to IAA degradation as a nutrient source, given the limited availability of easily assimilable carbon and nitrogen in the substrates.

Prado et al. (2019b) evaluated the production of indole derivatives by *T. harzianum* in SSF using various agro-industrial by-products with 1% tryptophan addition and reported a maximum production of 97.3 μg mL^{-1} when using wheat bran as a substrate. A higher production was reported by Prado et al. (2019a) with *Aspergillus flavipes* cultivated on soybean bran, achieving 655 μg mL^{-1} with 1.5% tryptophan supplementation. These findings highlight the considerable variability in indole

derivative production depending on the microorganism, culture medium, and process conditions. Given that no exogenous tryptophan was added in the present study, the observed production is highly promising and may contribute to enhanced P acquisition and plant growth.

Regarding the total flavonoid profile, a maximum of 2.2 mg g^{-1} DM was reached after 120 hours of cultivation, equivalent to 218.4 mg L^{-1}, representing a sixfold increase compared to the initial flavonoid content in the substrates (0.36 mg g^{-1} DM). The use of *Trichoderma* species as inoculum in fermentation processes to enhance flavonoid production is rarely reported in the literature. However, some studies indicate that *Trichoderma* application in plants can increase their flavonoid content, suggesting that this microorganism plays a role in the synthesis of these compounds. Imran et al. (2023) investigated the application of culture filtrates from three *Trichoderma* spp. in tomato leaves and found a significant increase in total flavonoid content. When treated with a *T. harzianum* strain, plants exhibited a maximum flavonoid content of approximately 0.85 mg g^{-1}, corresponding to a 3.5-fold increase. Similarly, Pascale et al. (2017) reported a significant increase in the polyphenol content in *Vitis vinifera* when applying live spores of a *T. harzianum* strain as well as a secondary metabolite (6-pentyl-a-pyrone).

Other microorganisms have also been explored for their ability to enhance flavonoid content of some substrates. Zhao et al. (2023) investigated the transformation of total flavonoids in mulberry leaves via SSF and achieved a threefold increase (24.42 to 72.55 mg rutin equivalents g^{-1} dry weight) using *Aspergillus cristatus*. Likewise, Xiao et al. (2021) reported a 1.3-fold increase in total phenolic content in black soybeans after SSF with *Eurotium cristatum*. Thus, the sixfold increase in total flavonoid content observed in this study is highly promising. It may contribute to several plant development benefits, including enhanced phosphorus and nutrient acquisition, increased resistance to pathogens and abiotic stress, improved nutritional content, and higher overall yield (Shah and Smith, 2020).

5.3.4 Scale-up: 22 L packed-bed bioreactor

After optimizing key process parameters and analyzing the temporal profiles of biomolecules of interest in the 0.5 L PBBs, the scale-up to a 22 L PBB was evaluated. Considering the dimensions of the 0.5 L PBB, the superficial air velocity (Eq. 2)

corresponding to the optimal airflow rate determined in the Box-Behnken design (100 mL min^{-1}) is approximately 0.5 mm s^{-1}. To maintain this velocity in the 22 L PBB, an airflow rate of approximately 1500 mL min^{-1} was required. This same flow rate was previously used by Sala et al. (2022), for the same strain and 22 L PBB, and no issues related to temperature rise, drying, or O_2 limitation were reported. However, after conducting the first batch, a pronounced temperature increase was observed. In response to this, two modifications were implemented for the second batch: the addition of 20% wood chips (WC) as bulking agent and an increase in airflow rate to 2000 mL min^{-1}.

Regarding the cultivation time, a duration of 4 days had initially been selected, as Fig. 5.4 indicates that the profiles of spores, indole derivatives, and total flavonoids began to stabilize after 96 hours. However, during the first batch in the 22 L PBB, it was observed that O_2 consumption started later compared to the 0.5 L PBBs. In response, the cultivation time was extended to 144 hours. The process conditions and some results for each batch are summarized in Table 5.3. As mentioned in Section 2.2.4, alongside the 22 L PBB batches, the same inoculated material was distributed in three 0.5 L PBBs to compare results and identify potential scale-up issues. These results are also presented in Table 5.3.

Table 5.3. Operating conditions and main results for the two batches conducted in the 22 L packed-bed bioreactor.

	Batch 1		Batch 2	
	22 L	0.5 L	22 L	0.5 L
Substrates proportion (BD:WS)	6:4	6:4	6:4	6:4
WC (%)	-	-	20	20
Inoculum size (spores g^{-1} DM)	1.00×10^5	1.00×10^5	1.00×10^5	1.00×10^5
Air flow (mL min^{-1})	1500	100	2000	100
Cultivation time (hours)	144	144	144	144
Maximum sOUR (g O_2 kg^{-1} DM h^{-1})	4.72	5.04 ± 0.44	3.65	3.21 ± 0.43

BD: beer draff; WS: wheat straw; WC: wood chips; DM: dry matter; sOUR: specific oxygen uptake rate; COC: cumulative oxygen uptake rate; ACP: acid phosphatase.

Table5.3. Continuation.

	Batch 1		Batch 2	
	22 L	0.5 L	22 L	0.5 L
Maximum COC (g O_2 kg^{-1} DM)	327.93	319.54 ± 30.72	246.40	219.25 ± 35.77
Maximum temperature (°C)	41.50	25.00	41.50	25.00
Average temperature (°C)	27.56	25.00	28.99	25.00
Average sporulation (spores g^{-1} DM)	2.64×10^9	$1.27 \times 10^{10} \pm 1.80 \times 10^9$	1.47×10^9	$5.52 \times 10^9 \pm 6.53 \times 10^8$
Average ACP activity (U g^{-1} DM)	0.74	2.93 ± 0.27	0.50	2.42 ± 0.21
Average total flavonoids (mg g^{-1} DM)	0.44	1.86 ± 0.17	0.54	1.16 ± 0.09
Average indole derivatives (µg g^{-1} DM)	687.84	568.61 ± 62.55	497.50	471.95 ± 41.06

BD: beer draff; WS: wheat straw; WC: wood chips; DM: dry matter; sOUR: specific oxygen uptake rate; COC: cumulative oxygen uptake rate; ACP: acid phosphatase.

Fig. 5.5 presents the temperature profiles along with the maximum and average values recorded at different radial and longitudinal positions within the PBB. A total of 6 temperature sensors were placed inside the bioreactor, as illustrated in Fig. 5.5a. The profiles for both batches revealed significant overheating in the central regions (r = 0), particularly at z = L/2 and z = L. These regions exhibited much higher temperatures compared to other positions, as shown in Fig. 5.5b and 5.5c for the batches 1 and 2, respectively. Temperature peaks observed every 24 hours were attributed to environmental fluctuations caused by direct sunlight received by laboratory windows.

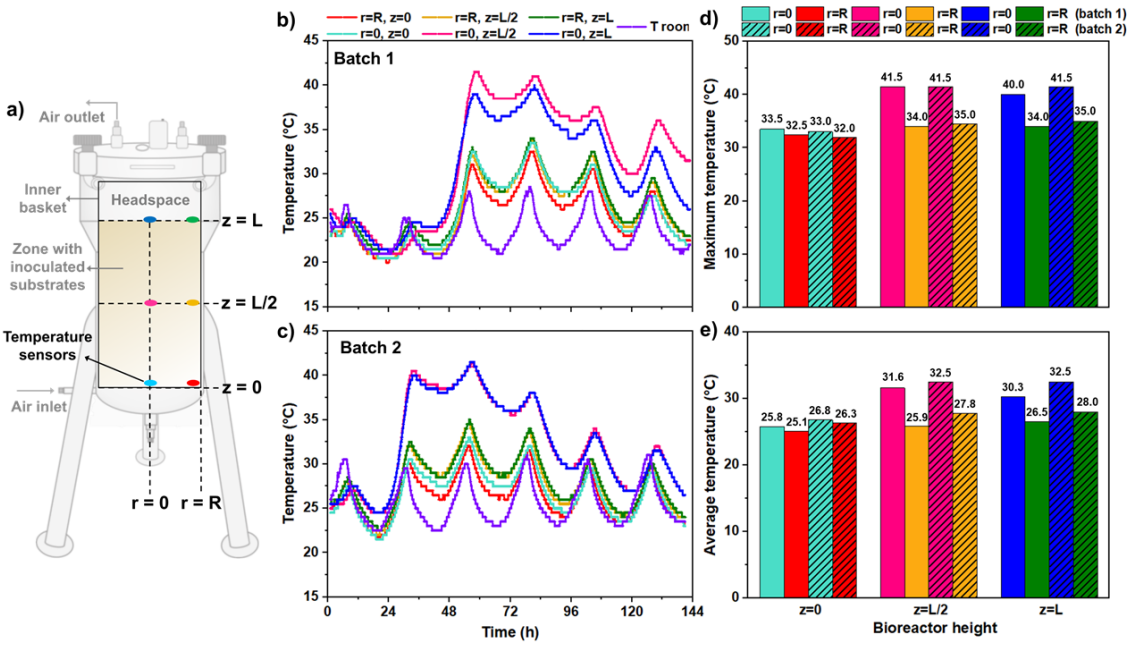

Fig. 5.5. Thermal behavior during SSF in the 22 L packed-bed bioreactor: a) position of temperature sensors inside the bioreactor; b) temperature profiles over time for the two batches; c) maximum and d) average temperatures recorded at each sensor position.

When comparing the temperature profiles of both batches, it was noted that the temperature rise in batch 1 occurred later than in batch 2, with a delay of approximately 24 hours. This corresponds to the delayed O_2 consumption observed in batch 1, likely due to lower ambient temperatures at the start of cultivation. The maximum and average temperatures recorded at each position in the bioreactor are shown in Fig. 5.5d and 5.5e for batches 1 and 2, respectively. Overall, the highest temperatures were recorded near the center of the bioreactor (r = 0) and farthest from the air inlet (z = L/2 and z = L), while the lowest temperatures were near the walls (r = R) and closest to the air inlet (z = 0). The maximum recorded temperature was 41.5°C at the central position (r = 0, z = L/2) in batch 1, and the same temperature was reached at the top center in batch 2 (r = 0, z = L). The highest average temperatures were also recorded at these positions, with values of 31.6°C and 32.5°C for batches 1 and 2, respectively. The overall average temperature across all positions was 27.6°C for batch 1 and 29.0°C for batch 2.

These temperature gradients are common in SSF processes using PBBs, where overheating typically does not occur near the air inlet, as this region receives fresh air that has not yet transported the metabolic heat. In contrast, temperatures are higher

farther from the air inlet due to the advection phenomenon (Rodrigues et al., 2022; Casciatori et al., 2024). Radial heat transfer by conduction contributes to lower temperatures near the bioreactor walls.

Given the pronounced temperature difference of 16.5°C above the optimal sporulation temperature of 25°C for the strain (Sala et al., 2020), and the challenges of scaling up SSF processes, further improvements are needed. Agro-industrial waste typically has low thermal conductivity, which combined with the small air flow rates used to avoid bed drying, reduces both static and dynamic thermal conductivities, making heat removal difficult. This leads to inevitable axial and radial temperature gradients, especially when the bioreactor diameter is large (Casciatori et al., 2016).

Although the addition of WS creates empty spaces in the bed to facilitate heat removal, it was observed that the bed had compacted by 6 cm at the end of batch 1. For batch 2, 20% WC was added, as it has greater mechanical resistance than WS and could prevent compaction. It is important to note that the percentage of WC added was relative to the total mass packed in the bioreactor. In addition to this, the air flow rate was increased to 2000 mL min^{-1}, which corresponds to an increase of approximately 33%. However, despite a lower compaction of 4 cm in batch 2, these strategies were not sufficient to prevent overheating.

In contrast, the maximum temperature reached in the work of Sala et al. (2022) was around 30°C with an average of 25.7°C after 6 days of cultivation using a bed with 40% BD and 60% WC. Ghoreishi et al. (2024) also used a 22 L PBB with 56% grass as substrate and 44% bulking agent, evaluating both pruning waste and WC. They reported no significant overheating, with a maximum temperature of 31°C for both bulking agents. However, spore and IAA production were higher with WC, likely due to less compaction and improved aeration. Grass as a substrate generates less heat compared to BD and WS, as it is nutrient-poor and leads to slower microbial growth.

Given these considerations, further improvements are necessary for the scale-up of the process to improve heat dissipation. Future work may involve exploring higher air flow rates and proportions of WC. According to Perez et al. (2019), when scaling up PBBs, the ratio between superficial air velocity and bed height should be maintained. However, even maintaining this ratio, the authors observed a significant decrease in enzyme production and an increase in overheating in the pilot-scale process compared to the bench scale.

Despite the challenges related to scaling up the process and the need for improvement, the maximum sOUR and COC values achieved in the 22 L bioreactor were similar to those achieved in the 0.5 L bioreactors, as shown in Table 5.3. The profiles of both batches are presented in Fig. 5.6a, where it can be seen that the peaks occurred around 70 and 40 hours for batches 1 and 2, respectively. As mentioned, the delayed peak in batch 1 was likely due to exposure to lower temperatures at the beginning of the process. The lower values observed in batch 2 are probably due to the use of 20% WC, leading to a lower proportion of more easily assimilated substrates.

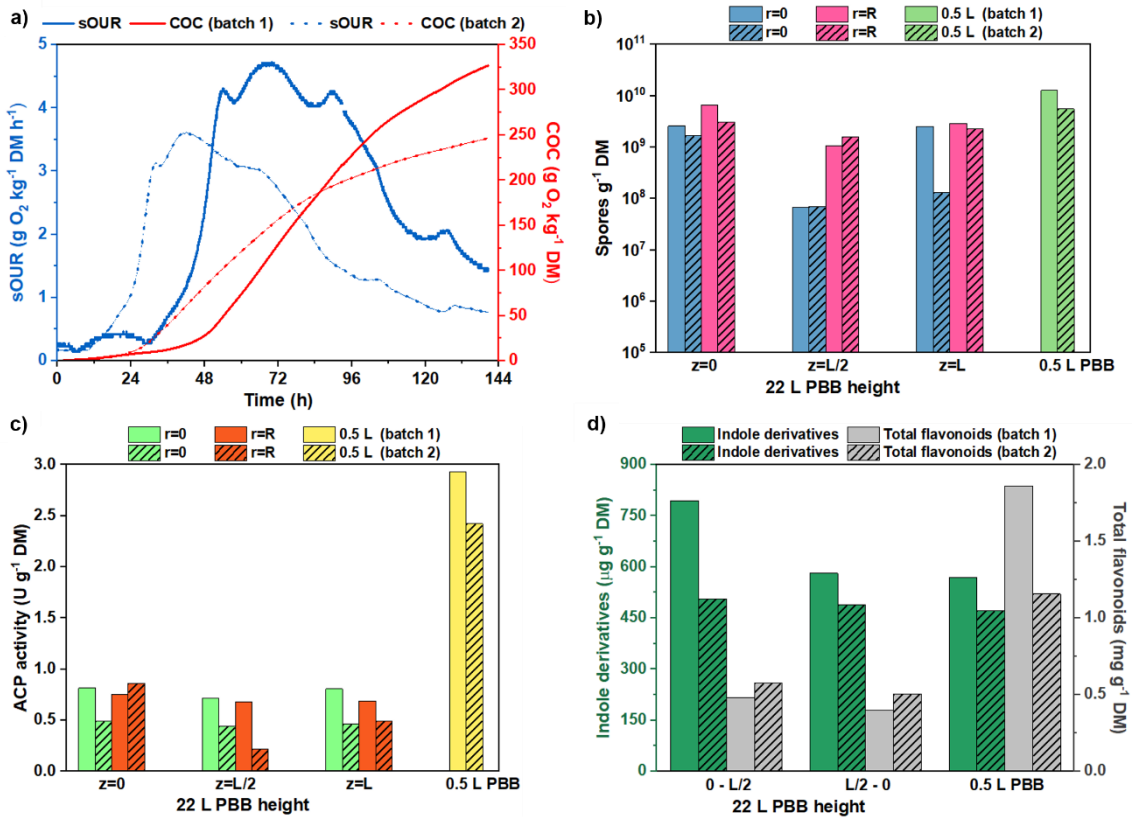

Fig. 5.6. Results from SSF process in the 22 L packed-bed bioreactor (PBB), compared to the 0.5 L PBB. Profiles of a) Specific oxygen uptake rate (sOUR) and Cumulative oxygen consumption (COC), b) spore production, c) ACP activity, and d) production of indole derivatives and total flavonoids. z represents the axial position in the bioreactor (with z = 0 at the fresh air inlet and z = L at the opposite end of the bed), and r represents the radial position (with r = 0 at the center and r = R at the wall).

Sala et al. (2022) and Ghoreishi et al. (2024) reported maximum sOUR values of 3.3 and 1.1 g O_2 kg^{-1} DM h^{-1}, respectively. When comparing these values with the results obtained here, it is evident that, there was significant O_2 consumption, indicating good microbial growth. The average spore production, considering all regions of the bioreactor, was 2.6×10^9 and 1.5×10^9 spores g^{-1} DM for batches 1 and 2, respectively (Table 5.3). Sala et al. (2022) achieved a maximum spore production of 1.7×10^9 spores g^{-1} DM after 6 days of cultivation, reinforcing that, despite the overheating, the yield obtained in the present study was still satisfactory. However, the values obtained in the bench scale are approximately 5 and 4 times lower than those obtained in the 0.5 L bioreactors, for batches 1 and 2, respectively, as shown in Table 5.3. Additionally, as expected, spore production was lower in regions with pronounced temperature increases, with values of 7×10^7 spores g^{-1} DM in the central region (r = 0, z = L/2), as shown in Fig. 5.6b. Sala et al. (2020), who evaluated the effect of temperature on the strain studied here, reported a substantial decrease in spore production above 32°C.

Overheating had even more pronounced negative effects on ACP activity, as shown in Fig. 5.6c. The average values were approximately 4 to 5 times lower than those obtained in the 0.5 L PBBs for batches 1 and 2, respectively, as presented in Table 5.3. This suggests that overheating may have impaired the synthesis and excretion of ACP (Vasileva-Tonkova et al., 1996).

Similarly, the production of total flavonoids was also negatively affected during the scale-up, as shown in Fig. 5.6d. It is important to note that in the values presented in Fig. 5.6d, the initial amount of total flavonoids was discounted. The average amounts of total flavonoids produced were approximately 4 and 2 times higher in the 0.5 L bioreactors for batches 1 and 2, respectively, as shown in Table 5.3. Flavonoids are thermosensitive molecules, which explains the significantly lower values obtained in the 22 L bioreactor. Additionally, their synthesis by fungi is impaired at high temperatures (Jiang et al., 2018).

On the other hand, the production of indole derivatives was higher in the 22 L bioreactor compared to the 0.5 L bioreactor, particularly in batch 1, as shown in Fig. 5.6d and Table 5.3. In batch 1 the proportion of BD was higher, which contains more indole compounds that may be precursors for indole derivative synthesis. The superior results observed in the lab scale are likely related to the higher temperatures reached during cultivation. It is well established that environmental factors influence IAA

production. The effect of temperature varies according to each strain and process conditions. Napitupulu et al. (2019) evaluated the effect of temperature on IAA production by a *T. harzianum* strain in submerged fermentation and reported an optimal temperature of 27°C, which differed from the optimal growth temperature of 30°C. In contrast, Ghoreishi et al. (2023) found that the highest IAA production by the strain studied here occurred at 30°C, whereas maximum sporulation was observed at 25°C. These findings highlight the need for further in-depth studies on the influence of temperature on IAA production.

5.4. Conclusions

This study demonstrated the potential of *Trichoderma harzianum* cultivated through SSF in PBBs to produce beneficial metabolites that enhance P acquisition by plants. BD and WS proved to be effective substrates, providing an alternative to traditional rice-based production. Although the strain was not effective in solubilizing inorganic P, it produced ACP and efficiently released organic P from the substrates, demonstrating potential for P mobilization. Under optimized conditions, the process led to high sporulation at both lab and bench scales - approximately 1×10^{10} spores g^{-1} DM in 0.5 L PBBs and 2×10^{9} spores g^{-1} DM in 22 L PBBs, using an inoculum size of 1×10^{5} spores g^{-1} DM - along with the synthesis of bioactive compounds indirectly involved in P acquisition, such as indole derivatives and flavonoids. However, scale-up to 22 L led to an overheating of 16.5°C, negatively impacting the production, of ACP and flavonoids. This highlights an opportunity in SSF bioreactor design: efficient heat dissipation to maintain performance at larger scales. Future research should focus on exploring new bioreactor designs, aeration strategies, and heat removal techniques. In overall, the findings reinforce the strain's potential for sustainable agricultural bio-input formulations aligned with circular economy principles.

References

Agosin, E., Volpe, D., Mun~ oz, G., San Martin, R., Crawford, A., 1997. Effect of culture conditions on spore shelf life of the biocontrol agent *Trichoderma harzianum*. World J. Microbiol. Biotechnol. 13(2), 225-232.

Ahmed, N., Shim, S., Won, S., Ra, C., 2018. Struvite recovered from various types of wastewaters: Characteristics, soil leaching behaviour, and plant growth. L. Degrad. Dev. 29, 2864–2879.

Anwar, S., Ali, S., Sardar, A.A., 2009. Citric acid fermentation of hydrolysed raw starch by Aspergillus niger IIB-A6 in stationary culture. Sindh University Research Journal (Science Series) 4, 01–08.

Bader, A.N., Salerno, G.L., Covacevich, F., Consolo, V.F., 2020. Native *Trichoderma harzianum* strains from Argentina produce indole-3 acetic acid and phosphorus solubilization, promote growth and control wilt disease on tomato (Solanum lycopersicum L.). J. King Saud Univ.-Sci. 32(1), 867-873.

Bric, J.M., Bostock, R.M., Silverstone, S.E., 1991. Rapid in situ assay for indoleacetic acid production by bacteria immobilized on a nitrocellulose membrane. Appl. Environ.

Busato, J.G., Ferrari, L.H., Chagas Junior, A.F., da Silva, D.B., dos Santos Pereira, T., Paula, A.M., 2021. *Trichoderma* strains accelerate maturation and increase available phosphorus during vermicomposting enriched with rock phosphate. J. Appl. Microbiol. 130(4), 1208-1216.

Casciatori, F.P., Bück, A., Thoméo, J.C., Tsotsas, E., 2016. Two-phase and two-dimensional model describing heat and water transfer during solid-state fermentation within a packed-bed bioreactor. Chem. Eng. J. 287, 103–116.

Casciatori, F.P., Laurentino, C.L., Taboga, S.R., Casciatori, P.A., Thomeo, J.C., 2014. Structural properties of beds packed with agro-industrial solid by-products applicable for solid-state fermentation: experimental data and effects on process performance. Chem. Eng. J. 255, 214–224.

Casciatori, F.P., Mafra, N.S.C., Rodrigues, N.A., Sales, E.H., Maia, M.M.S., Dias, A.C.P., Grajales, L.M., 2024. Flow configuration and packing density of sugarcane bagasse and wheat bran affecting enzymes production by solid-state fermentation. BioEnergy Res. 17(1), 187–197.

Chattaraj, S., Mitra, D., Ganguly, A., Thatoi, H., Mohapatra, P.K.D., 2024. A critical review on the biotechnological potential of Brewers' waste: Challenges and future alternatives. Curr. Res. Microb. Sci. 100228.

Chien, S.H., Prochnow, L.I., Tu, S., Snyder, C.S., 2011. Agronomic and environmental aspects of phosphate fertilizers varying in source and solubility: An update review. Nutr. Cycl. Agroecosyst. 89, 229–255.

Dorta-Vásquez, R., Valbuena, O., Pavone-Maniscalco, D., 2019. Solid-state fermentation of paper sludge to obtain spores of the fungus. EuroBiotech J. 3(2), 71-77.

Gao, L., Sun, M.H., Liu, X.Z., Che, Y.S., 2007. Effects of carbon concentration and carbon to nitrogen ratio on the growth and sporulation of several biocontrol fungi. Mycol. Res. 111(1), 87-92.

Ghoreishi, G., Barrena, R., Font, X., 2023. Using green waste as substrate to produce biostimulant and biopesticide products through solid-state fermentation. Waste Manag. 159, 84-92.

Ghoreishi, G., Barrena, R., Sánchez, A., Font, X., 2024. Solid-state fermentation to produce biostimulant agents from green waste: A circular approach at lab-scale. Chem. Eng. J. 502, 158057.

IFA, 2023. Phosphate rock resources and reserves. Available from: https://www.fertilizer.org/wp-content/uploads/2023/04/2023_Argus_IFA_Phosphate_Rock_Resources_and_Reserves_Final.pdf [Accessed on: March 2025].

Ikram, S., Huang, L., Zhang, H., Wang, J., Yin, M., 2017. Composition and nutrient value proposition of brewers spent grain. J. Food Sci. 82(10), 2232-2242.

Imran, M., Abo-Elyousr, K.A., Mousa, M.A., Saad, M.M., 2023. Use of *Trichoderma* culture filtrates as a sustainable approach to mitigate early blight disease of tomato and their influence on plant biomarkers and antioxidants production. Front. Plant Sci. 14, 1192818.

Jiang, F.C., Zhang, H.N., Wu, D., Feng, N., Zhang, Z., Zhang, J.S., Yang, Y., 2018. Kinetic models for the effect of temperature on flavonoid production in liquid submerged fermentation by *Phellinus baumii*. Biotechnol. Appl. Biochem. 65(5), 739-747.

Klaic, R., Gava Junior, M., Florencio, C., Ribeiro, C., Farinas, C.S., 2021. Biological solubilization of phosphate rock by solid-state cultivation to produce eco-friendly fertilizers. Pesq. Agropec. Bras. 56.

Klaic, R., Plotegher, F., Ribeiro, C., Zangirolami, T.C., Farinas, C.S., 2017. A novel combined mechanical-biological approach to improve rock phosphate solubilization. Int. J. Miner. Process. 161, 50-58.

Li, R.X., Cai, F., Pang, G., Shen, Q.R., Li, R., Chen, W., 2015. Solubilisation of phosphate and micronutrients by *Trichoderma harzianum* and its relationship with the promotion of tomato plant growth. PLoS One 10(6), e0130081.

Li, W., Zhao, L., He, X., 2022. Degradation potential of different lignocellulosic residues by *Trichoderma longibrachiatum* and *Trichoderma afroharzianum* under solid state fermentation. Process Biochem. 112, 6-17.

Lima, F.A., Rola, J.C., Gomes de Freitas, M.M., de Almeida Afonso, J.M.M., Resende, M.M., 2022. Acid phosphatase immobilization and production study by *Trichoderma* spp. in soybean molasses. Chem. Eng. Technol. 45(5), 979-984.

Mascarin, G.M., Matsumura, A.T.S., Weiler, C.A., Kobori, N.N., Silva, M.E.da, Berlitz, D.L., Matsumura, A.S., 2019. Produção industrial de *Trichoderma*. Embrapa. Available at: [https://www.embrapa.br/busca-de-publicacoes/-/publicacao/1119282/producao-industrial-de-trichoderma].

Massardi, M.M., Massini, R.M.M., de Jesus Silva, D., 2020. Caracterização química do bagaço de malte e avaliação do seu potencial para obtenção de produtos de valor agregado. J. Eng. Exact Sci. 6(1), 0083-0091.

McDowell, R.W., Pletnyakov, P., Haygarth, P.M., 2024. Phosphorus applications adjusted to optimal crop yields can help sustain global phosphorus reserves. Nat. Food 5(4), 332-339.

Mercl, F., García-Sánchez, M., Kulhánek, M., Košnář, Z., Száková, J., Tlustoš, P., 2020. Improved phosphorus fertilisation efficiency of wood ash by fungal strains *Penicillium* sp. PK112 and *Trichoderma harzianum* OMG08 on acidic soil. Appl. Soil Ecol. 147, 103360.

Meyer, M.C., Mazaro, S.M., da Silva, J.C., 2019. Trichoderma: uso na agricultura.

Napitupulu, T.P., Kanti, A., Sudiana, I.M., 2019. Evaluation of the environmental factors modulating indole-3-acetic acid (IAA) production by *Trichoderma harzianum* InaCC F88. In: IOP Conf. Ser. Earth Environ. Sci., 308(1), 012060. IOP Publishing.

Nieto-Jacobo, M.F., Steyaert, J.M., Salazar-Badillo, F.B., Nguyen, D.V., Rostás, M., Braithwaite, M., Mendoza-Mendoza, A., 2017. Environmental growth conditions of *Trichoderma* spp. affects indole acetic acid derivatives, volatile organic compounds, and plant growth promotion. Front. Plant Sci. 8, 102.

Nyhan, L., Sahin, A.W., Schmitz, H.H., Siegel, J.B., Arendt, E.K., 2023. Brewers' spent grain: An unprecedented opportunity to develop sustainable plant-based nutrition ingredients addressing global malnutrition challenges. Journal of J. Agric. Food Chem. 71(28), 10543-10564.

Pascale, A., Vinale, F., Manganiello, G., Nigro, M., Lanzuise, S., Ruocco, M., Lorito, M., 2017. Trichoderma and its secondary metabolites improve yield and quality of grapes. Crop Prot. 92, 176-181.

Porras, R.C.S., Ghoreishi, G., Sánchez, A., Barrena, R., Font, X., Ballardo, C., Artola, A., 2025. Solid-state fermentation of green waste for the production of biostimulants to enhance lettuce (Lactuca sativa L.) cultivation under water stress: Closing the organic waste cycle. Chemosphere 370, 143919.

Prado, D.Z., Okino-Delgado, C.H., Zanutto-Elgui, M.R., Silva, R.B.G., Pereira, M.S., Jahn, L., Ludwig-Müller, J., Silva, M.R., Velini, V.D., Fleuri, L.F., 2019a. Screening of *Aspergillus*, *Bacillus* and *Trichoderma* strains and influence of substrates on auxin and phytases production through solid-state fermentation. Biocatal. Agric. Biotechnol, 19, 101165.

Prado, D.Z., Oliveira, S.L., Okino-Delgado, C.H., Auer, S., Ludwig-Müller, J., Da Silva, M.R., Fleuri, L.F., 2019b. *Aspergillus flavipes* as a novel biostimulant for rooting-enhancement of Eucalyptus. J. Clean. Prod. 234, 681-689.

Richardson, A.E., Simpson, R.J., 2011. Soil microorganisms mediating phosphorus availability update on microbial phosphorus. Plant Physiol. 156(3), 989-996.

Rodrigues, N.A., Buffo, M.M., Casciatori, F.P., Farinas, C.S., 2024. New approaches for solubilization of phosphate rocks through solid-state fermentation by optimization of oxalic acid production. Bioresour. Technol., 408, 131165.

Rodrigues, N.A., Katayama, E.T., Casciatori, F.P., 2022. Alternative strategies to perform solid-state cultivation in a multilayer packed-bed bioreactor: Continuous and cyclic operations. Chem. Eng. J., 448, 137726.

Said, S.D., 2007. Spore production of biocontrol agent *Trichoderma harzianum*: Effect of C/N ratio and glucose concentration. J. Rekayasa Kimia & Lingkungan 6(1), 35-40.

Sala, A., Artola, A., Sánchez, A., Barrena, R., 2020. Rice husk as a source for fungal biopesticide production by solid-state fermentation using *B. bassiana* and *T. harzianum*. Bioresour. Technol. 296, 122322.

Sala, A., Barrena, R., Sánchez, A., Artola, A., 2021b. Fungal biopesticide production: Process scale-up and sequential batch mode operation with *Trichoderma harzianum* using agro-industrial solid wastes of different biodegradability. Chem. Eng. J. 425, 131620.

Sala, A., Vittone, S., Barrena, R., Sánchez, A., Artola, A., 2021a. Scanning agro-industrial wastes as substrates for fungal biopesticide production: Use of *Beauveria bassiana* and *Trichoderma harzianum* in solid-state fermentation. J. Environ. Manag. 295, 113113.

Santos, M.D.D., Blatt, C.T.T., 1998. Teor de flavonóides e fenóis totais em folhas de Pyrostegia venusta Miers. de mata e de cerrado. Braz. J. Bot. 21, 135-140.

Shah, A., Smith, D.L., 2020. Flavonoids in agriculture: Chemistry and roles in biotic and abiotic stress responses, and microbial associations. Agronomy 10(8), 1209.

Shi, W., Zhu, Y., Xing, Y., Wu, H., Ying, Y., 2024. Enhancing phosphorus-solubilizing microorganism potential for alleviating plant phosphorus limitation through amino acid co-application. Appl. Soil Ecol. 204, 105714.

Sun, R., Tomkinson, J., 2002. Comparative study of lignins isolated by alkali and ultrasound-assisted alkali extractions from wheat straw. Ultrason. Sonochem. 9(2), 85-93.

Tabatabai, M.A., Bremner, J.M., 1969. Use of p-nitrophenyl phosphate for assay of soil phosphatase activity. Soil Biol. Biochem. 1(4), 301-307.

Urso, J.H., Gilbertson, L.M., 2018. Atom conversion efficiency: A new sustainability metric applied to nitrogen and phosphorus use in agriculture. ACS Sustain. Chem. Eng. 6, 4453–4463.

Valencia, J.C., Castro, B.L., 2004. Aspectos biológicos de aislamientos de *Trichoderma* sp. antagónicos a *Rosellinia bunodes*.

Vasileva-Tonkova, E., Balasheva, D.M., Galabova, D., 1996. Influence of growth temperature on the acid phosphatase activity in the yeast *Yarrowia lipolytica*. FEMS Microbiol. Lett. 145(2), 267-271.

Wang, L., Guan, H., Hu, J., Feng, Y., Li, X., Yusef, K.K., Gao, H., Tian, D., 2022. *Aspergillus niger* enhances organic and inorganic phosphorus release from wheat straw by secretion of degrading enzymes and oxalic acid. J. Agric. Food Chem. 70(35), 10738-10746.

Xiao, Y., Huang, Y., Chen, Y., Fan, Z., Chen, R., He, C., Wang, Y., 2021. Effects of solid-state fermentation with Eurotium cristatum YL-1 on the nutritional value, total phenolics, isoflavones, antioxidant activity, and volatile organic compounds of black soybeans. Agronomy 11(6), 1029.

Zhang, F., Meng, X., Yang, X., Ran, W., Shen, Q., 2014. Quantification and role of organic acids in cucumber root exudates in *Trichoderma harzianum* T-E5 colonization. Plant Physiol. Biochem. 83, 250-257.

Zhang, J.D., Yang, Q., 2015. Optimization of solid-state fermentation conditions for *Trichoderma harzianum* using an orthogonal test. Genet. Mol. Res. 14(1), 1771-1781.

Zhao, Q., Yan, X., Yue, Y., Yue, T., Yuan, Y., 2023. Improved flavonoid content in mulberry leaves by solid-state fermentation: Metabolic profile, activity, and mechanism. Innov. Food Sci. Emerg. Technol. 84, 103308.

Chapter 6

6. Conclusions

The development of biofertilizers from the biological solubilization of low-reactivity phosphate minerals is an emerging technology that still faces several challenges before becoming competitive with existing market products. This work contributes to advancing this field by proposing and evaluating biotechnological strategies based on solid-state fermentation to increase the efficiency of phosphate rock solubilization, exploring indirect mechanisms to enhance phosphorus acquisition by plants, and assessing the scalability of these processes in packed-bed bioreactors. Considering all the steps undertaken and the proposed objectives, the key conclusions are as follows:

- Sequential experimental designs aimed at optimizing oxalic acid production by *Aspergillus niger* demonstrated that the type of agroindustrial waste significantly influences the type of organic acid produced. Among the tested substrates, the combination of sugarcane bagasse and soybean bran directed the metabolism toward oxalic acid production. Moreover, methanol acted as a key metabolic modulator, favoring acid accumulation over biomass formation. Once the optimal methanol concentration was established, high solubilization efficiencies were achieved for the Bayóvar, Registro, and even the Itafós rocks - the latter being of igneous origin and thus less reactive;
- Scaling up the optimized solubilization process to a multilayer packed-bed bioreactor highlighted the challenges of maintaining laboratory-level yields, likely due to difficulties in retaining methanol - a volatile compound - at optimal concentrations throughout the process;
- Drying the fermented solids within the bioreactor proved effective, reducing moisture content to below 5% (wet basis), thereby preserving microbial viability and acid phosphatase activity over a 34-day evaluation period. This approach streamlines downstream processing by consolidating cultivation and drying operations, minimizing contamination risks, and extending product shelf life - making it a promising strategy for industrial application;
- The application of biofertilizers in a soil-plant system proved effective in replacing 50% of the chemical fertilizer dosage. No significant differences in

plant development were observed between the treatment containing 50% biofertilizer and the control treatment containing 100% chemical fertilizer. These findings indicate the potential of these bioinputs to reduce chemical fertilizer use and support more sustainable agriculture;

- The cultivation of *Trichoderma harzianum* on beer draff and wheat straw resulted in high production of spores and key metabolites that enhance phosphorus acquisition by plants, such as indoleacetic acid and flavonoids. Aeration and substrate compositions that ensure high porosity were critical to promoting robust microbial development. These results highlight the multifunctional capabilities of *T. harzianum*, which, beyond its established role as a biological control agent, can also enhance phosphorus uptake by plants;
- The SSF process of *T. harzianum* in a 22 L packed-bed bioreactor under optimized conditions yielded promising results, with sporulation levels only one order of magnitude lower than those observed at laboratory scale. However, improved heat dissipation strategies are essential to enhance process performance at larger scales, as significant overheating (up to 16.5°C) notably impaired the production of acid phosphatase and total flavonoids.

Overall, the results of this thesis confirm the potential of SSF-based biofertilizers produced with *Aspergillus niger* and *Trichoderma harzianum* as viable alternatives to conventional fertilizers. Nonetheless, challenges remain, particularly those related to process scale-up.

Chapter 7

7. Suggestions for future work

Considering the findings of the present thesis, the following suggestions are proposed to guide future research:

- Explore alternative metabolic modulation strategies beyond methanol to induce high organic acid production and, consequently, improve the efficiency of phosphate rock solubilization;
- Evaluate the production of a biofertilizer composite containing *Aspergillus niger*, phosphate rock, and the elements identified in this work as inducers of high oxalic acid production: soybean bran and methanol;
- Evaluate the solid-state fermentation process of *Trichoderma harzianum* using beer draff and wheat straw as substrates in a multilayer packed-bed bioreactor operated in continuous mode, aiming to minimize overheating issues and increase process yield;
- Assess the viability of fermented solids dried in the the packed-bed bioreactor itself over an extended storage period (> 6 months) under different conditions (refrigeration and room temperature).